CZECH TECHNICAL UNIVERSITY IN PRAGUE
Faculty of Civil Engineering
Department of Architectural Engineering

SIMPLIFIED DYNAMIC THERMAL MODELS OF BUILDING CONSTRUCTIONS IN CONTACT WITH THE GROUND: SLAB-ON-GROUND

DOCTORAL THESIS

Zdenko Malík

Doctoral study programme: Civil Engineering
Branch of study: Building Engineering

Thesis supervisor: prof. Ing. Jan Tywoniak, CSc.
Supervisor – specialist: Ing. Pavel Kopecký, Ph.D.

Prague, 2023

CZECH TECHNICAL UNIVERSITY IN PRAGUE
Faculty of Civil Engineering
Thákurova 7, 166 29 Praha 6

DECLARATION

Ph.D. student's name: Zdenko Malík

Title of the doctoral thesis: Simplified dynamic thermal models of building constructions in contact with the ground: slab-on-ground

I hereby declare that this doctoral thesis is my own work and effort written under the guidance of the tutors Prof. Ing. Jan Tywoniak, CSc. and Ing Pavel Kopecký, Ph.D.
All sources and other materials used have been quoted in the list of references.

The doctoral thesis was written in connection with research on the projects:

- SGS17/008/OHK1/1T/11: Simplified dynamic thermal model of a slab-on-ground floor
- SGS16/011/OHK1/1T/11: Impact of moisture and pressure on the thermal properties of soil

In Prague, on 30.3.2023 …….

signature

ACKNOWLEDGEMENTS

I would like to thank my supervisors, prof. Ing. Jan Tywoniak, CSc and Ing. Pavel Kopecký, Ph.D. for their support, guidance, feedback, and patience. I would also like to thank my colleagues and management at UCEEB CTU for their understanding and support during these years. Thanks also belong to my family and friends for their undying support, patience and the questions "are you about done with your thesis?". Special thanks belong to Mgr. et Mgr. Kristýna "Čiči" Bůžková for pushing me towards deadlines.

https://doi.org/10.14311/dis.fsv.2023.006

Abstract in Czech

Práce analyzuje problematiku zjednodušeného dynamického modelování tepelného chování podlah na zemině. Požadavky na energetickou účinnost budov a související požadavky na tepelně technické vlastnosti obálky budovy se v nedávné minulosti výrazně zpřísnily. Efektivní navrhování budov s takto nízkou spotřebou energie vyžaduje co nejpřesnější vyhodnocení množství variant návrhu budovy v raných fázích návrhu. Zvýšená přesnost obecně vede k prodloužení doby výpočtu, a ztěžuje tak efektivní návrh.

Konstrukce ve styku se zeminou jsou z hlediska výpočtů tepelných ztrát jedním z nejproblematičtějších konstrukcí vzhledem k velkému 3D bloku zeminy. Práce poskytuje přehled různých existujících přístupů k řešení tohoto problému. Následně využívá shromážděné informace k návrhu metody pro konstrukci náhradního 1D modelu podlahy na zemině použitelného v RC modelování.

Model se skládá ze dvou samostatných 1D problémů, kde každý představuje jinou zónu podlahy na zemině. Jeho geometrická interpretace je založena na ekvivalentním rozměru podlahy. Hodnoty geometrických vlastností navrženého modelu byly zjištěny jemným laděním při zohlednění různých kombinací vstupních parametrů (geometrie objektu a míra tepelné izolace). Vyladěné hodnoty byly následně zpracovány matematickou regresí s cílem nalézt rovnice popisující jejich závislost na vstupních parametrech.

Model byl testován za různých okrajových podmínek s ohledem na řadu kombinací vstupních parametrů porovnáváním s referenčními 3D FEM simulacemi. Testy zahrnovaly samostatné testování při ročních harmonických okrajových teplotách a také použití modelu v roční tepelné simulaci celé budovy vystavené hodinovému profilu venkovní teploty vzduchu pro Prahu v rámci roku.

Byla zkoumána i možnost rozšíření modelu tak, aby zohledňoval účinky případné svislé tepelné izolace po obvodu. Navržené řešení tohoto problému bylo rovněž testováno při ročních harmonických okrajových teplotách.

Výsledky vypočtené pomocí vyvinutého náhradního 1D modelu se ve všech provedených testech s dobrou spolehlivostí shodovaly s referenčními výsledky. Výpočetní čas se zkrátil z několika hodin potřebných pro 3D FEM výpočty na několik minut. Díky tomu se vyvinutý model stává použitelným nástrojem v raných fázích navrhování budov pro zajištění návrhu energeticky účinných budov. Známá omezení navrženého modelu a náměty pro další vývoj jsou uvedeny v závěru této práce.

Klíčová slova: podlaha na terénu; tepelné chování budov; dynamické simulace budov; zjednodušené modelování chování budov; výpočetní nástroje

Abstract in English

This thesis analyses the problematics of the simplified dynamic thermal modelling of slab-on-ground floors. The energy efficiency requirements for buildings and related requirements for thermal performance of the envelope have significantly tightened in the recent past. An efficient design of buildings with such low energy consumption requires a precise assessment of multiple variants in the early design phases. Increased precision generally leads to increased computation times and therefore makes it difficult to evaluate large numbers of design options.

Constructions in contact with the ground are one of the most difficult problems in terms of heat loss calculations due to the large 3D block of soil. The thesis provides an overview of different existing approaches to overcome this issue. It then uses the gathered information to propose a method to construct a surrogate 1D model of a slab-on-ground floor usable in RC modelling.

The model consists of two separate 1D problems, each representing different zone of the slab-on-ground floor. Its geometrical interpretation is based on the equivalent floor dimension. The values of geometrical properties of the proposed model have been found through fine-tuning in different test cases. The fine-tuned values have then been processed by mathematical regression to find equations describing their dependency on selected input parameters.

The model has been tested under different boundary conditions considering a range of input parameters against reference 3D FEM simulations. The tests included standalone testing under annual harmonic boundary temperatures and performance in a whole-building annual thermal simulation exposed to an annual hourly outdoor air temperature profile for Prague.

A possibility to extend the model in order to account for the effects of vertical thermal insulation around the slab's perimeter has been investigated. The proposed solution to this problem has also been tested under annual harmonic boundary temperatures.

The results calculated using the developed surrogate 1D model have matched the reference results with good confidence in all performed tests. The computation time has decreased from several hours needed for 3D FEM calculations to several minutes. This renders the developed model to be a usable tool in early building design phases to ensure the design of energy efficient buildings. The known limitations of the proposed model and topics for further development are outlined at the end of this thesis.

Keywords: slab-on-ground floor; building thermal performance; dynamic building simulation; simplified building performance modelling; simulation tools

Table of content

Nomenclature

Following nomenclature is used in the work carried out within this thesis (Chapters 3 to 6). Nomenclature in other chapters is taken over from the original referred sources and explained within the text.

Geometrical properties

a, b	[m]	Floor plan dimensions (or a parameter in general formula)
d	[m]	Thickness (or a parameter in general formula)
h	[m]	Height
A	[m^2]	Area
P	[m]	Exposed perimeter
B'	[m]	Equivalent floor dimension
l	[m]	Length
α	[m]	Width

Physical properties

Θ	[°C]	Temperature
T	[K]	Thermodynamic temperature
t	[s, min, hour]	Time
q	[W/m^2]	Specific heat flux
L	[W/m]	Thermal permeability
Q	[W]	Heat flux
λ	[W/(m•K)]	Thermal conductivity
k	[W/K]	Thermal conductance
ρ	[kg/m^3]	Specific volume
c	[J/(kg•K)]	Specific heat
R	[m^{2}K/W]	Thermal resistance

Statistical properties and operators

Δ, PMRE	[%]	Mean relative error (MRE)
GoF	[%]	Goodnes of Fit
μ	[-]	Correlation coefficient
Δ		Difference

Superscripts and subscripts

1D, 2D, 3D	Dimensionality of the model used for obtained results
*	Moving average value
e, i	External or internal
si	Internal surface
f	Floor
slab	Slab
ref	Reference

1. Introduction

Motivation and aim of the thesis

There is a worldwide effort to decrease society's energy consumption and greenhouse gas emissions. The space conditioning of buildings represents a large contributor to both of these aspects. Its negative effect can be minimized by the optimization of both the building envelope and building energy systems. Building envelope optimization can largely impact the overall energy consumption and therefore the sizing and efficiency of building energy systems.

Optimization requires a comparison of multiple variants. These variants should at different design phases provide reliable and comparable data. In the early design phases, it is beneficial to evaluate a large number of variants in a short time. As the energy consumption in the designed buildings is decreasing rapidly, the accuracy of the models plays a crucial role. The latest development has led to heavily insulated above-ground structures. The impact of ground-coupled heat transfer on overall building performance is therefore increasing.

> *"One of the most complex configurations to model in detail, both in the dynamic simulation of buildings and in the analytical quasi-steady-state calculations, is the thermal dispersion through the walls and the floor in contact with the ground."* [1][1]

This is caused by the large block of ground adjacent to the structure itself. Most of the building components have two parallel surfaces directly exposed to the boundary conditions facing each other, making it easier to be represented by 1-dimensional models. The 3-dimensional block of ground adjacent to the slab construction affects the 'external' boundary temperature of the slab and makes it variable along its external surface.

3D simulations are demanding in terms of time consumption and also computational power requirements. This issue can be solved by introducing simplified or surrogate models. Simplifications, however, decrease the model's accuracy. In the early design phases, when comparing a large number of conceptual variants, some level of inaccuracy is acceptable.

This thesis aims to develop a straightforward surrogate numerical model of slab-on-ground heat transfer. The goal is to provide a model based on one-dimensional heat conduction, which will sufficiently simulate the in-nature three-dimensional problem. The

[1] G. Pernigotto, A. Prada, M. Baratieri, P. Baggio, and A. Gasparella, 'Modelling Of The Thermal Behavior Of Walls And Floors In Contact With The Ground', presented at the International High Performance Buildings Conference, Purdue, 2012, vol. 2012.

aim is to create a model with minimum input parameters based on the slab-on-ground geometry and its thermal resistance.

Such a model can be used for fast calculation of transient heat conduction through the ground in whole-building simulation models.

Methodology

This thesis works within this scope and limitations:

- Model deals with a standalone building.
- Model should sufficiently simulate the 3D problem described in the ČSN EN ISO 10211:2020 [2] in terms of the ground-body dimensions.
- Model should sufficiently simulate typical slab-on-ground setups within the standard parameters of the construction and soil in the Czech Republic.
- The resulting model should only consist of 1D partial problems.
- The effect of the vertical perimeter insulation should be reflectable.

The work is organized in a step-by-step top-to-bottom fashion, first analyzing the substitution possibilities of 3D models by 2D models. Then, the substitution of the reference model (3D or 2D) by a 1D model is started using the following methods:

Finite element method (FEM): Finite element method is used to compute the approximations of the real solutions to partial differential equations describing the space- and time-dependent physical problems. Within this thesis, FEM is used to evaluate heat conduction within the 3D and 2D models. The results serve as a reference for further simplifications.

Fine-tuning: The results obtained from simulation on the developed model should match the reference results. For this purpose, a set of specific tuning cases with different values of input variables are evaluated. The values of individual parameters in the developed model are adjusted with focus on the match of results.

Regression analysis: The relationship between the dependent surrogate 1D model parameters and the slab-on-ground variables (geometry, thermal resistance) is investigated using regression analysis.

Comparison of results: The results obtained from the proposed surrogate 1D model are compared to reference 3D FEM model results under different boundary conditions.

Thesis outline

The thesis is structured into three main parts: Chapter 1 provides the introduction describing primarily the aim and methodology of the thesis.

Chapter 2 describes the state of the art. It looks into the benefits of fast and precise building performance modeling in the global context. It also addresses the influence of

ground-coupled heat transfer on the overall building performance modeling accuracy. This chapter describes the limitations of simplified models of this phenomenon and looks into the existing modeling approaches.

Chapter 3 describes the development process of the surrogate thermal model of a slab-on-ground construction. As per the methodology described above, this process consists of multiple subsequent steps. Therefore, this chapter provides a partial discussion of the results in each step and conclusions for the use of these results in the following steps. Overall discussion and conclusions are presented at the end of this thesis.

2. State of the art

2.1. Global context of energy efficiency in buildings and requirements

The energy consumption in buildings (residential and non-residential) accounted for 30 % of the world's energy consumption and 28 % of the world's emissions in 2018 according to [3], 35 % of the energy consumption and 38 % of the CO_2 emissions in 2019 [4] and 36 % of the energy consumption and 37 % of the CO_2 emissions in 2020 [5]. [3] also states, that the global energy consumption for space heating has decreased by 1 % from 2010 to 2018 but still accounted for one-third of total global energy consumption in buildings. On the other hand, the space cooling demand rose more than 33 % from 2010 to 2018. If the increasing floor area of buildings is taken into account, the space heating intensity per unit of floor area decreased by 20 % from 2010 to 2018 and the space cooling intensity rose by 8 %. Space conditioning (heating and cooling) therefore accounted for approximately 12 % of global energy consumption in 2018.

Standards that specify the minimum energy performance requirements for buildings are established by building energy codes. However, at present, mandatory or voluntary building energy codes are implemented in fewer than 85 countries worldwide. These codes have been proven to be a cost-effective means of enhancing the energy performance of residential and commercial buildings, be it new constructions or refurbishments [6]. The countries with such codes already in place are usually working on their continuous evolution to achieve higher energy effectiveness. These codes usually don't only cover the U-values of the building envelope, but at the same time set the requirements for ventilation systems and overall building energy performance.

The energy efficiency of buildings is a widely researched topic. Fig. 2-1 shows the number of research papers published in the Elsevier journals when searching the database for "energy efficiency in buildings" between 1999 and 2021 [7]. The number of published articles has a strongly rising tendency. According to the CORDIS database, 333 projects have been supported by the European Union which are linked to the "energy efficient buildings" query with the total EU contribution exceeding 1.3 billion € (as of 31.12.2021) [8].

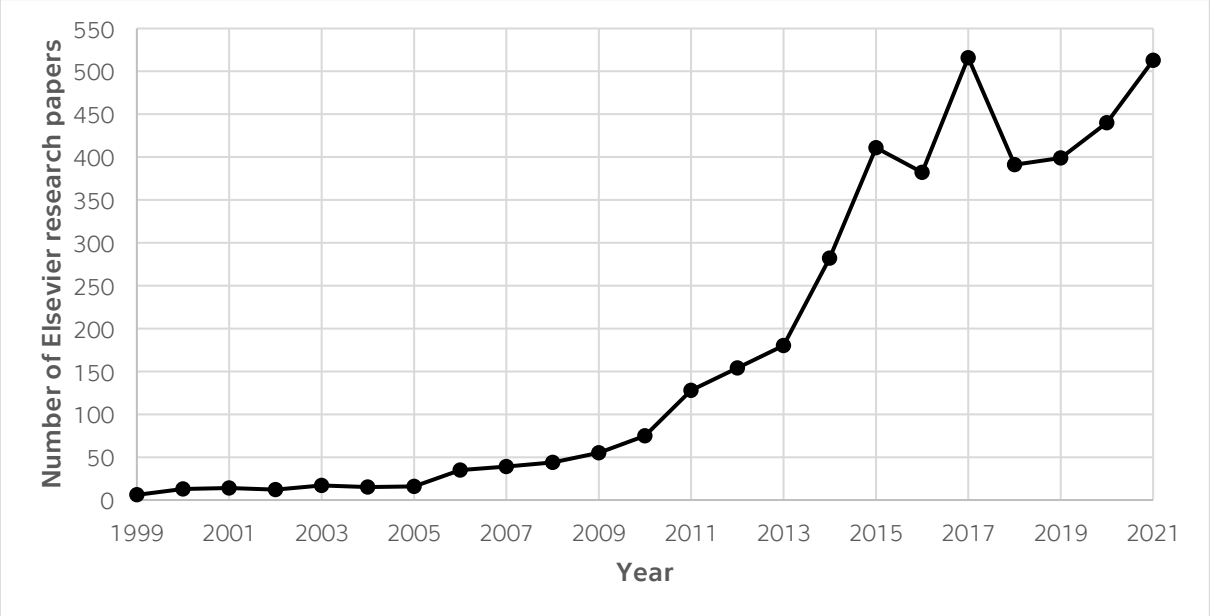

Fig. 2-1 Number of Elsevier papers matching the search query "energy efficient buildings"

There is no universally used definition of energy efficient buildings or building energy efficiency. Janmejoy and Manjari [9] define it as a building that *"creates comfortable living conditions inside the dwelling with the least possible amount of energy consumption maximizing efficiency in the use of resources."*[2] Mahmudul [10] provides a slightly more concrete definition: "*The energy efficiency of a building is the extent to which the energy consumption per square metre of floor area of the building measures up to established energy consumption benchmarks for that particular type of building under defined climatic conditions."*[3] Fairey and Goldstein [11] define energy efficiency as *"the provision of a constant level of energy service while using less energy*".[4] They then summarize several metrics used to rate energy efficiency: EUI, the HERS index, the zEPI Index and the percent-better-than-a reference-code. Energy Use Index (EUI) is one of the most widely used metrics to track building energy efficiency and is defined as the energy consumption per unit of conditioned floor area. The energy performance of a building is the outcome of the interplay between an engineered system, operation and maintenance

[2] J. Gupta and M. Chakraborty, '15 - Energy efficiency in buildings', in Sustainable Fuel Technologies Handbook, S. Dutta and C. Mustansar Hussain, Eds. Academic Press, 2021, pp. 457–480. doi: 10.1016/B978-0-12-822989-7.00016-0.

[3] H. Mahmudul, 'Investigation of Energy Efficient approaches for the energy performance improvement of commercial buildings', Queensland University of Technology, Brisbane, Australia, 2013. [Online]. Available: https://eprints.qut.edu.au/61050/1/M._Hasan_Thesis.pdf

[4] P. Fairey and D. B. Goldstein, 'Metrics for Energy Efficient Buildings: How Do We Measure Efficiency?', presented at the 2016 ACEEE Summer Study on Energy Efficiency in Buildings, Washhington, D.C., 2016. [Online]. Available: https://www.aceee.org/files/proceedings/2016/data/index.htm

(O&M) practices, and the demands and behavior of the building's occupants [12]. These three dimensions of energy performance are to large extent autonomous.

The trends in energy efficiency do in reality move in the direction of benchmarking. These EUI benchmarks are centrally determined at national or international levels using standards and directives. These benchmarks today do not only refer to the end-use energy but also primary energy consumption. If we were to only focus on heating and cooling energy demand, the ultimate goal throughout Europe would be 15 kWh/m^{2}a, which is the Passive House standard. The PH standard presents the possibility of heating energy savings of up to 90 % when compared to older existing buildings and up to 80 % when compared with new buildings (comparison within Germany) [13].

Energy efficient buildings which also aim for low energy consumption (be it nZEB or Passive House) become much less robust than the buildings built in the past. That requires a very precise design of the building carefully assessing the heat losses and gains. Furthermore, the effective operation of the designed systems become more crucial.

On one side, therefore, stands an effective design. Here the trend is clear: minimize the heat losses and efficiently manage the heat gains in summer and winter. Precise simulation tools are needed for the building construction design and subsequent HVAC sizing.

The use of models and simulations however does not end at the design phase anymore. Simplified but precise models are being used for effective system operation and optimization. So much so, that these models can be used for predictive control of the systems considering estimated boundary conditions and operation, to maximize efficiency. These model predictive control (MPC) systems can be also used to minimize the carbon footprint by shifting the loads to times when its impact is lower (e.g. when more renewable energy is produced to cover the demand) [14].

Building space conditioning energy

Energy consumption of buildings depends significantly on the requirements used for the indoor environment and building design and operation [15]. The main purpose of buildings is to provide a satisfactory indoor environment for their occupants. The historical development of the Indoor Environment Quality (IEQ) in Danish dwellings has been conducted in [16]. This research shows, that only modest IEQ improvements have been made when comparing the buildings built in the last 150 years in Denmark. The data further shows no overall thermal indoor environment improvements. The authors attribute this to the general goal to increase winter comfort, which has consequently led to a decrease in summer comfort. Based on this research it can be said, that buildings

built 150 years ago can provide an indoor environment comparable to the one in buildings of today. The main difference is just the amount of energy needed.

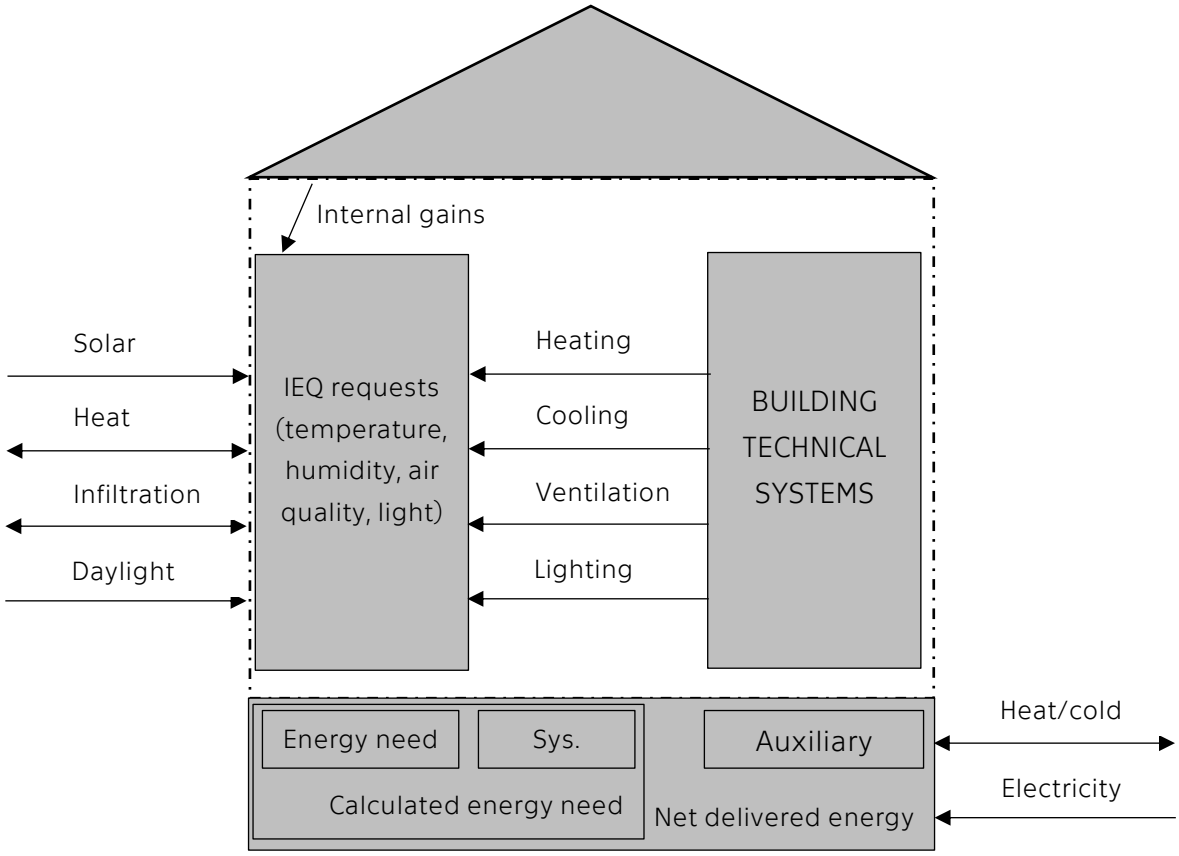

Fig. 2-2: Building energy needs and delivered energy

Space conditioning energy consumption comprises many factors. If we only focus on the consumption for space heating and cooling, it can be schematically described as in Fig. 2-2. Individual systems maintaining specific parts of the IEQ introduce not only their own energy need but may also affect the others. Increased requirements for internal air quality may, for example, lead to increased ventilation. This introduces larger heat gains or losses which the cooling and heating systems respectively have to deal with. That is why the scheme also includes daylight, lighting (insufficient daylight causes the demand for artificial light introducing internal heat gains), and ventilation. Thermal conduction through the envelope is therefore just a part of a multi-variable heat balance equation.

The thermal behavior of a building is significantly influenced by the heat loss that occurs through the building elements that are in contact with the ground [17]. As the number of parameters affecting the thermal behaviour of individual buildings is large, it is rather complicated to generally quantify the ground-coupled heat transfer's importance in the whole building behavior According to Adjali, et.al [18] it can be, in certain circumstances, responsible for up to 50% of the total energy consumed concerning internal climate control. The IEA BESTEST technical report [19] investigating the ground-coupled heat

transfer related to slab-on-grade constructions states, that typical slab-on-grade floor heat loss can range from 15 % to 45 % of the annual heating load. Data mining performed by Zhou et.al [20] on 5615 households in Tianjin in China.

Thermal performance requirements

In the Czech Republic (Czechoslovakia at the time), the first heat transfer requirements for basic building constructions were specified in 1949 in the ČSN 1450-1949 standard (*Heat loss calculation for the central heating system design*). The first standard dedicated to the thermal protection of buildings was issued in 1962 (ČSN 73 0540) and has been revised and actualized several times since [21], [22]. The development of the required U-values for selected envelope constructions in the Czech Republic is shown in Fig. 2-3 [23]. Annex 1 offers the overview of this development in other European countries. From the figure, it can be seen, that the largest development has generally been made in the above-ground envelope – mostly in the windows, which have posed the largest heat loss potential. The ground-coupled construction can afford higher U-values as they are not exposed to extreme outdoor temperatures because the soil serves as a buffer. The U-value only considers the built construction, not the soil itself. That may be the reason for the requirements on the ground-coupled constructions not being tightened as much over time. More strict requirements on above ground envelope while "neglecting" the development of ground-coupled constructions rises the relative impact of the ground-coupled heat loss on overall building performance.

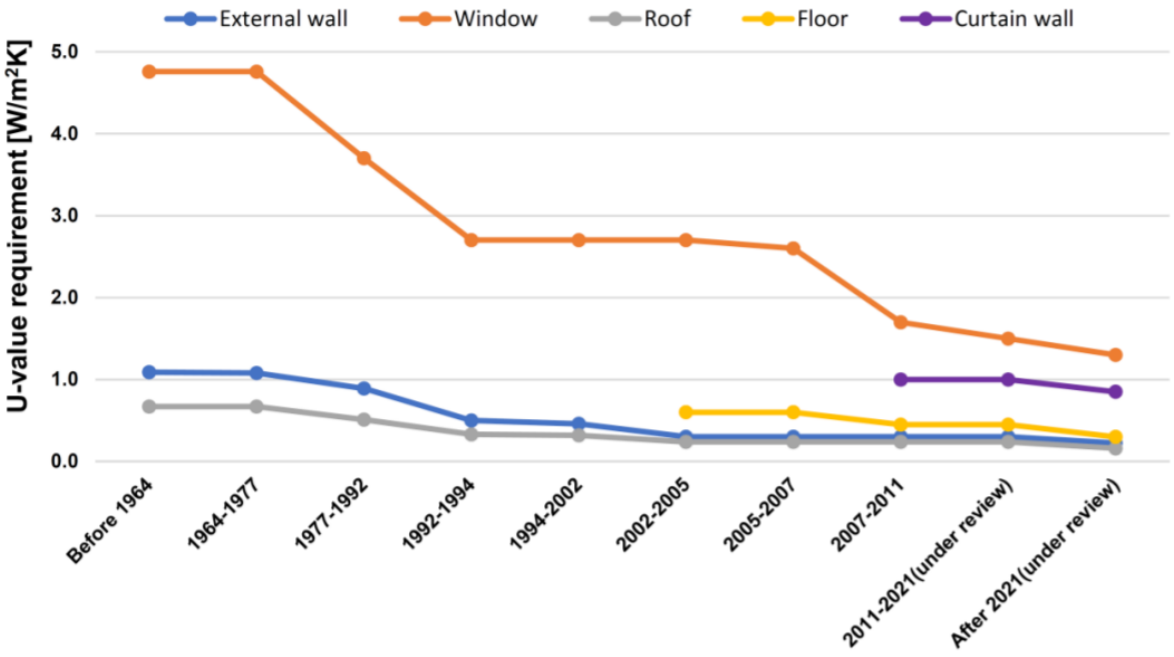

Fig. 2-3 Development of the required U-values for different building construction periods in the Czech Republic [23]

2.2. Ground-coupled heat transfer limitations

Most of the building envelope components are planar. They mostly have a constant thickness and the same order and thickness of material layers. This results in mostly uniform heat transfer through their boundary surfaces. Generally, in above-ground constructions, the heat transfer is only disrupted by thermal bridges and different construction joints (which can also be considered thermal bridges). The effect and behaviour of individual thermal bridges can be quantified and considered while still modelling the constructions quite simply in 1D models.

While in the case of above-ground envelope elements, their internal and external surfaces have approximately the same surface area, in the case of ground-coupled heat transfer the surface exposed to the exterior boundary temperature is generally much larger than the surface exposed to the interior boundary temperature. The 3D nature of the ground-coupled heat transfer leads to the uneven 'boundary' temperature on the outer surface of the built slab-on-ground construction. This can be seen in Fig. 2-4. Here the temperature distribution on the external surfaces of external walls and slab on the ground floor is shown in a steady-state heat conduction simulation when considering the 3D block of soil. Furthermore, in the case of transient internal and external boundary temperatures, this uneven 'boundary' temperature doesn't change with the same phase shift, amplitude or mean value at different parts of the outer surface as shown in Fig. 2-5.

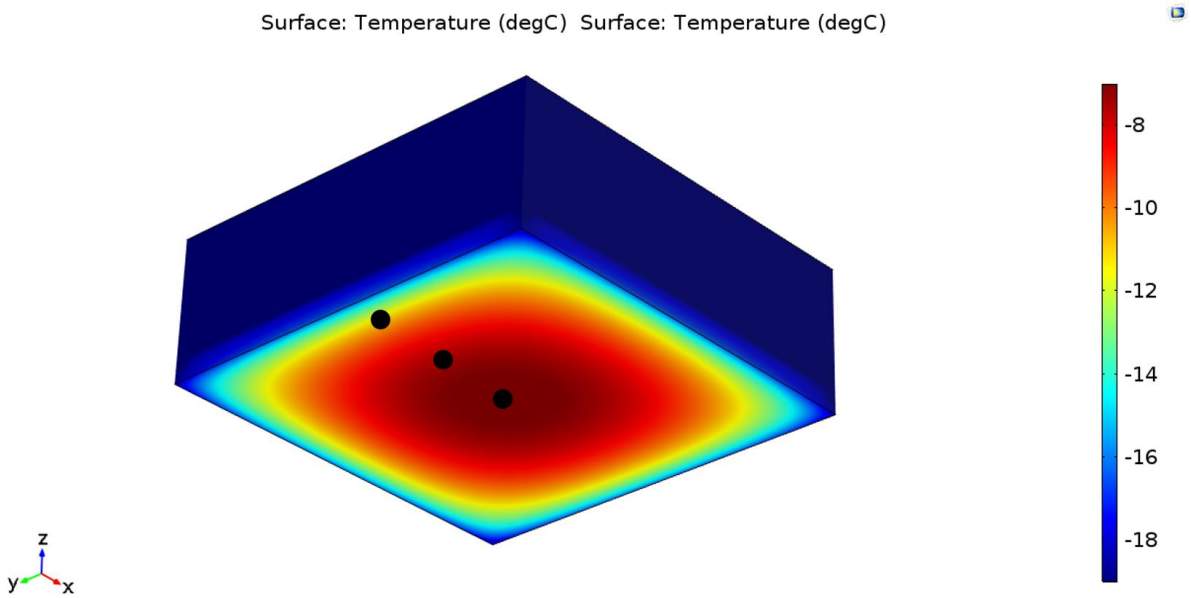

Fig. 2-4: Steady-state temperature distribution on the external surface of building envelope elements – slab on ground and exterior wall (shown from the bottom); points shown in the figure are locations for further analysis in Fig. 2-5

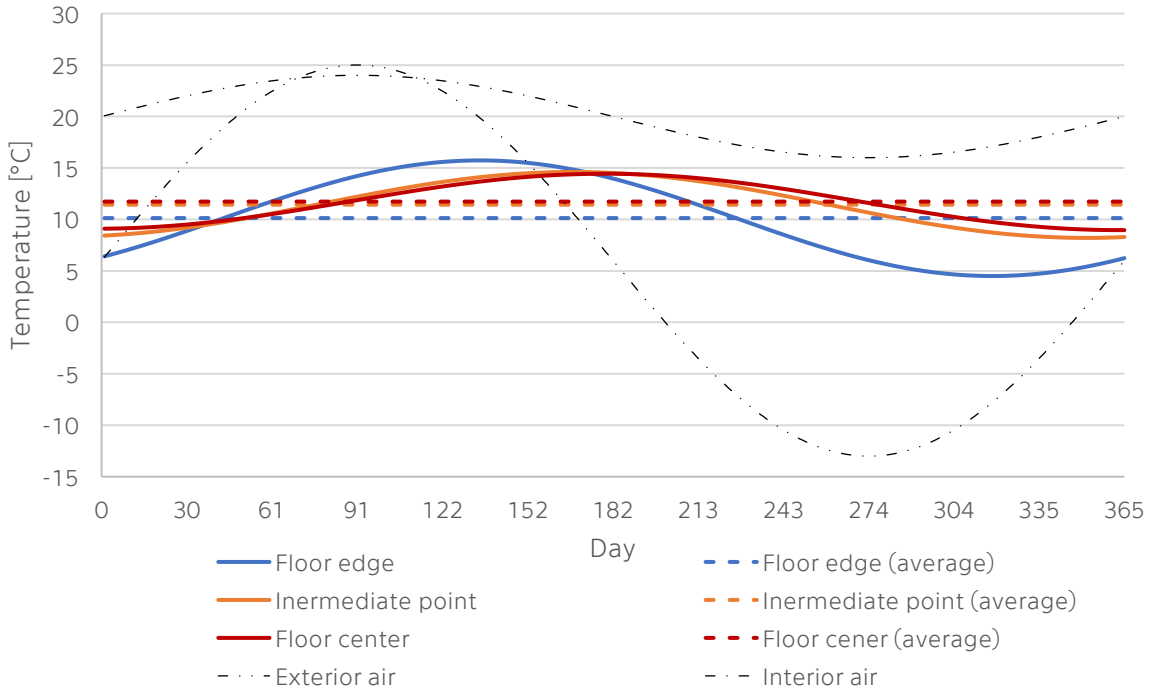

Fig. 2-5: Example of an annual temperature profile at different points under the slab-on-ground construction

Heat transfer in soil is a complicated process that encompasses several mechanisms, including conduction through soil grains, liquids, and gases; latent heat transfer involving evaporation-condensation cycles; sensible heat transfer via vapor and liquid diffusion and convection; and radiation in gas-filled pores. Conduction through the solid particles in the soil is typically the primary mode of heat transfer, although the presence of moisture in the soil can introduce additional transport mechanisms [24]. Its 3D nature combined with the large thermal capacity of the soil block results in large time shifts in the phase shift of the temperature fluctuation. Reliable modelling of such a complex phenomenon requires both quality input data and computational power/time. The disagreement among models used for calculating uninsulated slab-on-grade heat transfer can vary from 25 % to more than 60 % when comparing simplified models with detailed models [19]. This disagreement is dependent on the complexity of compared models, materials, and climate.

The general theory of ground-coupled heat transfer in buildings was summarized by Claesson and Hagentoft [25]. They also discuss the complexity of the problem. Apart from the already mentioned disproportion in areas exposed to individual boundary conditions and the three-dimensionality of the heat flow, they also mention the following:

- Inhomogeneous ground
  The thermal properties of the ground may not be homogeneous. Typically, the ground can be stratified in horizontal layers based on the soil occurring at a certain depth. The soil stratification can introduce another variable: different moisture

content within different soil layers. The conductivity in dry soil (less than 1 W/m•K) is often much smaller than in saturated soil (more than 2 W/m•K).
Another source of inhomogeneity can be large isolated bodies such as rocks. In real urban situations, where the building is not built as a solitary element, other buildings, their foundations as well as underground structures present other sources of uncertainty.

- Moisture migration
  Moisture flow, which is common in all building constructions can affect the energy flux. This effect is however judged to be negligible in most constructions as well as in the ground-coupled ones.
- Groundwater flow
  Flowing ground water may influence the energy flow as well. Hagentoft [26] states, that the groundwater's influence is typically small. He physically interprets it by the fact, that the groundwater receives heat from the ground under the building and moves downstream at a higher temperature. The energy harvested under the building is then released into colder ground downstream. This affects the isotherms under the building but does not change the building heat loss to any larger extent, except for rather extreme situations.
- Freezing
  Freezing presents two complications. First, the freezing/melting around the freezing point introduces latent heat processes. Secondly, the thermal properties of the ground change when it freezes. The heat conduction equation becomes non-linear as the thermal conductivity is a function of temperature. According to Hagentoft and Claesson is the error introduced by neglecting these phenomena small and negligible.
- Boundary conditions
  Detailed boundary conditions at the ground surface are complicated to describe. These may include already mentioned other buildings. The ground surface is also influenced by the radiative exchange with the sky and the wind velocity. Both depend on the specific conditions at a specific location on the ground surface (roughness, emissivity, view factors to the sky, greenery, etc.). To effectively account for these variables, Hagentoft and Claesson suggest the use of the mean below-ground temperature as the external boundary condition. They suggest the use of temperatures the mean value at one meter's depth in undisturbed ground, where most of the variations should be smoothed out.
- Snow
  Snow is a specific case of boundary condition and the heat flow is considerably influenced by it. Predicting snow occurrence in the design phase is quite complicated and therefore its effect on heat losses is complicated to quantify.
- Initial temperature distribution in the ground.

A new building presents a disruption in a previously periodically conditioned system with considerable inertia. Buildings are being designed for operation after the system 'adapts' to the new boundary conditions. The building performance after the building erection will therefore not match the calculated data right away. The extra heat loss due to thermal build-up after the building erection is reported to be 10 % to 20 %.

2.3. Ground-coupled heat transfer in building energy simulation tools

The most commonly used whole-building simulation software packages are TRNSYS, ESP-r, IES VE, IDE ICE, DOE-2 and EnergyPlus. These software packages can also serve as the computation core for other programs with a different user interface. For example, EnergyPlus is the computation core for DesignBuilder, OpenStudio or Honeybee. In this chapter, the approach to ground-coupled heat transfer within TRNSYS, ESP-r and EnergyPlus is described.

Ground-coupled heat transfer in ESP-r

ESP-r is a general purpose, multi-domain (building thermal, inter-zone air flow, intra-zone air movement, HVAC systems and electrical power flow) simulation environment which works on the principle of simulation follows description where additional technical domain solvers are invoked as the building and system descriptions evolve. ESP-r is capable of solving for zones, network mass flow, CFD, and electrical domains almost simultaneously. This software employs a variety of solution techniques for zonal, airflow, system, and electrical power domains. ESP-r continuously tracks and reports energy balances throughout the model at every zone, surface, and component. The solver descriptions include the zone solver, the mass flow solver for air, water, or mixed flows, the CFD solver, the system solver for dynamic system component models, and the electrical power solver, which handles both DC and AC electrical power distributions. [27].

The ESP-r Cookbook [28] lists the possible boundary conditions to be used for constructions in contact with the ground:

- predefined monthly ground temperature profile
- 3D ground model
- a BASESIMP foundation description

Instead of a more precise 3D ground model (according to [27] the majority of users works with 1D solvers only) a BASESIMP foundation description can be used [29]. It is a regression-based algorithm which estimates residential-foundation heat losses. Its structure allows the addition of new foundation configurations. This algorithm has been

derived from 33 000 parametric finite-element-based simulations. It divides the ground-coupled heat transfer into three components:

- Heat loss from foundation to ambient air, $Q_{\text{above-grade}}$ (t)
- Mean annual heat loss from foundation to soil, $Q_{\text{below-grade,average}}$
- Annual harmonic heat loss from foundation to soil, $Q_{\text{below-grade,harmonic}}$ (t)

For the heat flow from the basement then applies the following equation:

$$Q_{basement}\,(t) = Q_{above-grade}\,(t) + Q_{below-grade,average} + Q_{below-grade,harmonic}\,(t) \quad (2\text{-}1)$$

To solve this equation, the BASESIMP calculation algorithm consists of 3 steps:

First step is the solution of set of equations.

$$SUMUO = \left\{\frac{a_1 + b_1(height - depth) + \frac{c_1}{soilk}}{rsi^{d_1}}\right\} \cdot \left\{\frac{1}{e1 + (i1)(overlap)^{f_1}(rsi)^{g1}(height - depth)^{h1}}\right\} + \{j1\} \quad (2\text{-}2)$$

$$SUMUR = \left[\frac{\{q_2 + r_2(width)\} \cdot \{u2 + v2(soilk)\} \cdot \{w2 + x2(depth)\}}{(wtable)^{s2+t2(width)+y2(depth)}}\right] + \left[\frac{a2(depth)^{b2}(soilk)^{c2}}{(wtable)^{d_2}(rsi)^{e2+f2(soilk)+g2(depth)+h2(overlap)}}\right] \quad (2\text{-}3)$$

$$ATTEN = \{a3 + b3(soilk) + c3(depth)\} + \left\{\frac{e3 + f3(soilk) + g3(depth)}{(rsi)^{h3+i3\cdot overlap}}\right\} \quad (2\text{-}4)$$

$$PHASE = a4 + \frac{b4}{(rsi)^{c4}} \quad (2\text{-}5)$$

SUMUO, SUMUR ATTEN and *PHASE* are in the BASESIMP's predecessor BASECALC determined using a set of 2D FEM calculation using unit-temperature-excitation boundary conditions. BASESIMP used the results of these simulations to formulate the above stated equations using mathematical regression. The number of parameters for the calculation is quite excessive and their values are dependent on the type of construction being evaluated. An example of their values is shown in Fig. 2-6.

	no insulation		interior insulation from top of wall to 0.6m below-grade		interior full-height insulation		exterior insulation from grade to bottom of wall	
	average BC	variable BC	average BC	variable BC	average BC	variable BC	average BC	variable BC
a	0.784	0.756	0.892	0.856	0.717	0.663	0.794	0.753
b	0	0	-0.00590	0.00561	-0.0220	-0.0112	-0.00590	-0.00394
c	-0.0627	-0.0413	-0.0754	-0.0471	-0.0656	-0.0467	-0.0630	-0.0387
d	0.0159	0.0679	-0.0270	0.0393	0.0347	0.104	0.0180	0.0720
e	0.184	0.174	0.0620	0.0733	0.115	0.156	0.162	0.159
f	-0.00280	-0.00143	-0.00249	-0.00260	-0.00243	-0.00100	-0.00371	-0.00103
g	0	0	0.000398	-0.000492	0.00239	0.00123	0.000818	0.000511
h	0	0	-0.000624	-0.00143	0.000171	-0.00139	-0.000322	-7.61E-5
i	0	0	-0.000892	-0.000630	0.000786	0.00145	0.000390	0.000591
j	-0.000588	0.00370	0.00308	0.00552	0.00538	0.00814	-0.000890	0.00414
k	-0.00323	-0.00508	0.00186	-0.00130	-0.00690	-0.0103	-0.00413	-0.00627
l	0	0	0.00237	0.00224	-0.00685	-0.00276	-0.00348	-0.00226
m	0.0123	0.0178	0.0125	0.0151	-0.00593	0.00180	0.00266	0.0142
n	-0.0188	-0.0195	-0.0208	-0.0199	-0.0182	-0.0156	-0.0157	-0.0148
o	-0.0448	-0.0399	0	0	-0.0181	-0.0235	-0.0424	-0.0394
p	0	0	0.000230	-2.58E-5	0.000216	-0.000132	4.03E-5	-7.22E-5
q	0.00116	-0.000694	0.000637	-0.000985	7.41E-5	-0.00130	0.00137	-0.00103
r	0.00186	-0.00235	0.00189	-0.000349	0.00219	-0.000170	0.00206	-0.000156
s	0.00302	0.00259	0.00490	0.00408	0.00495	0.00211	0.00346	0.00205
RMS error	0.9%	0.9%	0.7%	0.5%	1.2%	0.8%	1.0%	0.9%
greatest deviation	2.2%	2.0%	1.5%	1.0%	3.0%	2.3%	2.3%	2.2%
range limits	$0 \le RSI \le 5$ (m²K/W) $0.85 \le k_{soil} \le 1.9$ (W/mK) $3 \le W \le 10$ (m) $0 \le D \le 2$ (m) $5 \le V \le 15$ (m)							

Fig. 2-6: Some of the correlation coefficient to be used in the BASESIMP calculation [30]

The second step is to perform the correction for three dimensional effects around corners using equations:

$$S_{ag} = SUMUO \cdot 2(length + width) \tag{2-6}$$

$$S_{bg,avg} = SUMUR \cdot \{2(length - width) + 4 \cdot width \cdot F_{cs}\} \tag{2-7}$$

$$S_{bg,var} = ATTEN \cdot \{2(length - width) + 4 \cdot width \cdot F_{cv}\} \tag{2-8}$$

$$PHASE = PHASE \tag{2-9}$$

S_{ag}, $S_{bg,avg}$ and $S_{bg,var}$ are three-dimensional shape factors in [W/K] for the individual heat transfer components; PHASE is the thermal response factor [radians]; $T_{basement}$ is the interior air temperature [K]; $T_{g,avg}$ is the annual-average ground surface temperature [K]; T_a is the exterior dry-bulb temperature; $T_{g,amp}$ is the amplitude of the annual harmonic of the ground-surface temperature [K]; and P_s is the phase lag of the ground-surface temperature cosine wave equal to the time between January 1 and the time of the coldest ground-surface temperature [radians].

The F_{cs} and F_{cv} scalar corner-coefficient factors and are again regression-based functions taking into account the thermophysical properties of the construction and adjacent soil and use the same correlation coefficients.

The last step is the actual heat loss calculation:

$$Q_{basement}\,(t) = Q_{above-grade}\,(t) + Q_{below-grade,average} + Q_{below-grade,harmonic}\,(t) \quad (2\text{-}10)$$

$$Q_{above-grade}\,(t) = S_{ag}(T_{basement} - T_a) \quad (2\text{-}11)$$

$$Q_{below-grade,average} = S_{bg,average}\left(T_{basement} - T_{g,avg}\right) \quad (2\text{-}12)$$

$$Q_{below-grade,harmonic}(t) = S_{bg,var}T_{g,amp} \cdot \sin\left(\omega t + PHASE - \frac{\pi}{2} - P_s\right) \quad (2\text{-}13)$$

For the purposes of the BASESIMP development, constant soil density and specific heat have been considered. If variability of these properties should be accounted for (on top of already variable soil conductivity) would result into drastically larger number of reference BASECALC simulations

The BASESIMP structure and the extent of investigated and described cases make it very useful for early-stage building energy simulations. It also makes BASESIMP both easy to implement and extensible.

The BASESIMP authors state, that any regression-based algorithm inherently sacrifices some accuracy: no correlation equation can perfectly represent a data set. The accuracy of the algorithm has been demonstrated by the authors and it has also been compared to the well-tested Mitalas method [31], [32]. The comparison for one case of a slab-on-grade foundation is shown in Fig. 2-7.

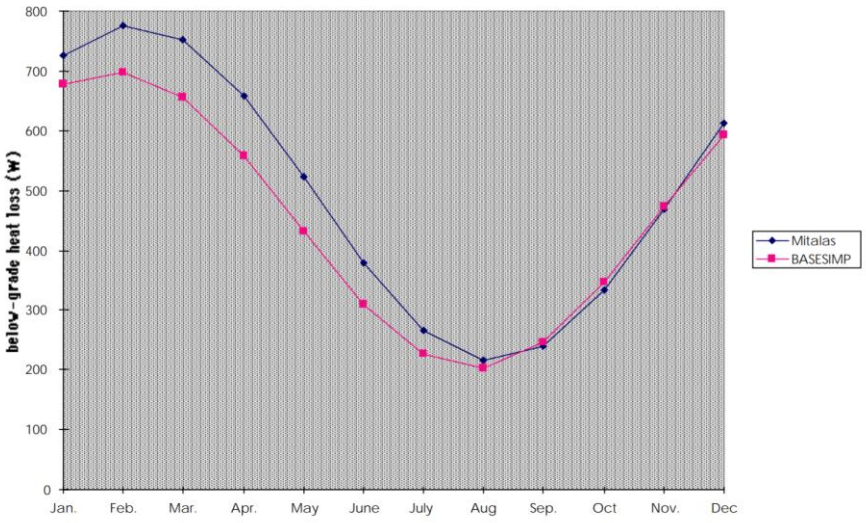

Fig. 2-7 BASESIMP vs. Mitalas (slab-on-grade) [29]

Energy Plus

Generally, the heat conduction calculations in EnergyPlus are one-dimensional. Also, the time shift caused by other building constructions is incomparable with the time shift caused by the soil mass. To be able to implement the ground heat transfer reliably into the model, a partial decoupling takes place. In order to calculate the zone energy balance, the temperature of the outside construction surface is crucial. Therefore, the problem gets separated into the zone balance and the ground heat transfer at the boundary between the slab construction and the ground.

In older Energy Plus versions (8.3 [33]) the ground heat transfer calculates the temperatures at the boundary surface, which are then used in the zone energy balance as the slab boundary temperatures. Bahnfleth's 3D ground heat transfer programs [34]–[36] modified by Clements are used to calculate these temperatures for the core and perimeter area as monthly averages or the average outside temperatures for the whole slab.

To model the heat transfer through ground-coupled constructions, EnergyPlus offers three calculation approaches:

- Ground heat transfer calculation using C and F factor constructions
- Ground heat transfer calculation using Site:GroundDomain:Slab
- Ground heat transfer calculation using Site:GroundDomain:Basement

For slab-on-grade constructions, the first two approaches are suitable. The C and F factor-based calculations aim to take into account the US building energy code and standards which use the mentioned factors. These in default do not specify detailed layer-by-layer materials of the construction. To be compatible with the EnergyPlus calculations, the component creates its own two-layer construction which matches the user-defined F factor (when talking about the floor constructions). This surrogate construction consists of a concrete layer (15 cm) with thermal mass and a massless thermal insulation layer.

A detailed layer-by-layer modelling approach is used when implementing the Site:GroundDomain:Slab component. According to the Input Output Reference [37], horizontal ground surfaces interact with the Site:GroundDomain object by utilizing the SurfaceProperty:OtherSideConditionsModel object.

The current version of Energy Plus (9.6 [38]) incorporates an open-source foundation heat transfer calculation tool Kiva [39]. The tool was designed to provide a framework for testing different approaches to simulate ground-coupled heat transfer within Kuris's doctoral candidacy [40]. Energy Plus uses Kiva's two-dimensional calculations. The simulations use the finite difference method. The two-dimensional calculations are based on the approximation introduced by Anderson [41]. The applicability of this approach for

transient boundary conditions has been independently analysed as a part of this doctoral thesis and it will be discussed in the following chapters.

TRNSYS

TRNSYS [42] (Transient System Simulation Tool, currently in version 18, is a modular simulation software designed to simulate the behaviour of transient systems. Building energy simulation is just one of its potential uses. The tool works with individual components (Types) describing individual parts of the system. These Types process their required inputs and produce outputs, which can then be processed by other types. For this purpose, a link between the relevant Types is created, describing the relation of between respective inputs and outputs.

After creating the diagram, the resulting input file is read and processed by the Kernel (computation engine). The engine iteratively solves the system, determines convergence and plots system variables. It can also determine thermophysical properties, invert matrices, perform linear regressions and interpolate external data files. The standard library of components (Types) consists of more than 150 types (weather data processors, HVAC equipment, heat pumps, multizone buildings, energy sources such as wind turbines, etc.)

Type 56 is used for the multizone building energy simulation (BES). The parameters of TYPE 56 are not defined directly in the TRNSYS input file. The building is described on a so-called building file (*.BUI). This file containing the necessary information about individual zones, such as loads, schedules, adjacencies constructions etc. then serves as an input file for Type 56.

To model ground coupling, TRNSYS 18 uses different subroutines. Within this chapter, the Type 77 and Type 49 are described. Type 77 can serve for calculation of a boundary condition for Type 49, but by itself it is not usable for sla-on-ground calculations. An overview of Type 1244, Type 1255 and Type 1267 is provided in Annex 2 of the thesis. The common denominator for all the Types dealing with the ground-coupling (therefore except Type 77) is the calculation of the sub-surface heat transfer using 3-dimensional conduction using a finite difference approach.

The basic Type77 is used to model the vertical temperature distribution in the ground. Its inputs include the annual mean ground surface temperature, its annual amplitude, the time in year when the minimum surface temperature occurs, and the soil thermal diffusivity. Type77 is based on the Kusuda model [43], which calculates the temperature of the undisturbed ground in given depth at given time of the year.

$$T = T_{mean} - T_{amp} exp\left(-depth\left(\frac{\pi}{365\alpha}\right)^{0.5}\right)\cos\left(\frac{2\pi}{365}\left(t_{now} - t_{shift} - \frac{depth}{2}\left(\frac{365}{\pi\alpha}\right)^{0.5}\right)\right) \quad (2\text{-}14)$$

In the above equation, α is the thermal diffusivity of the soil. It is computed inside the model using:

$$\alpha = \frac{k}{\rho Cp} \tag{2-15}$$

The soil temperature at various depths may be required for components buried in the ground that interact thermally with the soil, such as Type49. This Type is used useful as a first approximation in such cases but the interaction is only one-way. The soil temperature affects the building component but the temperature of the building will not in turn affect the soil temperature.

Type49:

- Is intended for Slab-on grade heat transfer calculation from Type56 multizone buildings.
- The data file is generally created using a TESS Plug-In for Google Sketchup.
- The slab edge heat transfer is not accounted for and the insulation can be added to the Type 56 walls. The model allows for skirt insulation to the depth of the footer (not between zones). Insulation in the model is mass-less and infinitesimally thin.
- The footer material is not accounted for.
- Only one soil layer is modelled
- Soil surfaces are uniform and horizontal
- The far-field heat transfer can be modelled as conductive or adiabatic and can be set for the X and Y directions independently, while the far-field temperatures are set by Kusuda correlation as a function of soil properties, time of year and depth.
- Deep earth heat transfer can be conductive or adiabatic, while the deep earth temperatures are set by Kusuda correlation (equation *(2-14)*).
- Near-field surface temperatures are set by Kusuda correlation as a function of soil properties, time of year and depth. The building does not impact the surface temperatures.
- Heat flows from Type 56 slabs are passed in as inputs. Average slab/soil boundary temperatures passed back to the Type 56 model.
- Sub-surface heat transfer is calculated using a 3-dimensional conduction using a finite difference approach.

Type 49 is a TRNSYS component for a multizone slab on ground. It uses a 3D finite difference model of the ground, which is solved using a simple iterative analytic method. The calculation is based on several assumptions and limitations:

- Soil is conductive only (moisture effects are neglected)
- Soil has homogenous properties in all its volume
- Thermal properties of the ground are not dependent on temperature
- Ground surface is flat
- The building does not affect the surrounding soil surface temperature.

The subroutine calculates the temperatures under the slab, which can then be used in the building simulation as the boundary temperatures of the slab-on-ground construction in 1D models.

User has to provide a "map" for the soil surface indicating the exposure of the individual computation nodes either to the multi-zone building or the ambient air. The noding then differentiates the soil into nodes under the slab, in the near field and in the far field (Fig. 2-8).

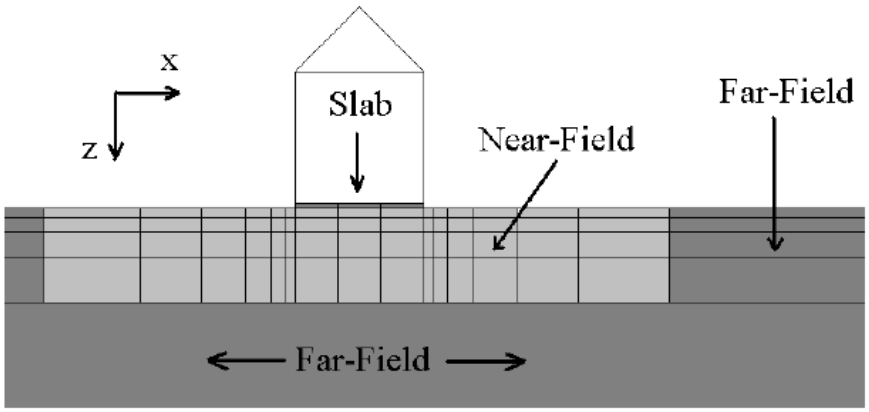

Fig. 2-8 Soil noding under and around the building

The noding starts at the edge of the slab with the smallest nodes (in order to precisely address the zone most exposed to the dynamic boundary conditions) and the size of the nods grows towards the centre of the floor. For this a Growth Factor is introduced. It can vary from 1.1 to 2 while the smallest nod size is usually between 0.01 m and 0.1 m. The combination of these values determines the calculation precision, but also the calculation time. For example, noding under the slab of 12×12 m can result in 144 nodes if the smallest node size is 0.1 m with the Growth Factor of 2. The number of nodes increases to 2 116 if the smallest node size is 0.02 m with the Growth factor of 1.2. The noding for both examples is illustrated in Fig. 2-9. Similar principle can be used when specifying nodes in the near field.

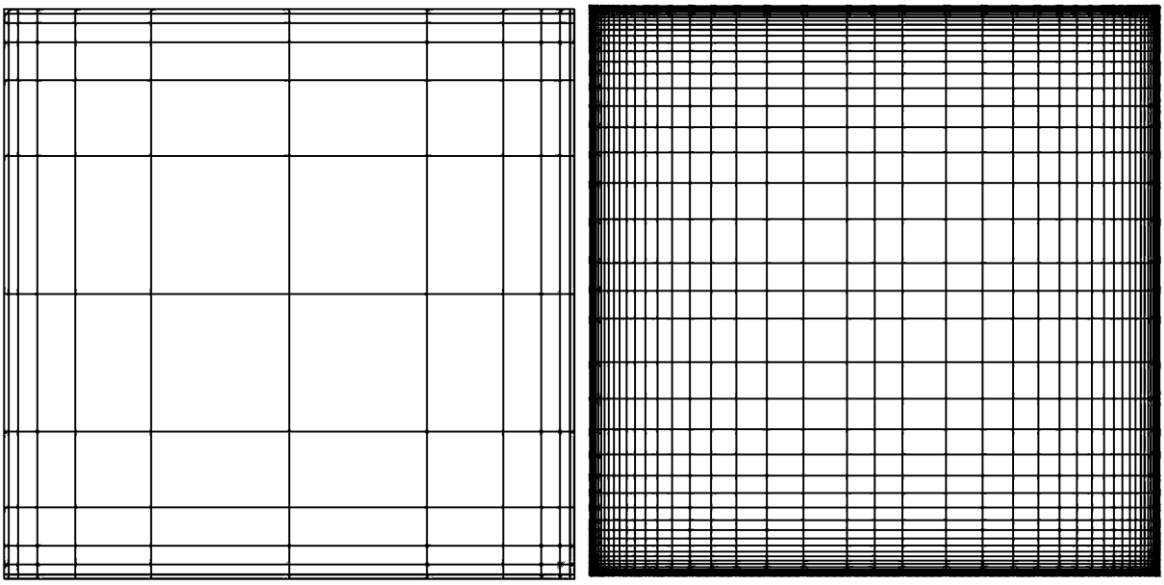

Fig. 2-9 Noding under a 12x12 m slab: minimal node size 0.1 m and growth factor 2 (left, 144 nodes); minimal node size 0.02 m and growth factor 1.2 (right, 2 116 nodes)

The near field is then surrounded by the far field. It can be either treated as an adiabatic boundary condition, or the previously mentioned Kasuda correlation can be used to determine the temperature of the far field at certain depth and time. In the later case the far field temperature is not affected by the temperature in the neighbouring near-field node.

For each node there are six partial heat fluxes from the neighbouring nodes/boundary conditions, which affect its temperature (five in some cases if the far-field is modelled as an adiabatic boundary condition. This leads to the solution of a large number of coupled differential equations for which an approximate analytical solver is used. Its advantage lies in the usability within the FORTRAN complier on which TRNSYS is built and also in the independency on the time step. Numerical solutions might under some circumstances expectable in a building simulation not converge. The analytical solution does not suffer from this limitation, but requires more time-consuming iterative calculation. Following equation describes the energy balance of each node:

$$m_{i,j,k} Cp_{soil} \frac{dT_{i,j,k}}{dt} = \sum \dot{Q}_{in} \tag{2-16}$$

where I,j,k are the special coordinates of each node; m is the mass of the individual node, T is its temperature and $\sum \dot{Q}_{in}$ is the sum of the six (five) individual heat fluxes into the node. In order to use the analytical solution, these equations are placed into the form:

$$\frac{dT}{dt} = aT + b \tag{2-17}$$

where a is a constant and b may be a function of time or the dependent variable. It can be assumed that b is constant over the timestep equal to its average value during the

timestep (while in fact in the case of soil nodes it is a function of the temperature of the adjacent nodes). Then the temperature for each node can be at any time calculated using:

$$T_{final} = \left(T_{initial} + \frac{\bar{b}}{a}\right) e^{a\Delta t} - \frac{\bar{b}}{a} \tag{2-18}$$

where:

$$\bar{b} = b(\bar{T}) \tag{2-19}$$

and:

$$\bar{T} = \frac{T_{final} + \frac{\bar{b}}{a}}{a\Delta t}\left(e^{a\Delta t} - 1\right) - \frac{\bar{b}}{a} \tag{2-20}$$

This approach allows for an iterative calculation until the temperatures converge. The assumption of constant b over the timestep is acceptable while using the typical timesteps in TRNSYS simulations being shorter than 1 hour.

Approach of Janssen and Christensen

BSim [44] is a PC tool for building simulations based on 1D heat transfer models. Janssen and Christensen [45] state, that BSim requires the translation of the originally 3D problem into a set of 1D processes. While dealing with this problem when simulating the hygrothermal behaviour of museum spaces in one specific case, they proposed an approach to achieve this translation.

Their simplification starts with adopting the Andeson's equivalent 2D geometry [41] as a reference for their final set of 1D models. This assumes that the 3D geometry can be translated into an equivalent 2D geometry based on the relation of the slab-on-grade's perimeter *P* and its area *A* resulting in the building's equivalent width *B′* in the 2D model.

$$B' = \frac{A}{P/2} \tag{2-21}$$

The heat flow through the slab-on-ground construction obtained from the 2D calculation (following the guidelines in EN ISO 13370 [46]) has to be multiplied by a half of the slab-on-ground's perimeter *P* to represent the actual heat flow from the building. Th authors have also assumed the symmetry of the heat flow about the model's vertical axis. They have therefore modelled only a half of the geometry using an adiabatic boundary condition along the building's vertical axis. This leads to the need of multiplying the results by the whole slab-on-ground's perimeter *p*.

Similar to the BASESIMP approach described previously, Janssen and Christensen use the superposition of different regimes. The regimes used here are as follows:

- Steady-state:
  - Interior temperature: constant at 1 °C;
  - Exterior temperature: constant at 0 °C;
- Transient interior:
  - Interior temperature: a harmonic variation with period 1 yr, average 0 °C, amplitude 1 °C, phase angle taken from measured interior temperatures;
  - Exterior temperature: constant at 0 °C;
- Transient exterior:
  - Interior temperature: constant at 0 °C;
  - Exterior temperature: a harmonic variation with period 1 yr, average 0 °C, amplitude 1 °C, phase angle taken from Danish DRY.

This approach is similar to the unit-temperature-excitation method used in BASECALC mentioned previously.

In order to determine the thickness of the soil layer they start with dimensioning it based on the equality of the 2D and 1D steady state heat flows. It generally means, that the steady-state heat flow has been calculated in the 2D simulation using the above stated boundary conditions. Then an equivalent 1D soil layer thickness has been calculated, which considering the soil thermal conductivity would result in the same steady-state heat flow. When verifying this design by calculating the heat flows in 2D and designed 1D model under the remaining two transient boundary conditions it has been found, that the results do not match sufficiently. Especially so under the transient exterior conditions.

The half of the characteristic width B' used for the model has therefore been discretised into 5 separate zones. Their width increased from the smallest one at the slab-on-grade's outer edge. For the building used in the study with the floorplan of 68×48.3 m and corresponding half of the equivalent width $B'/2$ = 14.1 m it meant the widths of 1m, 1m, 1m, 2m and 9.1 m. The reason for these values is not specified in literature. The soil thickness for these dimensions were then ranging from 0.9 m to 19.7 m respectively. The match of the results has been deemed sufficient and the floor has been modelled in BSim with 5 propositionally sized floor zones with the resulting soil layer thicknesses.

This approach seemingly requires two steps for each individual case: A reference 2D calculation and then individual fitting of surrogate soil block dimensions.

3. New surrogate model development

The scope of the model development within this thesis is to introduce a surrogate thermal model of a slab-on-ground floor. The results of the surrogate one-dimensional model should interpret the results of 3D calculations with a reasonable level of confidence. The work will be structured into two individual steps:

3D to 2D simplification: The model development starts with the assessment of usability of surrogate 2D models as a source of reference data for further simplifications. Obtaining reference data from 2D models can save time and computational power. But it may also introduce inaccuracy into the reference data sets.

Surrogate 1D model design: The further simplification then adopts the approach described by Janssen and Christensen [45] – to specify a set of soil elements under the modelled floor in order to match the reference results. The number of elements, however, is limited to two: one representing the building core zone and one to represent the building perimeter zone. Here, mathematical regression and fine-tuning are used.

The geometrical parameters of these surrogate elements are then their width and depth. Although it will have been shown the 3D to 2D simplification is not suitable for reference calculations, its geometrical interpretation will be used to fix the total width of the two proposed elements.

While individual steps are dependent on the results of previous work, for the reader's convenience they are structured into individual tasks. The respective parts are therefore divided into introduction describing why the step is relevant; hypothesis to be challenged; methods used; results and partial conclusion.

In the model development, different denominations of heat flux will be used based on the calculation method and corresponding physical dimension:

- q [W/m^2] is the specific heat flux and It is a result of 1D calculations
- L [W/m] is the thermal permeability of a 2D system. Within this thesis it is either obtained from
    - simulations on 2D models,
    - multiplication of the results obtained from 1D models by multiplying the results by corresponding element widths (L=q·width),
    - or by division of the results obtained from 3D models by specific length (L=Q^{3D}/length)
- Q^{1D} [W] is the total heat flux calculated from the results of 1D models (Q^{1D}=ΣL·length, where ΣL=Σ(q_i · width$_i$) for a set of partial 1D calculations)
- Q^{2D} [W] is the total heat flux calculated from the results of 2D models. Q^{2D}=L·length
- Q^{3D} [W] is the total heat flux resulting from 3D FEM simulations

3.1. 3D to 2D simplification

The use of 2D models as a reference for further simplification into a 1D model offers two potential benefits. Firstly, using 2D models for the reference data acquisition reduces the time and computational power requirements of reference simulations. Secondly, it offers a geometrical representation which can be more comprehensibly transformed into the desired 1D representation.

An intermediate 2D model for further simplifications has been used for example in previously mentioned approach by Jannsen and Christensen [45]. The use of 2D simulation results as a reference may, however, introduce an uncertainty of reference data. This uncertainty would then be transferred into the results of developed surrogate model and combined with the uncertainties stemming from the surrogate model development itself.

This chapter compares the results of 3D and 2D FEM models, evaluates the inaccuracy of 2D models and chooses the most suitable approach to reference data acquisition for further work. The findings of this part of the thesis have been published in [47].

Hypothesis

For 2D calculations of heat conduction through slab-on-ground floors, Anderson [41] has derived an equivalent floor dimension B' which is dependent on the slab area A [m^2] and the exposed perimeter P [m]:

$$B' = \frac{A}{P/2} \quad [\text{m}] \tag{3-1}$$

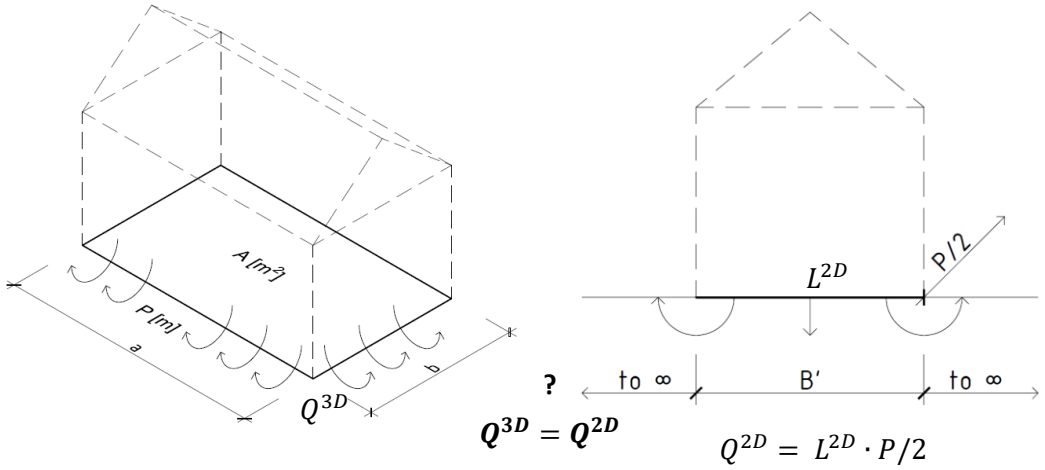

Fig. 3-1 Simple detached building geometry and parameters for Anderson's simplification (left) and the corresponding 2D model (right)

Fig. 3-1 shows a simple 3D geometry of a detached building with a slab-on-ground floor illustrating the parameters needed for Anderson's calculation and the resulting 2D geometry.

Simulations on 2D models based on this parameter are adopted in standards (EN ISO 13370 [46]) and are used in specific thermal simulation software such as HTflux [48]. It has also been accepted by Jannsen and Christensen [45] as a reference for further simplifications as mentioned before. Such models consider both defining properties of a building's floorplan and their geometry can be easily defined.

The premise of this simplification is, that the resulting heat fluxes obtained from simulations on these 2D models (in [W/m]) will sufficiently represent the real 3D heat fluxes when multiplied by the half of the floor's exposed perimeter ($P/2$):

$$Q^{3D} = Q^{2D} = L^{2D} \cdot P/2 \qquad [\mathrm{W}] \tag{3-2}$$

Anderson, however, published and tested this statement only for a steady thermal state. It is therefore essential to analyse its usability for simulations of a time-dependent annual heat transfer caused by periodic changes of interior and exterior temperatures.

Fig. 3-2 shows an approach to further reduce the 2D model. It uses the symmetry of the 2D model around its vertical axis. That allows to reduce the 2D model and reduce the computation time. This approach is commonly used in 2D simulations ([45], [48]). This step then changes the original equation into form:

$$Q^{3D} = Q^{2D} = L^{2D*} \cdot P \qquad [\mathrm{W}] \tag{3-3}$$

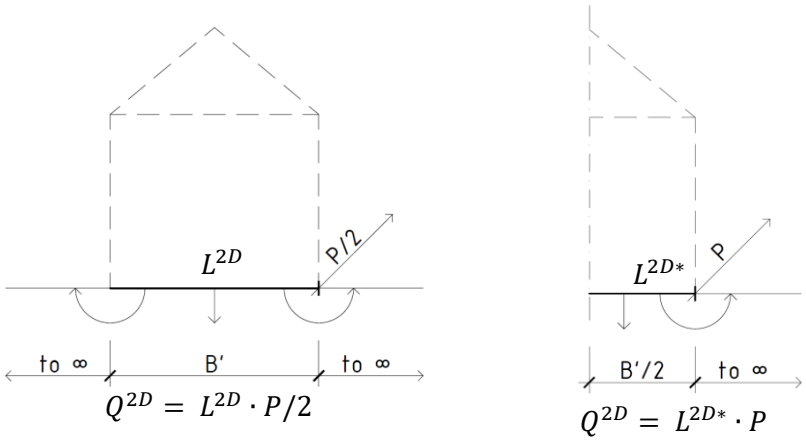

Fig. 3-2 Use of 2D model symmetry to further reduce the 2D model size

Method

Comparison: The hypothesis is tested by comparison of results obtained from simulations on 3D and 2D FEM models carried out using the Comsol Multiphysics software [49]. Heat fluxes through the inner surface of a slab-on-ground floor are compared. The hypothesis is tested for two scenarios: steady state boundary temperatures and annual harmonic boundary temperatures.

Geometry: Anderson's approach is based on treating the ground as a semi-infinite block (as it can be seen in Fig. 3-1). In numerical modelling (FEM, FDM,...) is this fact approached by using adiabatic (or other) boundary conditions at the edges of the soil block at sufficient distance. ČSN EN ISO 10211:2020 [2] sets this distances based on the building geometry. The distances suggested in the standard are used for both cases – 3D and 2D within this thesis to ensure comparability of results. The geometrical interpretation of the models used for comparison is shown in Fig. 3-3.

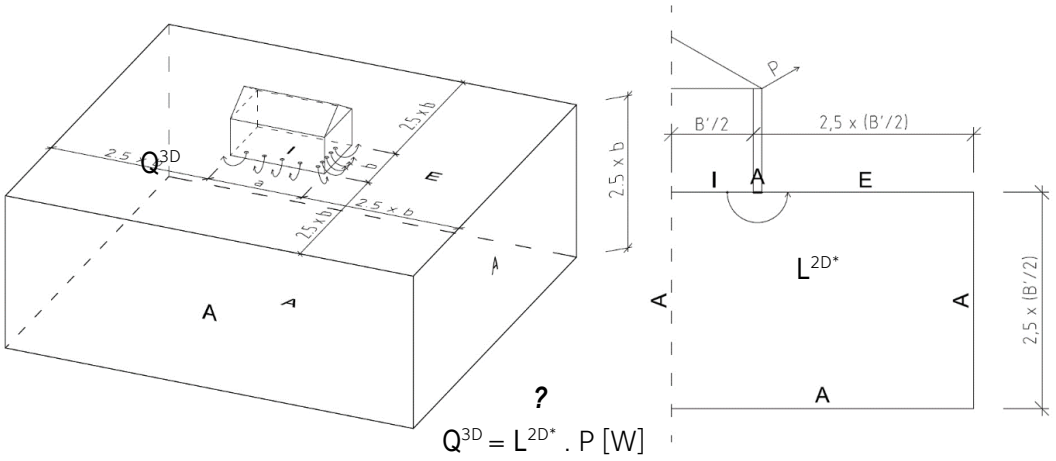

Fig. 3-3 3D (left) and 2D (right) model geometries for calculations: A – adiabatic boundary condition; I – interior boundary condition; E – exterior boundary condition

The standard dictates the introduction of an adiabatic boundary condition at the bottom of the ground domain. It can however also be assumed, that the boundary condition here is a constant temperature equal to the mean-annual outdoor temperature. This assumption is based on the temperature fluctuation damping by the mass of soil. Therefore, a comparison of the results for both deep-ground boundary conditions has been conducted. The results considering adiabatic and constant temperature boundary condition were practically identical. For further analysis, the suggested adiabatic boundary condition has been used.

Assumptions, fixed values and boundary conditions: The thermal accumulation in the floor slab itself has minimal effect in the annual perspective. Modelling of the slab due to its small thickness relatively to the soil domain would increase the number of finite elements in the three-dimensional calculation. These parameters have therefore been neglected. The slab has then been modelled only by its thermal resistance. This resistance has been merged with the surface resistance. The external walls have been considered by introducing an adiabatic boundary condition at their location.

Respecting the required U-values from the standard ČSN 73 0540-2:2011 [50] has the total thermal resistance on the interior boundary condition set according to equation:

$$R_{slab} = R_{si} + R_f = 3 \qquad [m^2.K/W] \qquad (3\text{-}4)$$

Thermal properties of the soil have been generally considered as the properties of an unknown soil according to ČSN EN ISO 13370:2019 [46] with the values λ = 2.0 W/(m.K); $\rho.c$ = 2.0 x 10^6 J/(m^3.K).

The use of a two-dimensional model as a suitable substitution for a three-dimensional model has been ctested using two sets of boundary conditions:

- steady state (for which was the concept of the equivalent floor dimension introduced in the first place) has been modelled for a constant temperature difference $\Delta\Theta$ = 37 °C.
- transient state used annual harmonic functions for internal and external temperature:

$$\theta_i = 4.\sin\left(\frac{2.\pi.t}{365} + \frac{3.19.\pi}{365}\right) + 20 \text{ [°C]} \quad (3\text{-}5)$$

$$\theta_e = 19.\sin\left(\frac{2.\pi.t}{365} + \frac{3.19.\pi}{365}\right) + 6 \text{ [°C]} \quad (3\text{-}6)$$

Metrics: The results obtained from two-dimensional models have been compared to the reference results from three-dimensional models by quantifying:

- relative error δ [%] for the steady-state cases

$$\delta = \left|\frac{Q^{2D} - Q^{3D}}{Q^{3D}}\right|.100 \quad [\%] \quad (3\text{-}7)$$

- Goodnes of Fit function *GoF* [%] for the transient cases

$$GoF = 100 \cdot \left(1 - \frac{\sqrt{\Sigma_{i=1}^{n}\left(Q_i^{3D} - Q_i^{2D}\right)^2}}{\sqrt{\Sigma_{i=1}^{n}\left(Q_i^{3D} - \overline{Q^{3D}}\right)^2}}\right) \quad [\%] \quad (3\text{-}8)$$

, where the lower index *i* specifies the order of a value within the annual course of the simulation and $\overline{Q^{3D}}$ is the mean-annual heat flux from a three-dimensional model.

Additionally, the total annual heat flux through the slab-on-ground construction has been investigated.

Set of samples: The Anderson's equation associates buildings with different floor areas with one common value of the equivalent building width *B'*. Because it is true for typical rectangular building floorplans, that the larger floor area also means larger exposed perimeter, are the intervals of the floor areas represented by the same *B'*-value rather small. In order to guarantee representative results, three-dimensional models have been constructed for multiple rectangular floor plans characterized by the same equivalent floor dimension *B'*. Also, a number of floor plans other than simple rectangles have been considered. The summary of simulated floor plans is shown in Fig. 3-4. It shows the 'simple' rectangular floor plans as well as the more complicated ones, which are further specified in Fig. 3-5 and Tab. 3-1. In Fig. 3-5 it can be seen, that the dispersion of floor

areas represented by the same equivalent floor dimension is relatively small – especially so for the smaller floor areas even when considering more complicated floor plans.

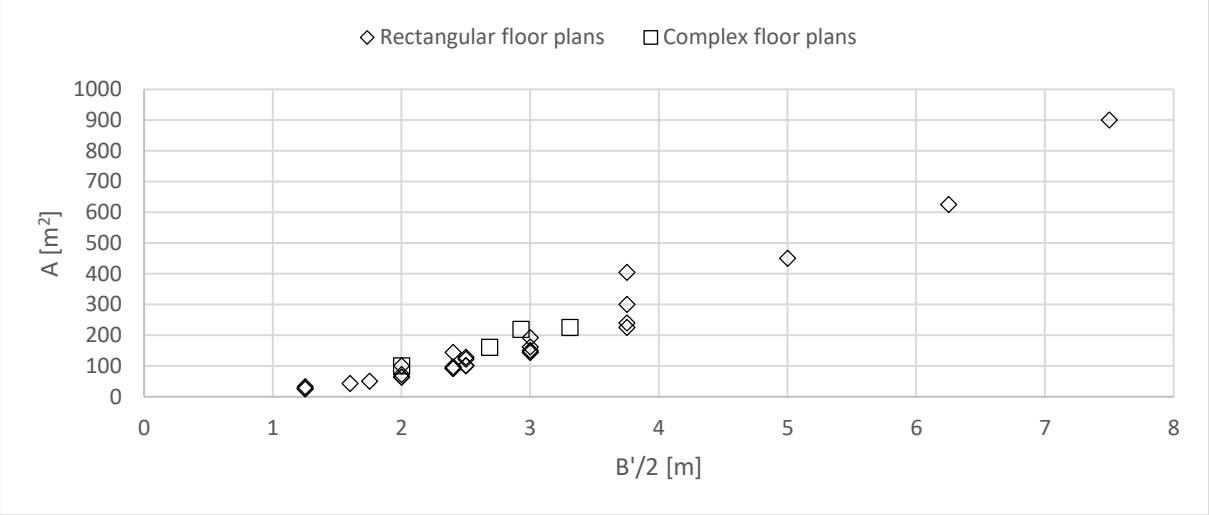

Fig. 3-4 Floor areas of considered floor plans related to their B'/2

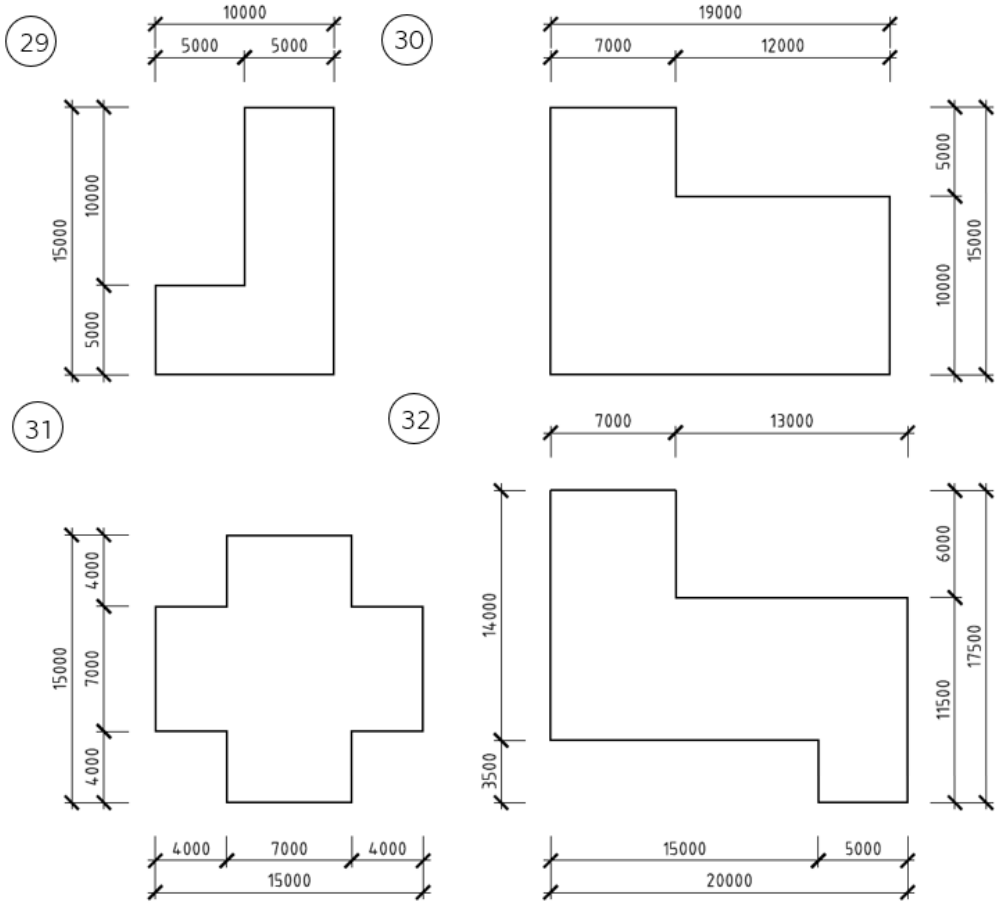

Fig. 3-5 Geometries of considered complex floor plans

Tab. 3-1 Characteristics of the complex floor plans

Floorplan number	A	P	B′
[-]	[m²]	[m]	[m]
29	100	50	4.00
30	225	68	6.62
31	161	60	5.37
32	219.5	75	5.85

Results

The comparison results for the steady-state scenario are shown in Tab. 3-2. It can be observed, that the relative error is for the 'simple' floor plans generally below 1 %. Also, the more complicated floor plans show low relative error. The cross-shaped floor plan (#31 in Fig. 3-5) is the one with the highest, yet still low, relative error of 2.66 %.

Tab. 3-2 Relative error of 2D vs. 3D calculation for selected floor plans under steady-state boundary temperatures

Nr.	a	b	A	P	B′	B′/2	Q^{3D}	L^{2D}	L^{2D}•P	δ
[-]	[m]	[m]	[m²]	[m]	[m]	[m]	[W]	[W/m]	[W]	[%]
1	5	5	25	20	2.50	1.25	249	12.3	247	0.85
2	6	10	60	32	3.75	1.88	553	17.2	552	0.24
3	8	12	96	40	4.80	2.40	835	20.9	837	0.16
4	8	8	64	32	4.00	2.00	581	18.1	581	0.09
5	9	9	81	36	4.50	2.25	716	19.9	717	0.11
6	10	15	150	50	6.00	3.00	1 228	24.7	1 234	0.48
7	12	20	240	64	7.50	3.75	1 836	28.9	1 849	0.67
29			100	50	4.00	2.00	906	18.2	908	0.16
30			225	68	6.62	3.31	1 789	26.5	1 801	0.68
31			161	60	5.37	2.68	1 329	22.7	1 364	2.66
32			220	75	5.85	2.93	1 808	24.3	1 819	0.58

The *GoF* values for the transient scenarios are shown in Fig. 3-6. Smaller floor plans show lower *GoF* values as the results obtained from two-dimensional models do not match the reference results as well. The dispersion of *GoF* values for the same B′/2 are relatively small and from a certain *B′*/2 value, the compliance rate stats to decrease.

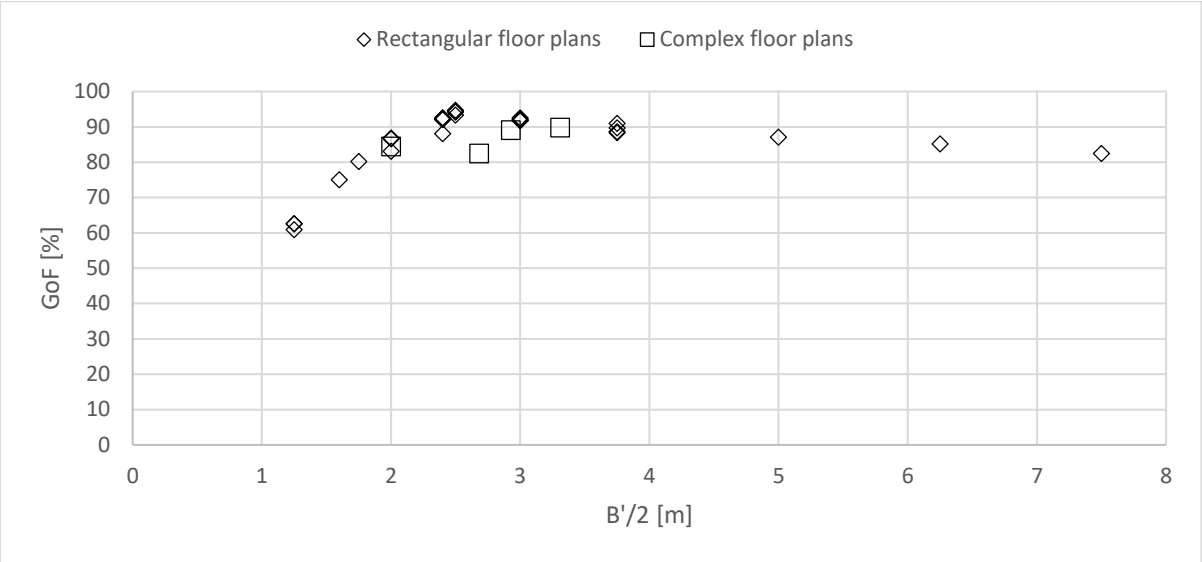

Fig. 3-6 GoF values of compared floor plan scenarios related to their B'/2

The ratio of total annual heat flux through the slab-on-ground (heat loss) obtained from the two-dimensional and three-dimensional models are shown in Fig. 3-7. The interval of these values is relatively small: <0.974; 1.022>. The values do not show any clear relation with the equivalent floor dimension.

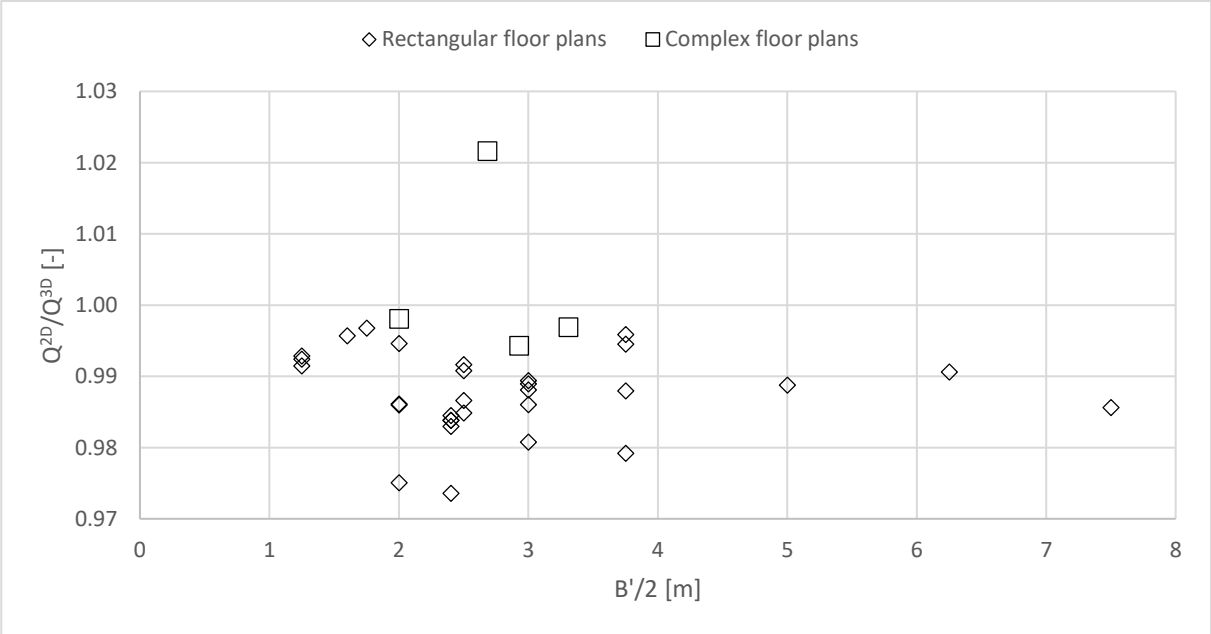

Fig. 3-7 Annual Q^{2D}/Q^{3D} ratio under harmonic boundary temperatures related to the floor plan's B'/2

The steady-state results indicate, that two-dimensional models constructed using the equivalent floor dimension introduced by Anderson yield very accurate results when compared with the reference three-dimensional models. This was expected as the concept has been introduced for the steady-state heat transfer through a slab-on-ground.

The transient harmonic boundary conditions introduce a larger discrepancy between the reference results and the results obtained from two-dimensional models. Smaller floors show lower values of *GoF*, but with the increasing floor size the values rise relatively fast. Approximately at $B'/2$ = 1.75 m (e.g. floor 7x7 m) the values of *GoF* reach 80 % and they do not decrease below this value for floor areas up to 900 m2 (30 x 30 m; *GoF* = 82.5 %)

The inaccuracy of two-dimensional models characterized by lower $B'/2$ may be attributed to the larger influence corners on the total heat flux. The inaccuracy of models of larger buildings may be at other hand attributed to the problematic FEM simulation of such a great ground domain in the chosen software. The large number of finite elements complicates the calculation due to the fact that the annual dynamic of harmonic boundary conditions effects the deeper parts of the ground domain with a significant delay. Therefore, while simulating larger domains, some instances occurred where even when simulating ten years of exposure to the boundary conditions, the system did not completely reach the quasi-stationary state. This could also be the cause of the decrease of *GoF* with growing value of B'/2>2,5 [m].

In retrospect, while completing this thesis, these obstacles might have been overcome by more sophisticated preconditioning of the system. The candidate, however, did not have the knowledge of how to implement such measures at the time of performing this analysis. These problems have been overcome in further model development.

Fig. 3-8 shows the comparison of the annual profile of the heat fluxes through a slab-on-ground with dimensions of 6.0 x 8.4 [m] ($B'/2$ = 1.75 m) obtained from a simulation on a three-dimensional and a two-dimensional model (after multiplication by the exposed perimeter *P*, see Fig. 3-3). The *GoF* value of 80.2 % may appear to be relatively low at the first sight. The graphical comparison of the results shown in Fig. 3-8 suggests, that it may be considered sufficient for general design praxis. It should be mentioned, that the soil properties in all models have been assumed constant and did not depend on temperature or moisture content. The degree of compliance described by the *GoF* value above 80 % can be considered after taking into account other sources of uncertainties as sufficient.

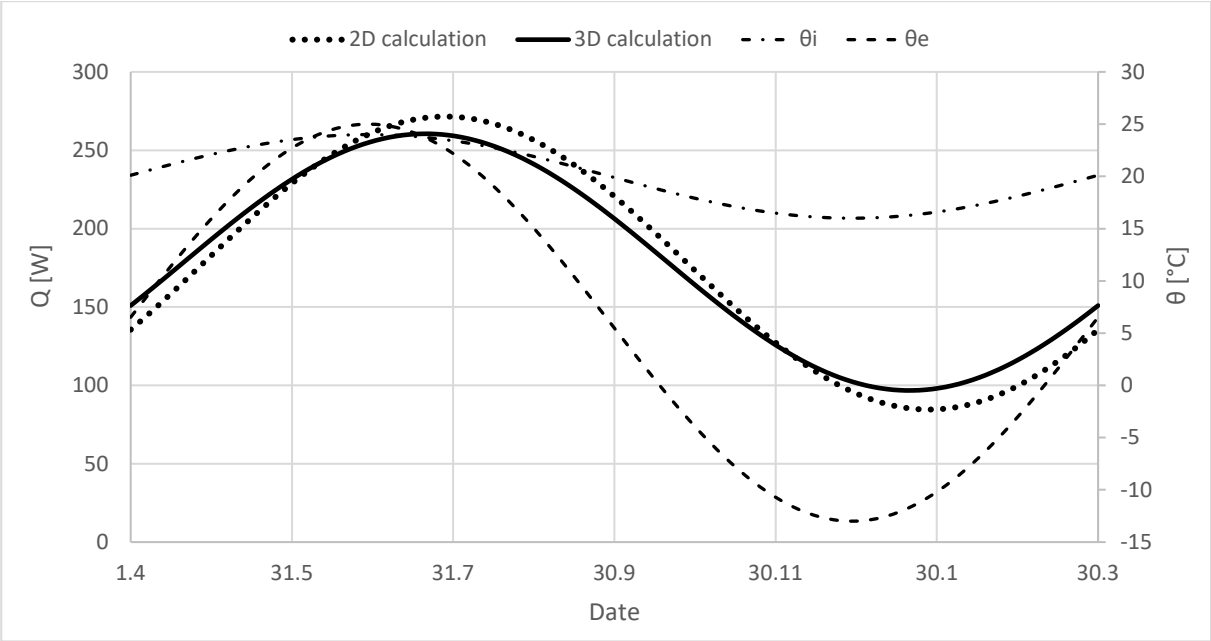

Fig. 3-8 Annual heat flux to the interior under harmonic boundary temperatures for the floor plan 6,0 [m] x 8,4 [m]; B'/2 = 1,75 [m]; GoF = 80,2 [%]

Partial conclusion

The results obtained from simulations on models with an adiabatic deep-ground boundary condition were identical with the results obtained from models with a constant deep-ground temperature. This may be caused by the sufficient depth of the boundary condition. Due to the gradual damping of the temperature amplitude is the amplitude at certain depth zero. No heat flux therefore occurs between the deep-ground boundary condition as the ground temperature near the boundary condition will be equal to the boundary temperature.

The results obtained from two-dimensional models constructed using the equivalent floor dimension (equation *(3-1)*) are for $B'/2 \geq 1{,}75$ [m] and considered soil properties comparable with the results from three-dimensional simulations. The deviation is comparable with deviations due to other model uncertainties.

While performing this study, a set of reference results (both from three-dimensional and two-dimensional models) has been created. The insight and data gained from this work has provided grounds for further model simplification described in following chapters. Based on the findings from this analysis, two-dimensional simulation results may be used as reference results for further simplifications in some instances.

The steady-state results show an excellent match between the reference results and the results from two-dimensional simulations. For the harmonic boundary conditions, it was found, that the simulation of smaller floor areas ($B' < 3.50$ m) on two-dimensional models is not as accurate when compared with the reference results.

It was found, that even though the two-dimensional simulation results are usable for building design, it would not be beneficial to use them as reference results for further simplification as this would inheritably increase the inaccuracy of the final models. It was however observed, that for different floor plans (with different floor areas) characterized by the same equivalent floor dimension B' applies (although L is itself a 2D characteristic, the superscript 3D is used to demonstrate it has been calculated from 3D calculation results):

$$\frac{Q^{3D}_{1\,(B'_1)}}{P_1} = \frac{Q^{3D}_{2(B'_1)}}{P_2} = \frac{Q^{3D}_{3(B'_1)}}{P_3} = \cdots = L^{3D*}_{(B'_1)} \tag{3-9}$$

This means, that even though the two-dimensional simulation results should not be used as the reference for further simplification, the reference results for a large sum of floor shapes can be obtained from one three-dimensional FEM model. Surrogate model geometry interpretation and parameters.

3.2. Geometry of the surrogate model: interpretation and parameters

This part of the thesis proposes a method to create a parametric set of 1D problems for slab-on-ground heat transfer calculations. The number of surrogate 1D problems is set to two – one representing the perimeter zone of the slab and one representing its core zone. It describes the logic of the proposed geometry interpretation; individual parameters and their function within the model. It then describes the process of their fine-tuning and the regression analysis in order to describe their dependency on the selected input parameters (slab-on-ground geometry and its thermal resistance).

The proposed model aims to calculate the heat transfer with sufficient accuracy when compared to reference calculations. Although the geometrical interpretation is based on a 2D geometry, the reference results are obtained from 3D FEM calculations. The reason for using 3D FEM calculations as a reference are the findings of the previous work – using 2D calculations for this purpose would inherently decrease the accuracy of the developed model.

To reduce the number of reference calculations, another finding of previous work is utilized. The transient heat fluxes through different slab-on-ground floors characterized by the same equivalent floor dimension can be mathematically reduced to the same equivalent 2D heat fluxes (thermal permeabilities) following the Anderson's [41] logic. This allows to calculate the reference results for multiple floor geometries using one 3D FEM model.

The 2D geometrical interpretation is used for practical reasons. Reducing the 3D geometry directly into a 1D interpretation would introduce two degrees of freedom to

substitute for. This would lead to numerous possible 1D interpretations for evaluation. Using the 2D geometrical interpretation, mathematically reducing the dimensionality of the 3D FEM results and setting the number of partial 1D problems to two, creates reasonable bounds for the model development. It gives us a straightforward way to identify parameters, their values and dependency on input parameters and to test the validity of the approach.

Hypothesis

The hypothesis to be tested is that it is possible to develop a surrogate model with geometry consisting of two one-dimensional elements for slab-on-ground floor heat transfer calculations. One element should represent the core zone of the floor 'neglecting' the boundary conditions dynamic. The other element should represent the floor perimeter zone exposed directly to the dynamic boundary temperatures.

The hypothesis further assumes, that the geometrical properties of these two elements can be described by functions considering two variables: floor geometry (characterized by the equivalent floor dimension B') and floor thermal resistance.

The envisioned geometrical interpretation of the developed surrogate model is show in Fig. 3-9. The left side shows the interpretation of heat transfer direction through the slab-on-ground in 2D. The right side then shows, how this interpretation will be translated into 1D problems – using surrogate soil elements of soil exposed to the boundary conditions.

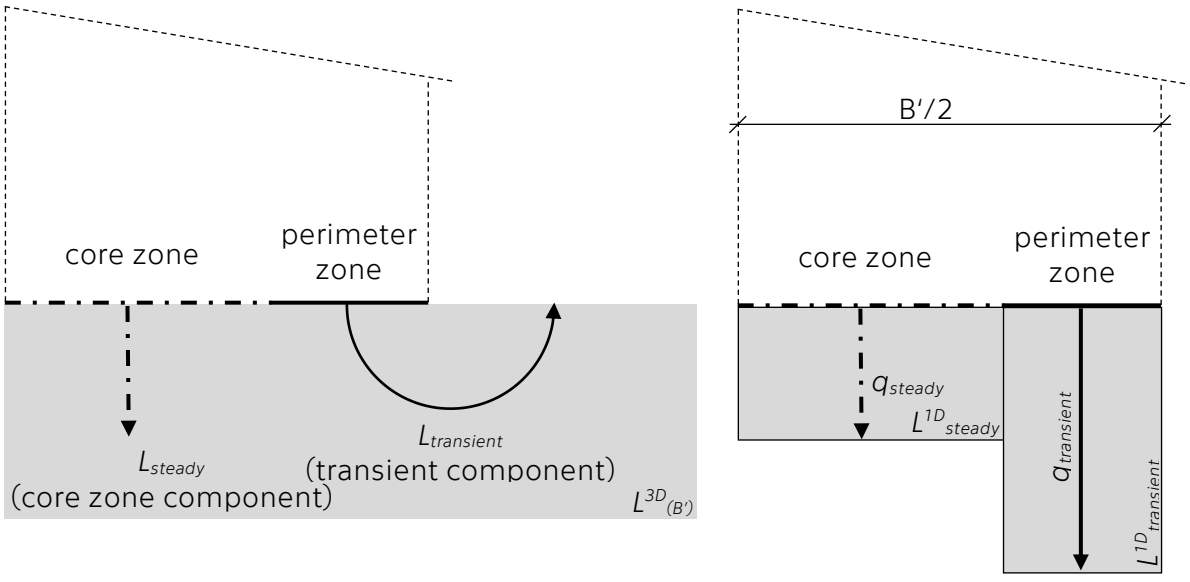

Fig. 3-9 Geometrical transition of the 2D geometrical representation to a set of 1D problems

This geometrical interpretation introduces three (four) geometrical properties of the model to be quantified (shown in Fig. 3-10):

- The length of the perimeter element ($l_{transient}$)
- The length of the core element (l_{steady})
- The width of the perimeter element (α)
- The width of the core element (when assuming a fixed overall width $B'/2$ and previously quantified α, this parameter becomes obsolete)

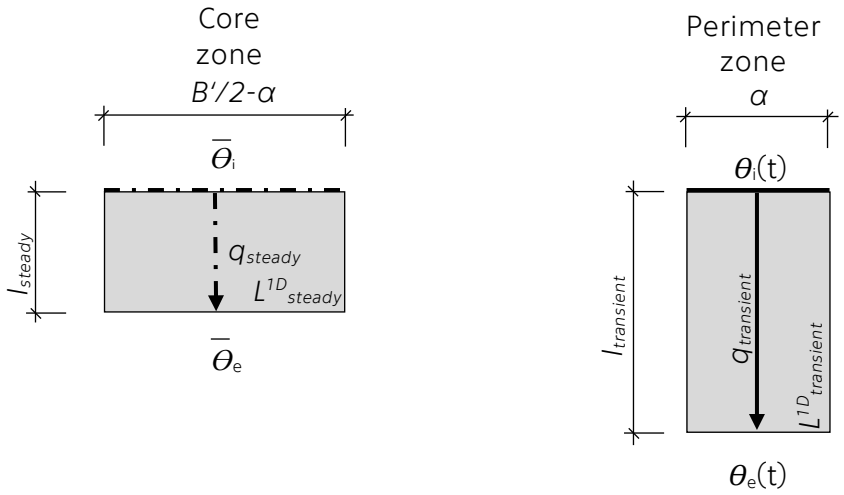

Fig. 3-10 Division into two separate 1D problems

This process of geometry reduction can be in regards to the heat transfer calculations summarized using:

$$\frac{Q_{ref}^{3D}}{P} = \; L_{ref}^{3D*} = L_{transient}^{1D} + L_{steady}^{1D} = q_{transient} \cdot \alpha + q_{steady} \cdot \left(\frac{B'}{2} - \alpha\right) \tag{3-10}$$

The example illustrated in Fig. 2-4 and Fig. 2-5 shows that the assumption of only steady heat transfer under the core zone is not physically correct. The hypothesis, however, assumes that all the dynamic behaviour of the entire system can be lumped into the perimeter zone's 1D representation.

Method

In essence, the development is a synthesis of two previously mentioned approaches. Janssen and Christensen [45] also used multiple one-dimensional elements to substitute the 3D soil domain. They, however, used this approach in one specific case without specifying any general guidelines for replicability in other cases. Their approach therefore requires a reference 2D simulation in order to determine the number of elements and their geometrical properties by fine-tuning. Also, all the elements are exposed to the dynamic boundary conditions in their approach. The BASESIMP [29] approach aimed to

create mathematical equations to determine three parts of the total heat transfer through the ground-coupled elements: $Q_{\text{below-grade,harmonic}}$ (t) (in the perimeter zone) and $Q_{\text{below-grade,average}}$ (t) (in the core zone) and $Q_{\text{above-grade}}$ (t). BASESIMP used the regression analysis of the 2D calculation results to determine the resulting equations.

When compared to these two influencing approaches, the developed model should have these advantages:

- When compared with Janssen and Christensen, the developed model will:
  - Always only use two soil elements.
  - Have the geometry of the soil elements defined based on floor geometry and thermal resistance without any additional reference 2D calculations.
- When compared with BASESIMP, the developed model will:
  - Have geometrical interpretation translatable into RC models allowing to work with finer than monthly timestep.
- When compared to both approaches, the developed model will:
  - Be based on more precise reference 3D FEM calculations instead of the 2D calculations.
  - Have lower number of variables and correlation coefficients.

It should be also noted, that BASESIMP has used a larger dataset for analysis also including other types of ground-coupled construction elements. It is therefore more versatile when used for building simulations.

Fine-tuning and its order: Fine-tuning is used to determine the values of the geometrical properties of the proposed model in each sample case. This means, that their values are adjusted in each case to match the results of 1D calculations and reference 3D FEM calculations. The 3D reference results have been translated into reference 2D results using the formula:

$$L_{ref}^{3D*} = \frac{Q_{ref}^{3D}}{P} \quad [\text{W.m}^{-1}] \tag{3-11}$$

When assuming annual harmonic boundary temperatures for the reference cases, the resulting heat fluxes through the slab-on-ground floors will also be harmonic. Therefore, the resulting heat flux course will in each case have three basic properties: average value, amplitude and time shift. The proposed elements in the developed model are, however, not both exposed to the harmonic boundary temperatures. This has a practical reason in the fine-tuning process. Having both elements exposed to the harmonic boundary conditions would lead to an infinite number of combinations of model parameter values making it impossible to find correlation equations in the following step – regression analysis.

The differentiation of boundary conditions between elements also differentiates the influence of the individual geometrical parameters on the resulting course of harmonic heat flux. This influence is summarized in Tab. 3-3. The element located at the edge of the building is exposed to transient boundary conditions. Its length $l_{TRANSIENT}$ influences the time shift of the heat flow (primary objective of the $l_{TRANSIENT}$ tuning), but also the amplitude and average value. Its width α has an influence on the heat flux amplitude (primary objective of the α tuning) and average value, but does not affect the time shift. The inner element is exposed only to yearly average temperatures and therefore finds itself in steady state. Its width is prescribed by the difference between $B'/2$ and α. Its length l_{STEADY} influences the yearly average value of the heat flow.

Tab. 3-3 *Influence of model parameters on the heat flux*

Model parameter	Affected quantity		
	Time shift	Amplitude	Average value
$l_{transient}$	✔	✔	✔
α	-	✔	✔
l_{steady}	-	-	✔

For the fine-tuning process, a set of reference 3D simulations was carried out first on floor plans with different characteristic length B'. Then, the parameter values of surrogate 1D model were tuned so that the results of the 1D model would correspond with reference results. Based on decreasing hierarchy of parameters described in Tab. 3-3 it was decided to proceed from the most to the least influential parameter. The tuning process for each parameter is described below in detail.

After the calculation of the reference 3D simulations and establishing $L^{3D^*}_{ref}$, the parameter $l_{TRANSIENT}$ was tuned. The tuning process was based on finding the time of maximum in reference heat flux course under given boundary conditions. The time of maximal specific heat flux $q_{TRANSIENT}$ computed on a partial surrogate 1D model (1D outer element if α = 1 m) under the same boundary conditions had to match the referential time. This ensures the match in time-shift of the resulting harmonic heat fluxes. This process is illustrated in a simplified manner in Fig. 3-11. For better visualisation, two vertical axes are used. The value of $l_{transient}$ within the 1D calculation has been repeatedly changed and the results were compared with the reference heat 3D FEM calculation results. Here it can be seen, how changing the $l_{transient}$ influences the resulting heat flux in its three parameters. In the shown case, the value of $l_{transient}$ will be approximately 3.5 m. In the actual fine-tuning within this thesis, the values of $l_{transient}$ have been tuned with the 1 cm precision.

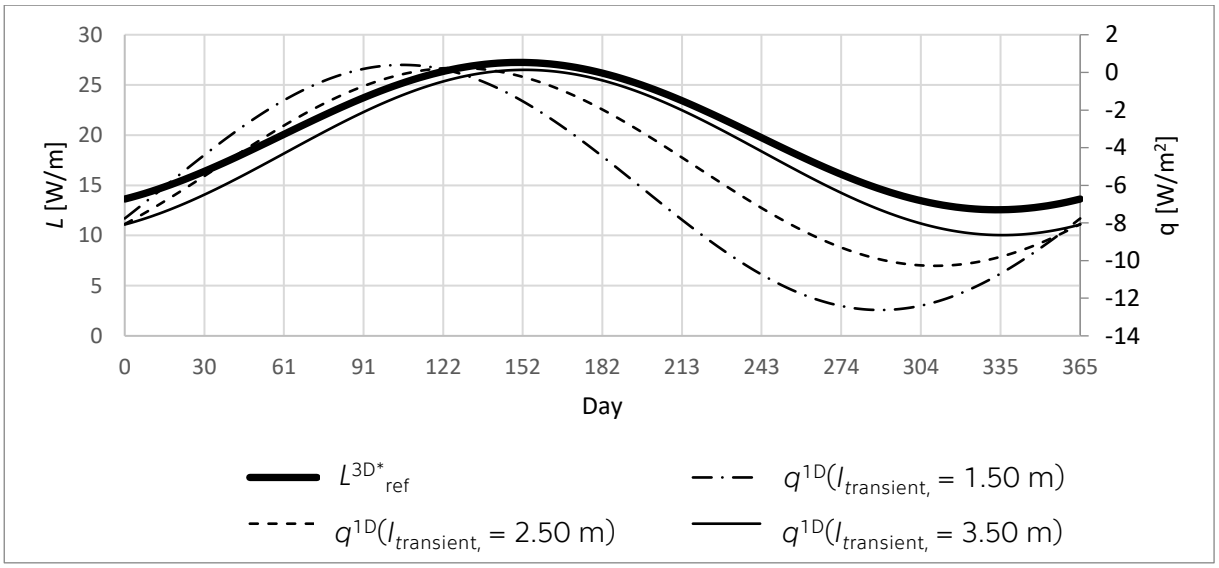

Fig. 3-11 Example of $l_{transient}$ fine-tuning process

After establishing the value of $l_{transient}$, the value of α has been investigated. The amplitude of heat flux course can be adjusted without affecting the time shift by multiplying it by the value of α. The value of α was found by dividing the differences between maximal and average heat flux from reference results and the results of 1D simulations using $l_{TRANSIENT}$ (Fig. 3-12).

$$\alpha = \frac{A(L^{3D}_{ref(t)})}{A(q_{transient(t)})} \quad [\text{m}] \tag{3-12}$$

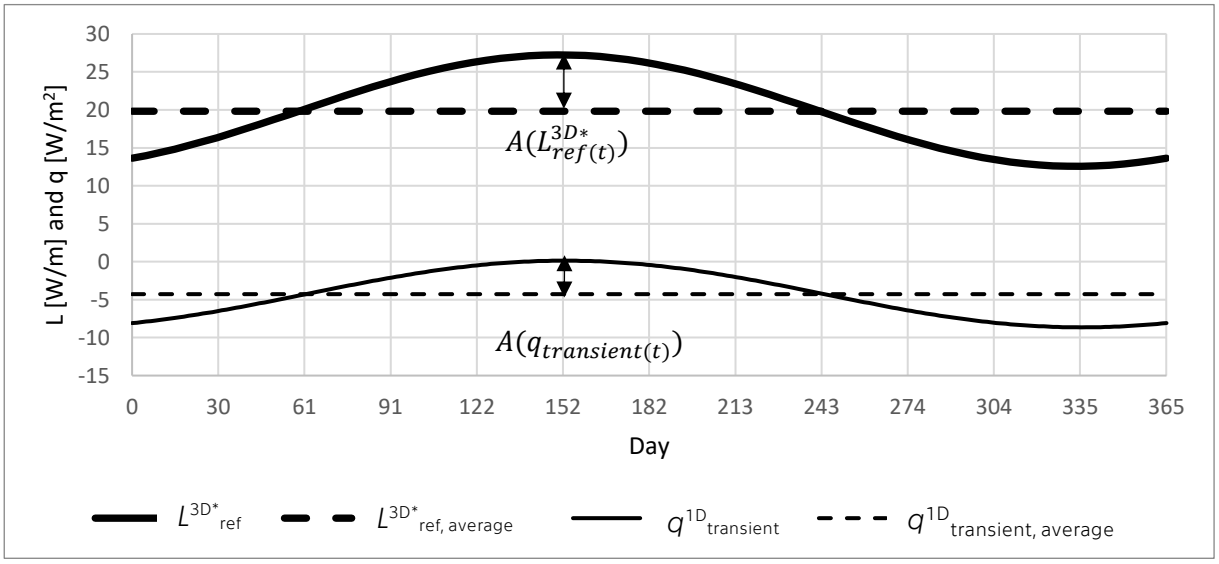

Fig. 3-12 Example of α fine-tuning after establishing $l_{transient}$

The comparison of the thermal permeability of the 1D perimeter-zone element is then calculated using the equation *(3-13)*. The comparison of the thermal reference thermal

permeability calculated on a 3D FEM model ($L^{3D^*}_{ref}$) and the resulting thermal permeability of the 1D perimeter-zone element ($L^{1D}_{transient}$) is shown in Fig. 3-13.

$$L^{1D}_{transient} = q_{transient} \cdot \alpha \quad [\text{W/m}] \tag{3-13}$$

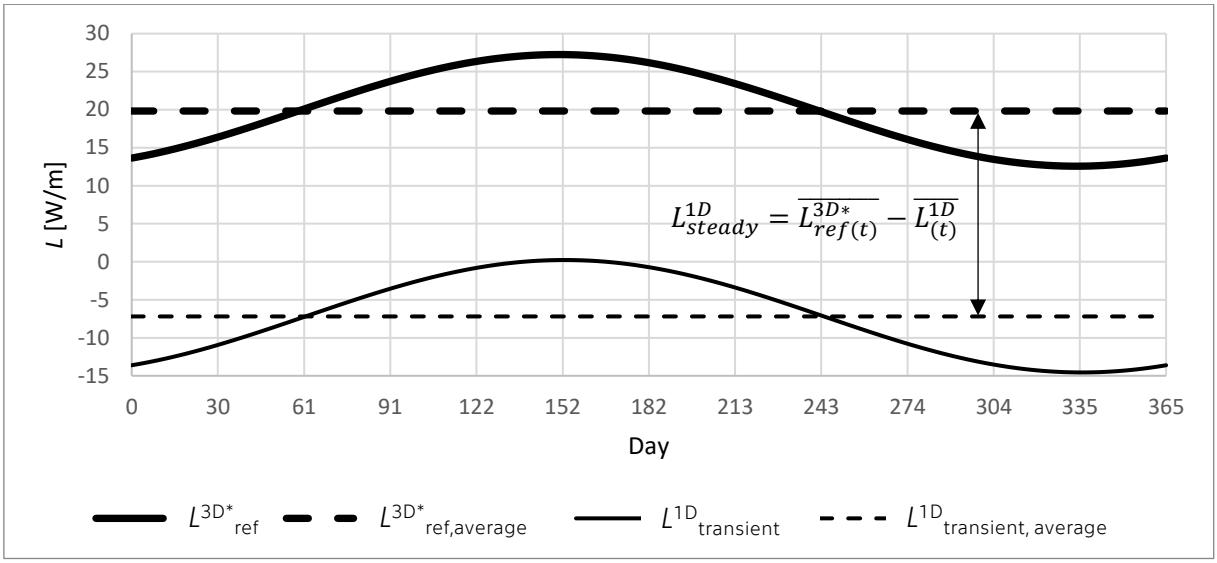

Fig. 3-13 Example of l_{steady} determination based of previously fixed $l_{transient}$ and α

The difference between the average values (and, at this point, also values at any given time) is a steady heat transfer to be covered by the core-zone element. The value of l_{steady} was a matter of solving a steady state heat transfer. Knowing the boundary temperatures, geometrical interpretation (width of the element $B'/2-\alpha$), the heat fluxes being compared and soil properties results into the equation:

$$l_{STEADY} = \left(\frac{\overline{\Delta T}.\left(\frac{B'}{2} - \alpha\right)}{\overline{L^{3D*}_{ref(t)}} - \overline{L^{1D}_{(t)}}} - R_{slab} \right).\lambda_{soil} \text{ [m]} \tag{3-14}$$

Regression analysis: The relationship between the dependent surrogate 1D model parameters and the slab-on-ground variables (geometry, thermal resistance) is investigated using regression analysis. For this purpose, the curve fitting application within the MATLAB software [52] has been used. The curve fitting procedure aims to construct a mathematical function that fits a set of data points the best.

In the case of function (y) dependent on one variable (x) ($y = f(x)$) the data set for curve fitting consists of the values of x and y obtained from an observation. The curve fitting than aims to solve the parameters of the function. If we aim to fit a linear function ($y = a \cdot x + b$) to a set of observed values of x and y, the curve fitting process searches for the values of parameters a and b for the function values to match the data set.

The process of curve fitting should, however, not only focus on perfect match of the constructed function and the given data points. It is also crucial to responsibly assume

the continuity of this match over the whole expected domain of the function's variables. The possible error can be mitigated by using sufficient number of data points.

After obtaining sufficient data sets, it is then necessary to determine the suitable mathematical equation type to be fitted. This can be achieved by examining the data set and estimating the function type (e.g. linear function, polynomial function, gaussian, trigonometric function, etc.) or testing different approaches and choosing the best fit. The MATLAB curve fitting application offers a wide range of preset regression models and includes an option to specify a custom equation form.

Assumptions, fixed values and boundary conditions: The floor was only considered by its thermal resistance. Thermal parameters of used soil were fixed to constant values of λ = 2.0 W/(m·K); $\rho \cdot c = 2.0 \times 10^6$ J/(m^{3}K) as recommended by the ISO 13370 standard [46] for unknown soil. Temperatures for the internal and external boundary conditions were set using the equations *(3-5)* and *(3-6)*.

Set of samples: Similar to the previous work and based on its partial conclusions, the reference results were obtained from a 3D FEM calculations using the COMSOL Multiphysics software [49] respecting the requirements of ISO 10211:2007 [2] for the soil block's dimensions as shown in Fig. 3-14. In order for the reference results to be usable within the proposed surrogate model geometry, the 3D reference results have been translated into reference 2D results using the equation *(3-11)*.

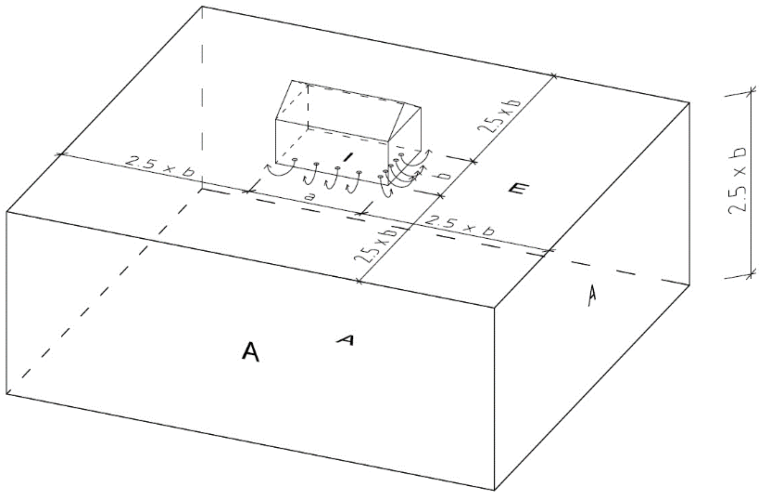

Fig. 3-14 Dimensions for the 3D FEM reference calculations

The reference floor plans are listed in Tab. 3-4. These have been chosen in order to include all the expected building sizes for the simulation of which the developed model could be used. Rectangular floor plans have been chosen for easier reference model setup. Based on the previous findings, these floor plans are for the purposes of the surrogate model development representative also for other geometries characterized by the same value

of *B′*. The number of floor plans has been found sufficient to ensure enough data points for the curve fitting procedure.

Tab. 3-4 Floor plans used to determine the 1D model parameters

	Floor dimensions		Area	Perimeter	Char. dimension
	a	b	A	P	B′
No.	[m]	[m]	[m²]	[m]	[m]
1	8	8	64	32	4
2	10	10	100	40	5
3	14	14	196	56	7
4	20	20	400	80	10
5	26	26	676	104	13
6	30	30	900	120	15

The reference calculations have been carried out on the models of all these floor plans considering the thermal resistance of the floor R_{slab} consisting of the slab's thermal resistance R_{slab} and the internal surface thermal resistance R_{si}, R_{slab} = {1; 2; 3; …; 8} [m².K.W⁻¹]. This set of thermal resistances should again ensure sufficient dataset for the curve fitting procedure and include all the presumed values to be expected when using the developed model.

Results

The results of the $l_{transient}$ fine-tuning are shown in Tab. 3-5 and Fig. 3-15. It shows the dependence of the tuned parameter on the building geometry (characterized by *B′*) for each considered case of thermal resistance of the floor construction. As the variance of the results caused by different values of R_{slab} for the same *B′* appears to be negligible, an average value has been calculated and used for the regression analysis. This way, the dependence of $l_{transient}$ on R_{slab} can be neglected and the curve fitting will only focus on of $l_{transient}$ on one variable – *B′*.

Tab. 3-5 Fine-tuned values of $l_{transient}$ [m] for the considered combinations of *B′* and R_{slab}

	R_{slab} [m²•K•W⁻¹]								avg.
B′ [m]	1	2	3	4	5	6	7	8	
4	3.86	3.80	3.72	3.74	3.72	3.71	3.70	3.69	3.74
5	4.27	4.24	4.14	4.20	4.16	4.17	4.17	4.16	4.19
7	4.93	4.93	4.84	4.91	4.86	4.90	4.89	4.89	4.89
10	5.67	5.69	5.56	5.68	5.60	5.67	5.67	5.66	5.65
13	6.18	6.21	6.09	6.21	6.14	6.20	6.20	6.20	6.18
15	6.44	6.48	6.34	6.48	6.42	6.47	6.47	6.47	6.45

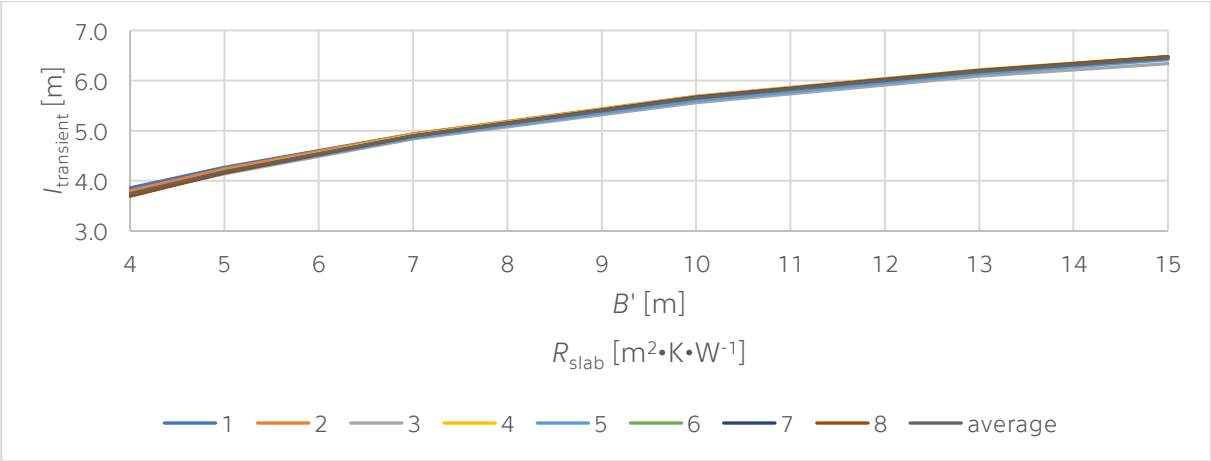

Fig. 3-15 Values of $l_{transient}$ yielded by fine-tuning

Fig. 3-16 shows the examples of possible curve-fitting using different types of function to fit the data set (average values of $l_{transient}$ from Tab. 3-5.). The types of function shown are: linear (left), power function (centre) and polynomial function of 2nd degree (right). Their mathematical notations are in equations *(3-15)*, *(3-16)* and *(3-17)* respectively. From the charts it can be seen, that the polynomial function fits the data set the best. Its confidence value is in this case $R^2 = 0.9992$, while the one of linear function is $R^2 = 0.9702$ and the one of power function is $R^2 = 0.9945$. It is possible, that other types of regression could provide even better fit to the considered datasets. The equation *(3-17)* has been, however, deemed sufficient for further work.

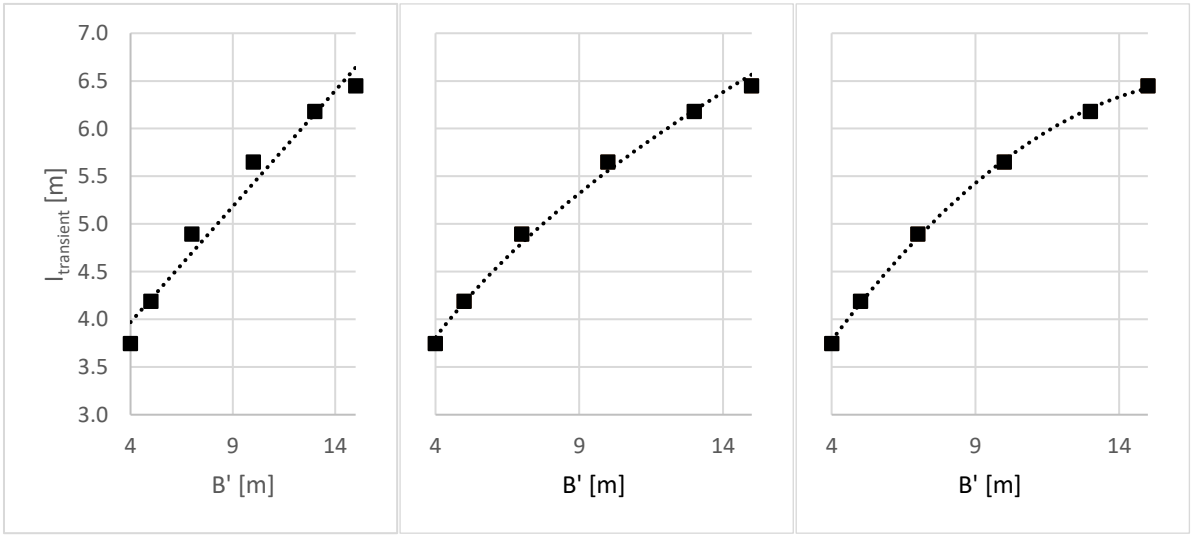

Fig. 3-16 Different curve fitting options for the $l_{transient}$: linear regression (left), power function (centre), polynomial function (right)

$$l_{transient} = 0.2427\ B' + 2.9994 \quad [\text{m}] \tag{3-15}$$

$$l_{transient} = 2.1555\ B'^{0.4113} \quad [\text{m}] \tag{3-16}$$

$$l_{transient} = -0.0149\ B'^{2} + 0.5234\ B' + 1.9219 \quad [\text{m}] \tag{3-17}$$

After establishing the dependence of the first model parameter $l_{transient}$ on the input parameters, the same dependence had to be established for the remaining two (α and l_{steady}). As the equation *(3-17)* does not match the original data set perfectly, the transient 1D calculations have been carried out using the newly calculated values of $l_{transient}$.

When comparing the results of reference 3D FEM calculations and the 1D transient calculations, it was possible to determine the desired values of α (Tab. 3-6 and Fig. 3-17) and l_{steady} in each reference case. In order to find the values of α, the comparison of amplitudes between the 3D and 1D calculation results has been used (equation *(3-12)*). Then it was possible to determine the values of l_{steady} by comparing the resulting average values of the heat fluxes using equation *(3-14)*.

Tab. 3-6 Fine-tuned values of α [m] for the considered combinations of B' and R_{slab}

	R_{slab} [m²•K•W⁻¹]							
B' [m]	1	2	3	4	5	6	7	8
4	1.25	1.13	1.08	1.05	1.04	1.03	1.02	1.01
5	1.39	1.26	1.21	1.19	1.17	1.16	1.15	1.15
7	1.69	1.56	1.51	1.48	1.47	1.45	1.45	1.44
10	2.25	2.13	2.08	2.06	2.04	2.03	2.02	2.02
13	2.91	2.80	2.75	2.73	2.72	2.71	2.70	2.70
15	3.37	3.27	3.23	3.20	3.19	3.18	3.17	3.17

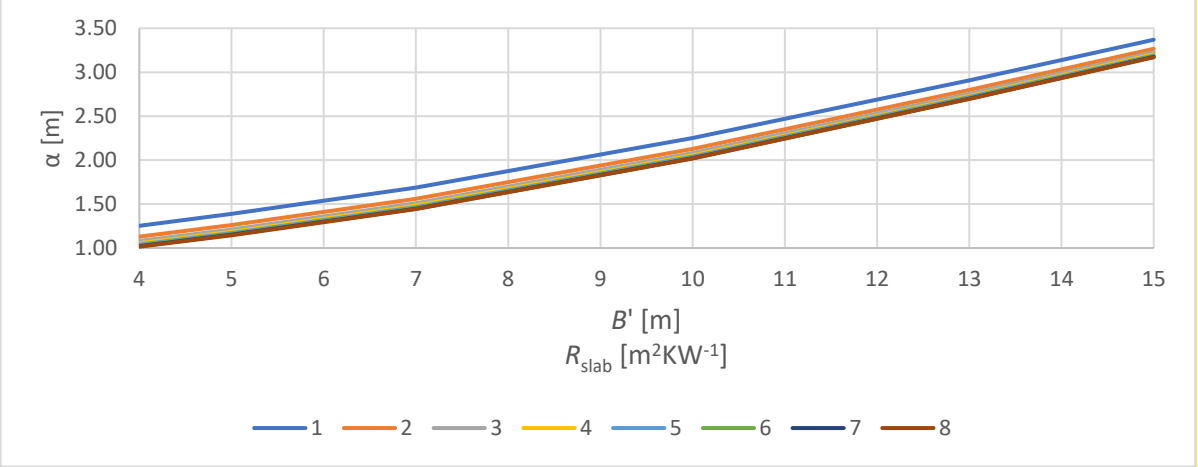

Fig. 3-17 Values of α yielded by fine-tuning

Values of parameter α depend on both R_{slab} and B'. Curve fitting process was used in two steps:

Finding a function for each curve shown in Fig. 3-17 describing the dependence of α on B' using the same type of function. It has been found, that this dependence can be best described by a function in form of:

$$\alpha = a \cdot \cos(B' \cdot b) + c \cdot \sin(B' \cdot b) + d \qquad (3\text{-}18)$$

, where parameters *a, b,c* and *d* will be a function of R_{slab}. After obtaining their numerical values for each case by the primary curve fitting, their dependence on R_{slab} has been analysed by secondary curve fitting. The secondary curve fitting has yielded the following mathematical functions:

$$a = -\frac{0.5199}{e^{0.7093 \cdot R_f}} - \frac{2.432}{e^{0.0007288 \cdot R_{slab}}} \tag{3-19}$$

$$b = 0.1004 - \frac{0.01405}{R_{slab}^{0.8722}} \tag{3-20}$$

$$c = 0.2053 + \frac{0.3041}{R_{slab}^{1.154}} \tag{3-21}$$

$$d = \frac{0.5214}{R_{slab}^{0.8604}} + 3.096 \tag{3-22}$$

By incorporating the parameter functions *(3-19)*, *(3-20)*, *(3-21)*, and *(3-22)* into the original equation *(3-18)*, the following notation for *α* has been obtained:

$$\alpha = \left(-\frac{0.5199}{e^{0.7093 \cdot R_f}} - \frac{2.432}{e^{0.0007288 \cdot R_{slab}}}\right) \cdot \cos\left(B' \cdot \left(0.1004 - \frac{0.01405}{R_{slab}^{0.8722}}\right)\right) + \left(0.2053 + \frac{0.3041}{R_{slab}^{1.154}}\right) \cdot \sin\left(B' \cdot \left(0.1004 - \frac{0.01405}{R_{slab}^{0.8722}}\right)\right) + \frac{0.5214}{R_{slab}^{0.8604}} + 3.096 \quad \text{[m]} \tag{3-23}$$

Tab. 3-7 shows the comparison of the desired values of *α* obtained using equation *(3-12)* and the values obtained using the proposed equation *(3-23)* (in brackets). When analysing these results, the value of R^2 of the proposed equation fitting the dataset is equal to 0.9999.

Tab. 3-7 Comparison of fine-tuned values of *α* [m] and values calculated using equation (3-23) (in brackets) for the considered combinations of *B′* and R_{slab}

	R_{slab} [m²•K•W⁻¹]							
B′ [m]	1	2	3	4	5	6	7	8
4	1.25 (1.26)	1.13 (1.13)	1.08 (1.1)	1.05 (1.08)	1.04 (1.07)	1.03 (1.05)	1.02 (1.04)	1.01 (1.04)
5	1.39 (1.39)	1.26 (1.25)	1.21 (1.22)	1.19 (1.2)	1.17 (1.19)	1.16 (1.18)	1.15 (1.17)	1.15 (1.16)
7	1.69 (1.7)	1.56 (1.56)	1.51 (1.52)	1.48 (1.5)	1.47 (1.49)	1.45 (1.48)	1.45 (1.47)	1.44 (1.46)
10	2.25 (2.26)	2.13 (2.12)	2.08 (2.09)	2.06 (2.07)	2.04 (2.06)	2.03 (2.05)	2.02 (2.04)	2.02 (2.03)
13	2.91 (2.91)	2.8 (2.79)	2.75 (2.75)	2.73 (2.73)	2.72 (2.72)	2.71 (2.71)	2.7 (2.71)	2.7 (2.7)
15	3.37 (3.38)	3.27 (3.26)	3.23 (3.23)	3.2 (3.21)	3.19 (3.19)	3.18 (3.19)	3.17 (3.18)	3.17 (3.18)

Tab. 3-8 and Fig. 3-18 show the desired values of l_{steady} calculated when comparing the reference 3D FEM results and proposed 1D models considering established $l_{transient}$ and α. These values have been calculated using the equation *(3-14)*. It can be seen, that the values are dependent on both input parameters B' and R_{slab}. Two-step curve fitting has been used to determine the regression function to describe this dependence (similar to the approach used for α).

Tab. 3-8 Fine-tuned values of l_{steady} [m] for the considered combinations of B' and R_{slab}

	R_{slab} [m²•K•W⁻¹]							
B' [m]	1	2	3	4	5	6	7	8
4	0.61	0.67	0.67	0.66	0.64	0.63	0.63	0.62
5	1.24	1.34	1.37	1.37	1.38	1.37	1.36	1.36
7	2.23	2.41	2.48	2.51	2.53	2.54	2.55	2.56
10	3.48	3.78	3.93	4.02	4.07	4.10	4.13	4.16
13	4.70	5.18	5.42	5.57	5.66	5.74	5.79	5.83
15	5.59	6.21	6.53	6.72	6.85	6.95	7.02	7.07

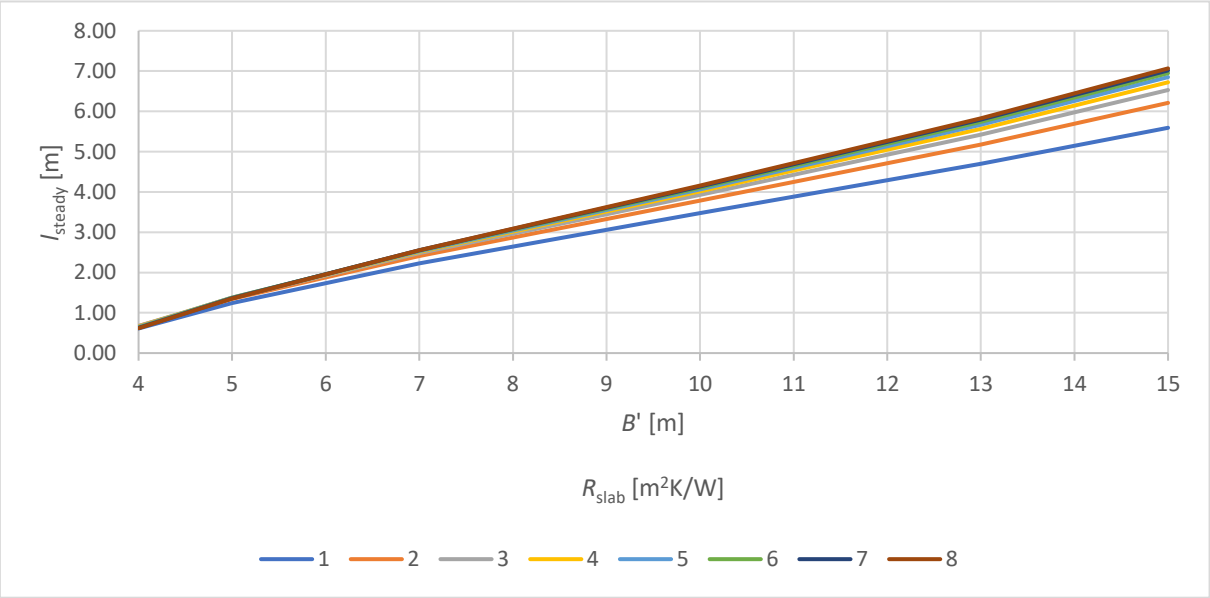

Fig. 3-18 Values of l_{steady} parameters yielded by fine-tuning

The regression process yielded the following mathematical notation for l_{steady}:

$$l_{\text{steady}} = B'.\left(0.5375.e^{0.008671\,.\,R_{slab}} - \frac{0.1791}{e^{0.5852.R_{slab}}}\right) + \frac{0.8109}{e^{0.2926.R_{slab}}} - 1.605.e^{0.003177.R_{slab}} \quad \text{[m]} \quad (3\text{-}24)$$

Tab. 3-9 shows the comparison of the desired values of l_{steady} obtained using equation *(3-14)* and the values obtained using the proposed equation *(3-24)(3-23)* (in brackets). When analysing these results, the value of R^2 of the proposed equation fitting the dataset is equal to 0.9987.

Tab. 3-9 Comparison of fine-tuned values of l_{steady} [m] and values calculated using equation (3-24) (in brackets) for the considered combinations of B' and R_{slab}

	R_{slab} [m²•K•W⁻¹]							
B' [m]	1	2	3	4	5	6	7	8
4	0.61 (0.76)	0.67 (0.8)	0.67 (0.8)	0.66 (0.78)	0.64 (0.76)	0.63 (0.75)	0.63 (0.74)	0.62 (0.73)
5	1.24 (1.21)	1.34 (1.29)	1.37 (1.32)	1.37 (1.32)	1.38 (1.31)	1.37 (1.31)	1.36 (1.3)	1.36 (1.3)
7	2.23 (2.09)	2.41 (2.27)	2.48 (2.36)	2.51 (2.4)	2.53 (2.42)	2.54 (2.43)	2.55 (2.44)	2.56 (2.45)
10	3.48 (3.42)	3.78 (3.75)	3.93 (3.92)	4.02 (4.02)	4.07 (4.07)	4.1 (4.11)	4.13 (4.14)	4.16 (4.18)
13	4.7 (4.74)	5.18 (5.22)	5.42 (5.48)	5.57 (5.63)	5.66 (5.73)	5.74 (5.79)	5.79 (5.85)	5.83 (5.9)
15	5.59 (5.63)	6.21 (6.2)	6.53 (6.52)	6.72 (6.71)	6.85 (6.83)	6.95 (6.92)	7.02 (6.98)	7.07 (7.05)

Partial conclusion

This part of work presented the development process of new surrogate model of heat transfer through insulated slab-on-ground floors. The developed model requires two input parameters: equivalent floor width describing the slab-on-ground geometry and the thermal resistance of the slab-on-ground construction. These parameters can be estimated by equations *(3-17)*,*(3-23)* and *(3-24)*. These equations have been found using regression analysis of values of these properties obtained from fine-tuning. The fine-tuning has been carried out using a set of reference 3D FEM calculations. The set of reference cases has been chosen to sufficiently represent the variety of input parameters combinations, which can be expected when using the model in the future. Further model verification and testing is needed in order to ensure its usability as a standalone tool, or within whole-building simulations.

The surrogate model was derived for one type of building foundation only – a simple slab-on-ground. This brings the question as to whether the model is applicable or can be further modified for other foundation types. These may include slabs on ground with vertical thermal insulation or partly underground floors. Geometry parameters of the proposed model depend on both building's geometry and the thermal resistance of the floor.

It is possible, that the dependence of model's geometrical parameters on the input parameters could have been described using different and simpler types of mathematical equations. The number of possible regression analysis solutions is practically infinite. The proposed equations have been considered to fit the fine-tuning results datasets with high confidence. One possible simplification can be assumed from Fig. 3-17 and Fig. 3-18. Here it can be seen that the parameter values considering $R_{slab} = \{1; 2\}$ [m² .K.W⁻¹] diverge from the other values the most. These values of thermal

resistance are not typically used nowadays in slab-on-ground floor constructions. Excluding these values from the fitting process would possibly eliminate R_{slab} from the final governing equations, or at least simplify the resulting equations.

4. New surrogate model verification and testing

The developed model and its usability have to be tested. The testing within this thesis consists of three approaches:

- First, the validity of the constructed mathematical equations for the model's geometrical properties is tested using the same approach as for their construction – comparing the results obtained on reference 3D models and on developed model. The basic input parameters (B' and R_{slab}) will be, however, different from the values used in model development. This will test, whether the data set for regression analysis used sufficient data over the expected domain of their values in simulations.
- Second, the results obtained from simulation on the developed model will be compared with results obtained by standardized calculation method for slab-on-ground floors in EN ISO 13370. The match of both calculations to reference 3D FEM calculations will be evaluated
- Third, the applicability of developed model in a whole-building simulation will be assessed. Thus far, the model development worked with the assumption of harmonic boundary temperatures. This means both boundary temperatures are known for the whole year beforehand. In building simulations, however, the internal boundary temperature is a solution of the zone thermal balance. It is therefore also dependant on the heat fluxes through the slab-on-ground. Furthermore, the external boundary temperature is not a harmonic function, when using hourly measured data. This will test how well the model handles the deviations of the external temperature from the harmonic assumption and the dependency of the internal boundary temperature on the model's own results.

4.1. Verification using input parameters not used for model development

The previous work has developed a surrogate 1D model of a slab-on-ground floor considering two input parameters – building geometry characterized by the equivalent floor dimension B', and the floor construction's thermal resistance R_{slab}. The geometrical interpretation of the model is shown in Fig. 4-2. The results of simulation on this model have to be multiplied by the slab-on-ground floor's exposed perimeter P in order to obtain the total heat flux through the construction:

$$Q^{1D} = P \ .(L^{1D}_{transient} + L^{1D}_{steady}) \quad \text{[W]} \quad (4\text{-}1)$$

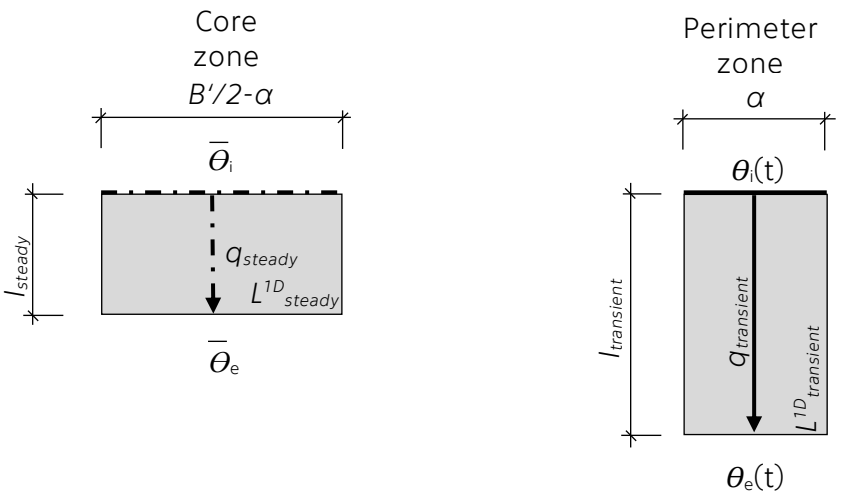

Fig. 4-1 Surrogate 1D model geometry and boundary conditions

Through the regression analysis it has been found, that the model's geometrical properties can be obtained using a set of governing equations *(3-17)*, *(3-23)* and *(3-24)*.

These equations have been obtained using data sets from simulations on a set of reference cases with defined input variables. The geometries used for the model development are characterized by the characteristic floor dimensions B' = {4; 5; 7; 10; 13; 15} [m] and floor construction's thermal resistance R_{slab} = {1; 2; 3; ...; 8} [m².K.W⁻¹].

This verification process aims to analyse the validity of the governing equations for other input parameters, than have been used in the development process. A set of four floor plans representing different type of buildings has been chosen. The reference 3D FEM simulations and the simulations using the developed model were carried out for this set of floor plans considering a set of slab thermal resistances R_{slab}. The boundary conditions are the same as in the development process.

Method

In order to test the resulting equations in different cases, a set of testing scenarios was selected- their geometrical description can be found in Tab. 4-1. The floor plans were all combined with R_{slab} = {1.5; 2.5; 3.5; ...; 7.5} [m².K.W⁻¹].

Tab. 4-1 Floor plans used for model validation

Residential building category	label	Floor plan dimensions				Floor plan characteristics	
		typical		chosen			
		a	b	a	b	A	B'
		[m]	[m]	[m]	[m]	[m2]	[m]
1-storey family house	F1	10 ÷ 17	10 ÷ 17	10	15	150	6.00
2-storey family house	F2	8 ÷ 13	8 ÷ 13	9	12	108	5.14
Small apartment building	A1	15 ÷ 36	10 ÷ 15	18	12	216	7.20
Large apartment building	A2	36 ÷ 100	10 ÷ 15	60	12	720	10.0

The same metrics as in 3.1 are used: Goodness of Fit (equation *(3-8)*) and Mean relative error (equation *(3-7)*).

Using the equations *(3-17)*, *(3-23)* and *(3-24)*, the values of geometrical parameters of the surrogate 1D models have been found. These are shown in Tab. 4-2.

Tab. 4-2 Geometrical parameters for the surrogate 1D models

	F1 (B′ = 6.00 m)			F2 (B′ = 5.14 m)			A1 (B′ = 7.20 m)			A2 (B′ = 10.0 m)		
R_{slab} [m².K.W⁻¹]	$l_{transient}$ [m]	α [m]	l_{steady} [m]	$l_{transient}$ [m]	α [m]	l_{steady} [m]	$l_{transient}$ [m]	α [m]	l_{steady} [m]	$l_{transient}$ [m]	α [m]	l_{steady} [m]
1.5	4.53	1.44	1.73	4.22	1.44	1.32	4.92	1.44	2.29	5.67	1.44	3.61
2.5	4.53	1.37	1.82	4.22	1.37	1.38	4.92	1.37	2.43	5.67	1.37	3.85
3.5	4.53	1.35	1.85	4.22	1.35	1.40	4.92	1.35	2.49	5.67	1.35	3.98
4.5	4.53	1.33	1.86	4.22	1.33	1.39	4.92	1.33	2.52	5.67	1.33	4.05
5.5	4.53	1.32	1.87	4.22	1.32	1.39	4.92	1.32	2.54	5.67	1.32	4.09
6.5	4.53	1.31	1.87	4.22	1.31	1.38	4.92	1.31	2.55	5.67	1.31	4.13
7.5	4.53	1.30	1.87	4.22	1.30	1.38	4.92	1.30	2.56	5.67	1.30	4.16

Results

Tab. 4-3 shows the validation results. All the values of *GoF* are above 95 %. The lowest value belongs to floor 60×12 m with R_{slab} = 1.5 [m².K.W⁻¹] (*GoF* = 95.6 %) and the best match was reached by floor 9×12 m with R_{slab} = 2.5 (*GoF* = 99.9 %). The *GoF* values are inversely proportional to the floor size if considering the same R_{slab}.

Tab. 4-3 Validation results

	GoF [%]				δ [%]			
R_{slab}	Floor plan				Floor plan			
[m²K/W]	F1	F2	A1	A2	F1	F2	A1	A2
1.5	99.6	99.8	99.7	95.6	2.01	1.41	1.62	4.75
2.5	99.9	99.9	99.9	95.8	1.03	0.69	0.76	4.21
3.5	99.9	99.9	99.9	96.0	0.68	0.72	0.65	3.79
4.5	99.9	99.9	99.9	96.4	0.74	0.91	0.71	3.43
5.5	99.8	99.8	99.9	96.7	0.83	1.05	0.77	3.16
6.5	99.8	99.7	99.8	96.9	0.92	1.17	0.81	2.96
7.5	99.8	99.7	99.8	97.1	0.98	1.27	0.87	2.81

Mean relative error exhibits no common increasing/decreasing tendencies relatively to the floor size, nor to the R_{slab}. Highest value shows the floor 60×12 m with R_{slab} = 1.5 [m².K.W⁻¹] (also worst *GoF* value, δ= 4.75 %). Lowest value belongs to the floor 18×12 m with R_{slab} = 2.5 [m².K.W⁻¹] (δ = 0.65 %). Comparison between reference results and results of proposed model for the floor 60×12 m with R_{slab}= 1.5 [m².K.W⁻¹] is shown in Fig. 4-2. This figure can be compared visually compared with a figure comparing the results of 3D FEM model and 2D FEM model from chapter 3.1 in Annex 3. There it can be seen, that the inaccuracy of both simplified models is comparable.

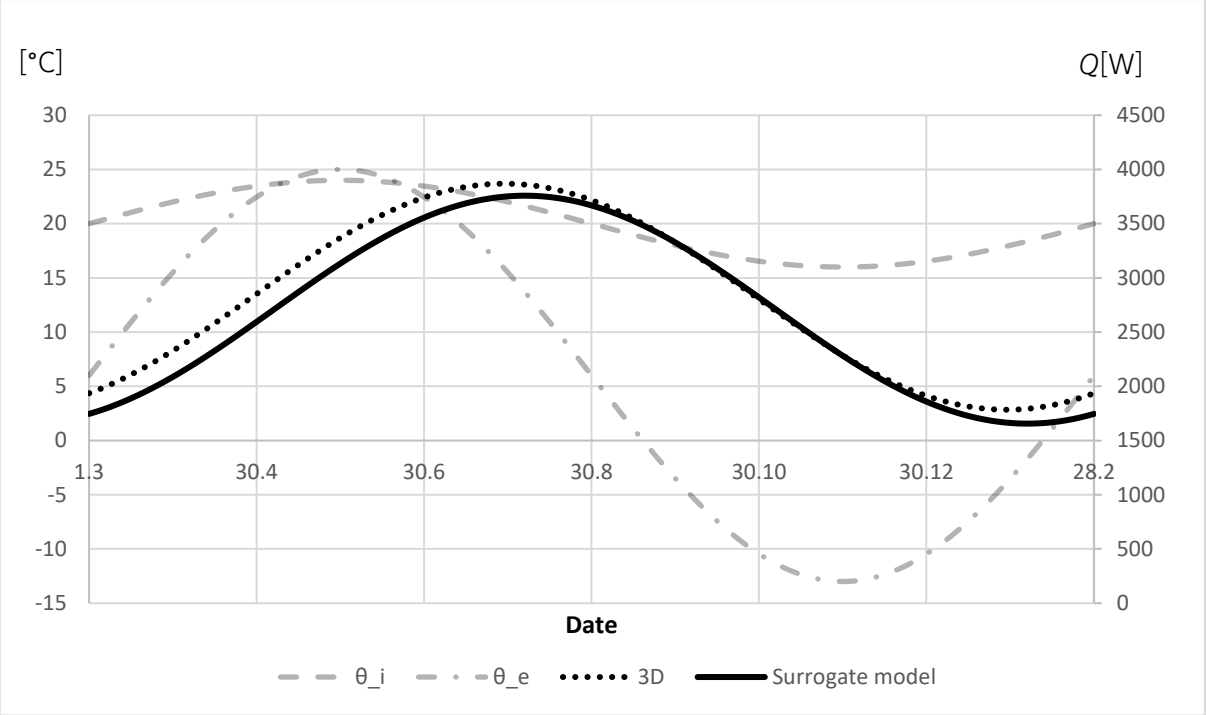

Fig. 4-2 Comparison of referential 3D results with surrogate model results for the worst case (A2; floor 60x12 m)

Partial conclusion

This part of the validation and testing has focused on comparison of the developed surrogate 1D model and the 3D FEM model behaviour considering the values of input parameters other than the ones used in the model development. The comparison has been carried out on 28 test cases considering different sizes of the buildings from a small family house to a large apartment building with different levels of slab-on-ground thermal insulation.

The comparison showed a good match between the results of the developed surrogate 1D model and reference 3D calculations. The worst value of *GoF* among the test cases was 95.6 % for a poorly insulated large apartment building. These results can be considered a good match for the technical praxis allowing the model to be used for fast preliminary calculations considering multiple design alternatives in the early stages of the building design process.

4.2. Comparison with EN ISO 13370

The standard 1D surrogate thermal model for slab-on-ground floors is included in the EN ISO 13370 [46]. This part of the thesis compares the results obtained from the standard 1D surrogate model and the surrogate 1D model developed within the thesis. The results of both models are also compared with reference 3D calculations.

EN ISO 13370 model structure

The EN ISO 13370 1D model consists of:

- Individual material layers of the slab-on-ground floor considering their thermal conductivity and thermal capacity,
- Soil layer (always 0.5 m) considering the soil's thermal conductivity and capacity, and
- Virtual layer only modelled as a thermal resistance.

The virtual layer ensures the correct value of the mean annual heat flux through the slab-on-ground system. Its thermal resistance is calculated from the slab-on-ground U-value. The standard specifies different U-value calculation methods, all of which also consider the equivalent floor dimension B' as an input.

The external boundary condition in this calculation is a virtual temperature Θ_v. Its purpose is to ensure the correct amplitude and phase shift of the heat flux. It can be calculated using a series of equations considering the course of the actual external temperature over time, building geometry and soil properties. In order to calculate the virtual temperature Θ_v, it is necessary to calculate the:

- Periodic penetration depth considering the soil thermal conductivity and capacity,
- Phase shift coefficients, and
- Periodic heat transfer coefficients.

The standard calculation focuses on monthly calculations. It mentions that this approach is applicable also for hourly simulations but does not specify how to obtain the fictive temperature values in this case.

Method

The results obtained from both simulation models have been compared with the reference 3D calculations. As the standard does not specify the process for hourly timestep calculations, the monthly-mean values of the heat losses have been compared. For this purpose, the standard EN ISO 13370 procedure has been conducted using MS Excel [53]. An Excel tool by Staněk [54] has been used as a reference for the calculations while compiling the workflow and for partial results check. The reference 3D results have been calculated using the COMSOL Multiphysics software [49] following the same principles as in previous parts of the thesis.

The geometry of the test cases, the boundary temperatures and the evaluation metrics are identical as in chapter 4.1. The total thermal resistance of the slab-on-ground construction has been limited to $R_{slab} = 3$ [m²K/W].

Apart from the MS Excel, the 1D calculations have also been conducted using COMSOL Multiphysics software using hourly timestep. The fictive boundary temperature profile in equation *(4-2)* has, however, been derived from the partial results of the MS Excel calculations. As the standard does not specify the workflow for obtaining the hourly fictive temperature, a harmonic function has been calculated from the monthly values. The monthly-average values of this function in hourly step had to match the monthly mean values calculated in compliance with the standard.

$$\theta_v = 10.27 \sin\left(\frac{\pi t}{365/2} + \frac{145.046\pi}{365/2}\right) + 6.013 \quad [°C] \tag{4-2}$$

Results

The comparison of results for the case of a 9×12 [m] is summarized in Tab. 4-4 and graphically visualized in Fig. 4-3. The same comparison for the other cases can be found in Annex 4.

The numerical values as well as the graphical interpretation suggest that the developed surrogate model yields more accurate results when compared to the standard calculation. This has been the case for all the considered test cases.

The EN ISO 13370 model results obtained from the MS Excel calculations and from the 1D FEM simulations have shown only negligible differences.

Tab. 4-4 Comparison of the mean heat fluxes through the slab-on-ground floors

	Q [W]		
month	Reference 3D model	ISO13370 model	Developed surrogate 1D model
January	306	260	304
February	369	370	368
March	428	472	428
April	474	539	470
May	484	554	481
Jun	458	511	457
July	404	423	406
August	337	313	339
September	274	210	277
October	231	143	236
November	221	129	227
December	245	172	252
PMRE [%]		17.5	1.0
GoF [%]		36.0	96.2

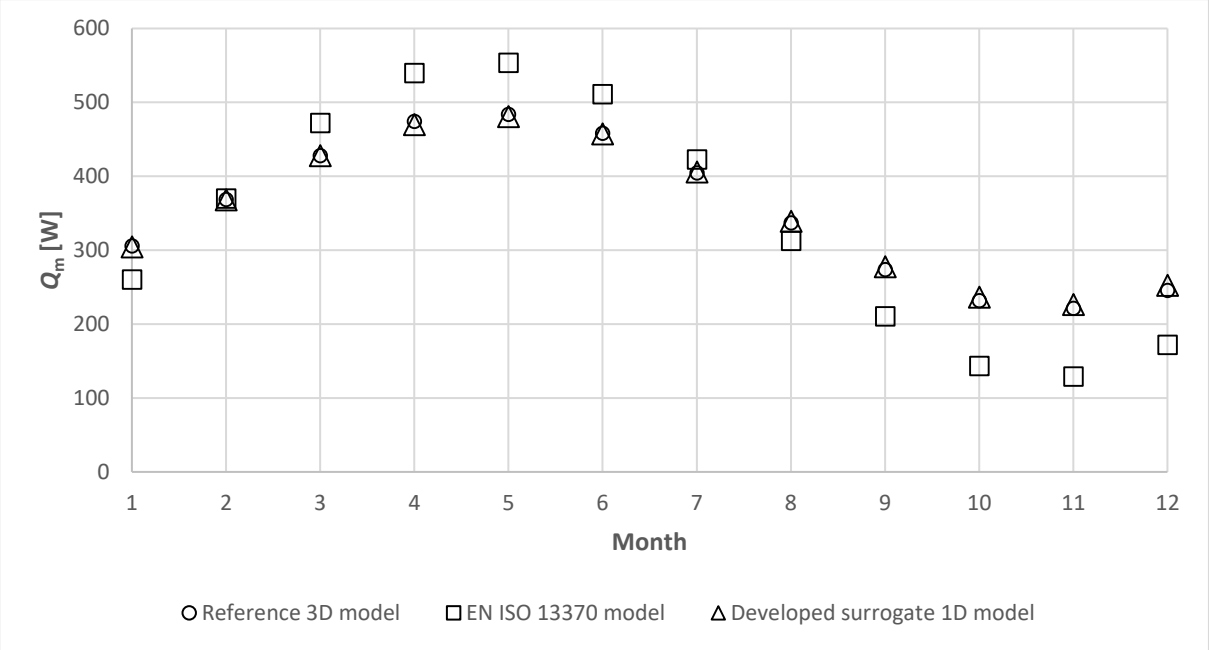

Fig. 4-3 Comparison of the mean heat fluxes through the slab-on-ground floors

Partial conclusion

A comparison of the results obtained from a reference 3D FEM calculation, a standard EN ISO 13370 1D calculation and a calculation on the developed surrogate 1D model has been carried out. The EN ISO 13370 calculation has been primarily designed to estimate the monthly mean heat fluxes through slab-on-ground floors. The monthly mean heat fluxes have therefore been calculated from the results of the 3D FEM calculations and the results from the developed surrogate 1D model respecting their timesteps.

The time shift of the resulting harmonic heat fluxes of both 1D calculations match the time shift of the results obtained from the reference 3D FEM simulation. When a calculation tool such as Staněk's MS Excel tool [54] is used, the standard EN ISO 13370 1D calculation is the matter of seconds. The calculation on the developed surrogate 1D model can take up to 9 minutes depending on the computation system, but the results match the reference results with much higher confidence.

The standard [46] mentions the 1D model can be used for hourly data. The workflow for this option is, however, not described in detail. The applicability of the developed surrogate 1D model using more dynamic hourly temperature data is the topic of the following work within this thesis.

4.3. Applicability in a whole-building simulation – heating energy demand

An analysis of applicability of the developed surrogate slab-on-ground floor model has been carried out. The purpose of this analysis was to test the interaction of the model with the thermal dynamics of the building when considering also other heat losses. The surrogate whole-building model is also simplified, and the modelling of other building components introduces additional inaccuracies. To mitigate the effect of these inaccuracies the models only consider heat conduction through the building envelope.

This analysis tests the applicability of the model considering two major changes in boundary conditions in comparison with the development and testing so far. The first major change is the external boundary temperature. So far, the external boundary temperature has been an annual harmonic function which was characteristic by very slow temperature changes over long increasing and decreasing periods. The external boundary condition used for this testing is the measured hourly dry bulb temperatures from Prague (Fig. 4-4). It is characteristic with larger diurnal temperature swings in both directions. It is desirable to determine how well can the surrogate model deal with this additional excitement of the boundary condition.

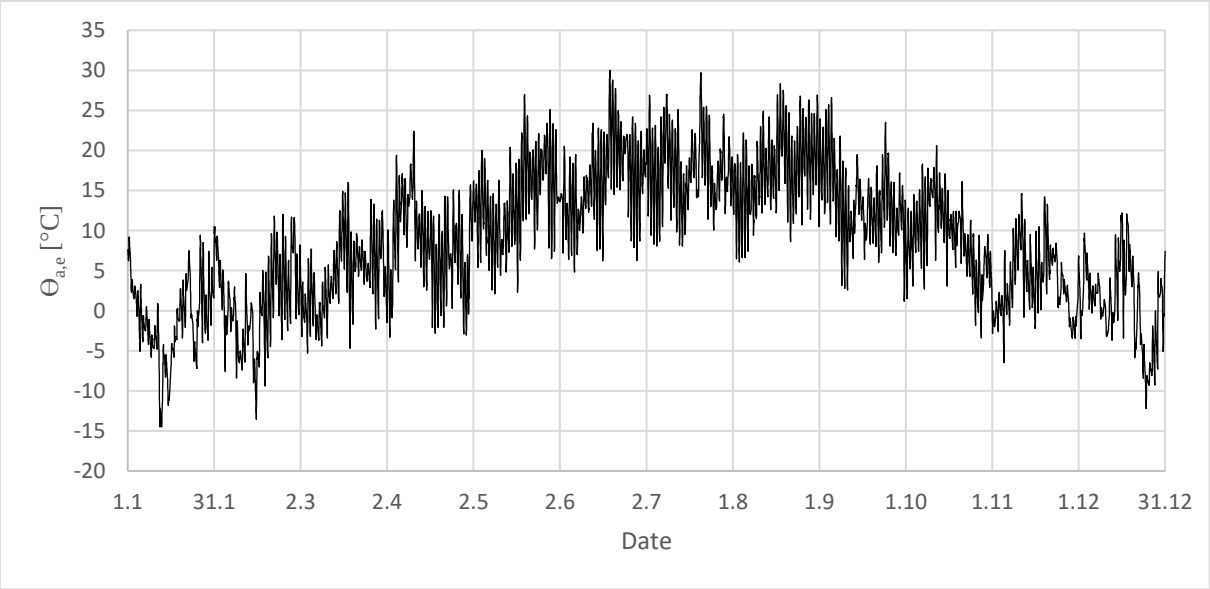

Fig. 4-4 External air temperature used in the simulation (hourly data)

The second major change is in indoor boundary temperature. So far, it has also been an annual harmonic function. This allowed for the assumption of the annual mean value necessary for the central zone component of the developed model. In the presented study, the indoor air temperature is a result of the heat balance equation, in which the heat flux through the slab-on-ground floor is an input. Although it would be possible to estimate the average indoor temperature, this analysis considers it unknown.

In this chapter, the reference 3D FEM model is described. As already mentioned, in order to eliminate inaccuracies of other components, some simplifications have been introduced – namely to eliminate the thermal bridges, which would be complicated to implement within the surrogate model of the building.

The analysis is divided into the construction and mutual verification of the models (without considering the ground-coupled heat flux) and the subsequent introduction of the ground-coupled problem into the models. This allows to quantify the effect of the developed slab-on-ground model on the simulation results. To evaluate these effects, the energy needed to maintain internal air temperature within specified range was observed.

Reference model

A 3D FEM model of a simple building has been constructed using COMSOL Multiphysics software [49]. The building dimensions were 7×7×2,5 [m]. A larger building would result into a massive ground domain when complying with the standard [2] suggestions leading to ineffective calculations with the computational possibilities available at the time of the analysis. The computation mesh of the constructed model for these dimensions consisted of more than 77 000 elements (see Fig. 4-5). This is caused by the meshing settings aiming to sufficiently describe the heat transfer within the walls and roof.

The model itself consists of four one-layer walls, roof, and the slab-on-ground. Geometrical parameters of these constructions are summarized in Tab. 4-5. Physical properties are then summarized in
Tab. 4-6. The slab-on-ground is only modelled as the total thermal resistance of $R_{slab} = 5$ m^{2}K/W while neglecting its mass. This value of thermal resistance corresponds to approximately 20 cm of EPS for thermal insulation and it is in compliance with the recommended value for passive buildings in the standard ČSN 73 0540-2:2011 [50].

Tab. 4-5 Geometrical parameters of the building components

Element	Amount [-]	d_1 [m]	d_2 [m]	d_3 [m]	V_{total} [m^3]
Wall	4	7	2.5	0.4	28.0
Roof	1	7	7	0.5	24.5
Zone 1	1	7	7	2.5	122.5
Slab-on-ground	1	7	7	-	-

Tab. 4-6 Physical properties of the building components

Element	c [J/(kg·K)]	λ [W/(m·K)]	ρ [kg/m^3]
Wall	1 000	0.1	1 800
Roof	1 500	0.08	1 000
Zone 1	1 000	5.0	29.67
Soil	1 000	2.0	2 000

The solar irradiance on individual surfaces or night radiation towards the sky has not been considered. The Zone 1 heat capacity also includes the capacity of eventual partition walls and furniture.

The reference model neglects the air convection inside the building. Instead, the air is modelled as a solid material with the constant equivalent thermal conductivity λ_{air} = 5 W/(m·K). The same assumption has been used by van Schijndel [55].

In order to eliminate the thermal bridges, the corners between the individual walls as well as between the walls and the roof are specially treated. In a horizontal section, the walls only connect in one point – the internal corner of the building. The rest of the corner, which would pose a thermal bridge, is then replaced with an adiabatic condition on the sides of the walls. The wall-roof corner is treated in a similar manner (in vertical section). Graphically is this solution shown in Fig. 4-6. The connection of the exterior walls to the ground domain is also modelled in a way that eliminates the heat transfer between these two elements. These adaptations allow us to assume only one-dimensional heat conduction in the individual above-ground components and therefore modelling them as one-dimensional in the surrogate model without additional inaccuracies.

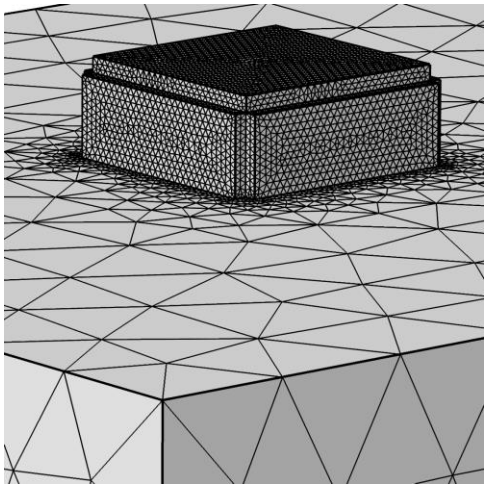

Fig. 4-5 Computational mesh in the reference 3D model

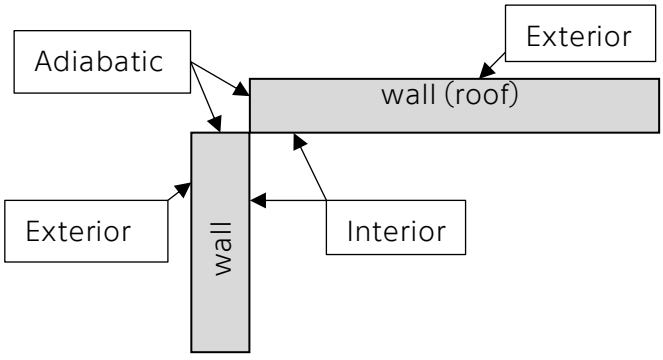

Fig. 4-6 Elimination of potential thermal bridges in the reference model

Surrogate 1D model

The surrogate 1D model has been constructed in the Matlab [52] and Simulink [56] environment as a system of thermal nodes with thermal capacity connected by thermal conductance. The previously described elimination of thermal bridges in the reference 3D FEM model allowed us to model each above-ground construction as a one-dimensional element. The walls have been discretized into 25 nodes, while the roof into 15.

The part of the model representing the slab-on-ground has been constructed using two parts representing the two soil elements (see Fig. 4-1). Their geometrical properties have been determined by the equations *(3-17)*, *(3-23)* and *(3-24)*, and their values are summarized in Fig. 4-3. These blocks are also modelled as one-dimensional elements. The transient-active block has been discretized into 15 nodes with thermal capacity. It is exposed to transient outdoor air temperature as a boundary condition. The steady-state block is only modelled as thermal conductivity/resistance. In the development of the model, the mean-annual temperature has been used as an outside boundary condition. In this instance, the outside boundary condition is time-dependent temperature – the moving average of the outdoor air temperature from the last 90 days. The RC scheme of the surrogate model is shown in Fig. 4-7 and the Simulink definition is shown in Fig. 4-9.

Tab. 4-7: Surrogate 1D model parameters

Parameter	Value [m]
B‘	3.50
B‘/2	1.75
lsteady	0.49
ltransient	3.57
α	1.01

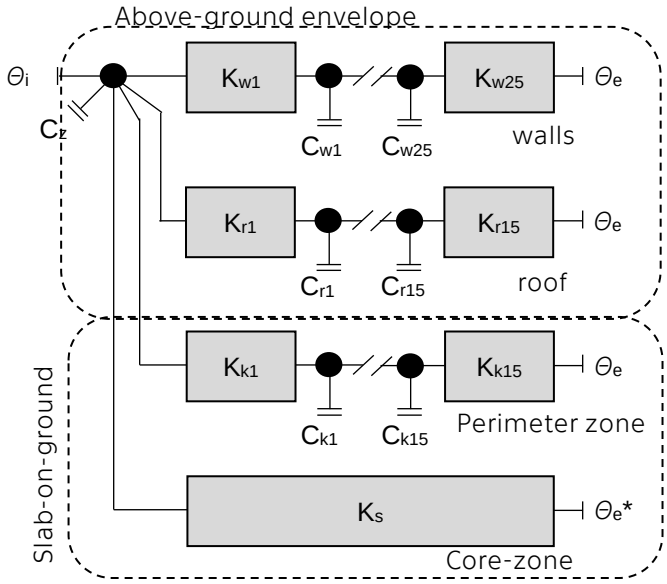

*Fig. 4-7 RC scheme of the surrogate building model Θ - temperature, K – thermal conductance C – node thermal capacity, z – thermal zone, w –wall, r – roof, subscripts: p – perimeter element, c – core element, I – interior, e – exterior, * - moving average temperature*

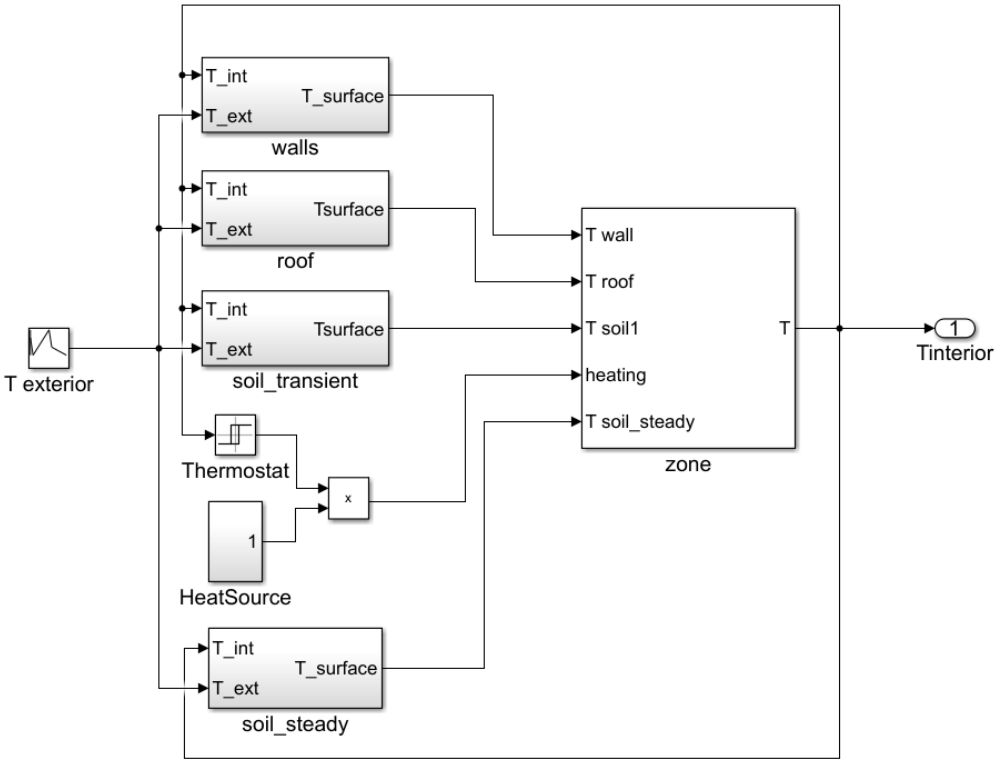

Fig. 4-8 Simulink definition of the model

Heat sources in the model

As the means for comparison the energy demand to maintain the internal air temperature within a specified range is used. This is achieved by addition of a heater and cooler, which are governed by a simple thermostat. Parameters of this simple HVAC system are summarized in Tab. 4-8.

In the reference 3D model, the whole volume of the zone is conditioned equally by the HVAC system. In the surrogate model it directly heats/cools the one zone node.

Tab. 4-8 Simple thermostat parameters

HVAC component	Turn on if:	Turn off if:	Power [W]
Cooling	$\Theta_i > 27$ °C	$\Theta_i < 24$ °C	1 000
Heating	$\Theta_i < 19$ °C	$\Theta_i > 23$ °C	1 500

Results – above ground envelope

When simulating the behaviour of the above-ground envelope without the effects of the slab-on-ground, the HVAC system only worked as a heater. Therefore, only the heating energy demand has been compared. The weekly sums are shown in Fig. 4-9, monthly sums then in Fig. 4-10. When comparing the weekly values, it can be observed that the surrogate model shows inaccuracies in both directions: in some weeks it overestimates the heating demand, in some it underestimates it. The largest difference is reported for the 23rd week (start of June), where the heating demand is overestimated when compared with the reference 3D model by 11.5 [kWh]. When considering the power of the heater of 1500 [W], it means 7.5 more heating hours. Monthly sums are rather well matched between the reference and surrogate model.

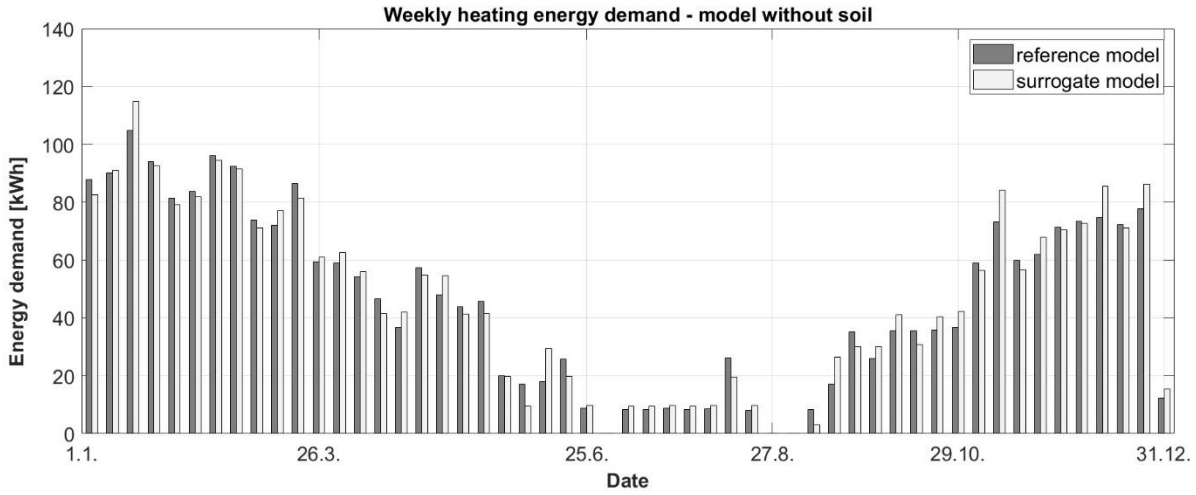

Fig. 4-9 Comparison of the results of reference and surrogate models of the -above-ground envelope – weekly energy demand

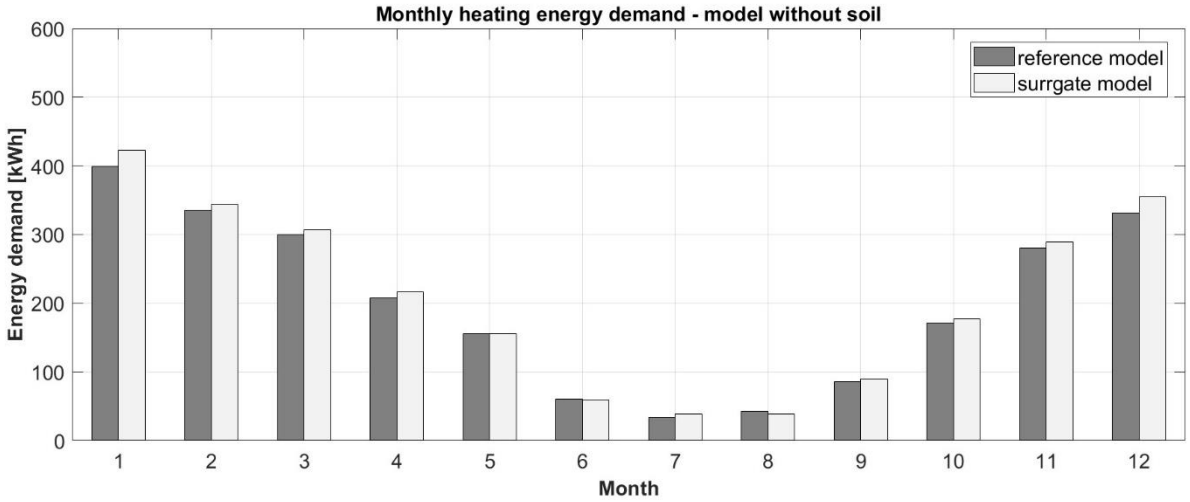

Fig. 4-10 Comparison of the results of reference and surrogate models of the -above-ground envelope – monthly energy demand

The surrogate model overestimates the annual heating demand by 87 [kWh] as shown in Tab. 4-9. Annual heating demands obtained from simulation on both, the reference 3D model and the surrogate model are comparable with the assumed demand simply calculated from the constructions' areas, their U-values and the mean-annual temperatures in the interior and exterior.

Tab. 4-9 Above – ground model: comparison of results

Model	Energy demand [kWh]
Reference model	2 406
Surrogate model	2 493
Surrogate model error	+87 (3.6 %)
Estimated demand	2 551

Results – whole building simulation

Neither in this case was the cooling system activated. Weekly heating energy demand comparison is shown in Fig. 4-11. Similarly to the above-ground only simulation, also here the surrogate model shows some inaccuracies. When comparing the individual values, these can be viewed as relatively well matching. Interesting might be the 34th week, where the reference model reports the need of 8 [kWh] and the surrogate model 0 [kWh]. In total numbers, the largest difference occurs in the 3rd week. The surrogate model underestimates the heating demand by 16 [kWh].

According to the monthly comparison shown in Fig. 4-12, the surrogate model slightly overestimates the energy demand in most of the months. The annual heating demand in the reference model is 3 123 [kWh], while in the surrogate 1D model it is 3 163 [kWh] resulting in the difference of 38.9 [kWh]. That represents an error of 1.25 [%] as shown in Tab. 4-10.

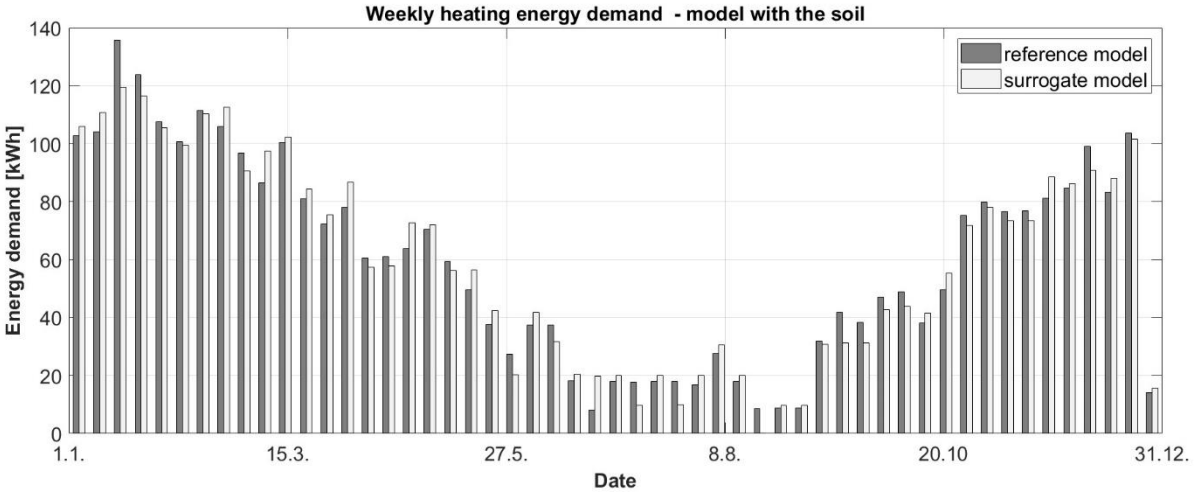

Fig. 4-11 Comparison of the results of reference and surrogate models of the whole building – weekly energy demand

Tab. 4-10 Whole building model: comparison of results

Model	Energy demand [kWh]
Reference model	3 123
Surrogate model	3 163
Surrogate model error	+38.9 (1.25 %)

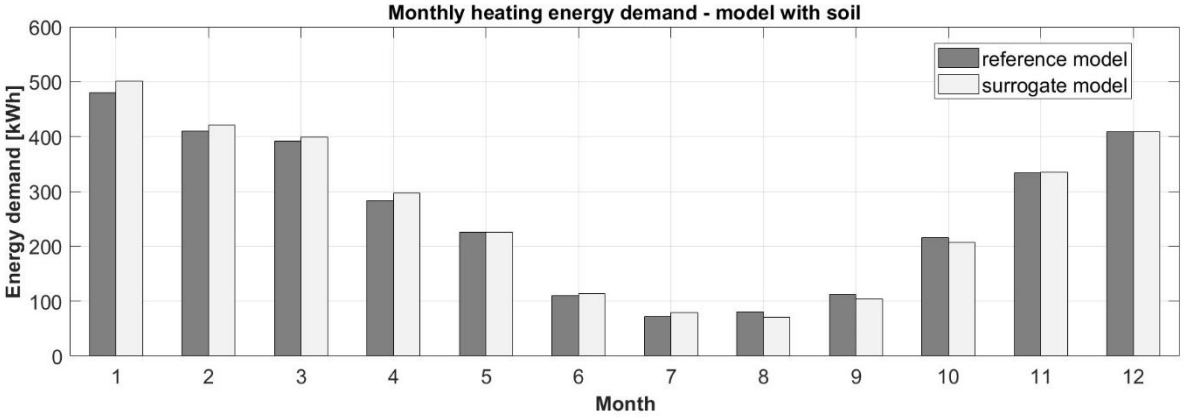

Fig. 4-12 Comparison of the results of reference and surrogate models of the whole building – monthly energy demand

Partial conclusion

The results suggest that the model of above-ground construction with a one-node internal zone itself introduces some inaccuracy, which is not significantly affected by the introduction of the surrogate slab-on-ground component.

Even the use of 3D FEM models brings a significant amount of uncertainties. It is practically impossible to model the whole building with all the physical phenomena occurring in reality. We believe, that when comparing the error of 20 % when comparing simulation results with an actual measurements of building performance can be

considered acceptable. From this point of view can the inaccuracy introduced by the developed surrogate slab-on-ground model considered as acceptable.

The results also show an overestimation of the monthly heating demands as well as the annual heating demands. As the error is in the direction of overestimation, it can be considered as an error on the safe side.

The source of this inaccuracy may for example be the fashion in which the availability of the heat source has been modelled. Furthermore, the tone has been discretized in the reference model into a number of finite elements, while it has only been modelled as one-node in the surrogate model. When the above-ground construction was observed in a free-float mode, the maximal temperature difference in the interior temperatures has been $\Delta T = 0.2$ [K].

The use of a surrogate model has brought a significant reduction in the computation time from 40 hours (3D FEM model) to 9 minutes (surrogate Matlab & Simulink model) on the same computer setup while maintaining an excellent accuracy. This accuracy is, however, respective to a significantly reduced reference case.

4.4. Applicability in a whole-building simulation – free-float temperatures

The developed model has performed with considerably good accuracy in the previous test. The test has, however, not fully analysed the problem caused by the internal air temperature being unknown. The temperature has been maintained in the specified range. Furthermore, the results suggest that the actual range of the internal air temperature has been even narrower than $\Theta_i \in <19;27>$ °C, as the heating occurred every week and the cooling element has never been triggered in the simulation. This would suggest, that the indoor air temperature has been maintained mostly between 19 °C and 23 °C preset for the heating element. This could be for the purposes of the calculation considered close to a constant temperature originally assumed in the model development for the core-zone element simulation. The free-float temperature test aims therefore to analyze the behavior of the whole-building system with Θ_i not maintained within any specified range.

Method

The same whole-building models (reference 3D FEM and surrogate 1D) are considered as in chapter 4.3 but without an active HVAC system. The simulations have been carried out using the outdoor air temperature while simulating 28 years from 1995 to 2022. This long range allows to analyze, whether the accuracy of the surrogate 1D model changes over time due to e.g. error accumulation. The hourly weather data has been obtained using the Oikolab service [57].

As the metrics for evaluation, the maximal annual difference and mean annual difference have been used. These have been applied for each calendar year while using a six-hour output timestep in simulations. The simulation outputs compared have been the interior air temperatures.

In order to assess the best approach to the internal boundary condition for the core-zone element in this kind of simulations, it has been considered in variants:

- Immediate internal air temperature,
- Moving average of the last:
  - 15 days,
  - 30 days,
  - 60 days,
  - 90 days,
  - 120 days,
  - 150 days,
  - 365 days.

Results

Figures Fig. 4-13 - Fig. 4-20 show the comparison of the free-float indoor air temperatures from the 3D FEM model and surrogate 1D model for the year 2005. Each figure shows this comparison for the selected variant of indoor boundary condition for the core-zone element..

It can be seen, that the 'worst performing' cases are the ones treating the indoor boundary temperature as the immediate indoor air temperature and as the moving average for the last 365 days. While these are the extremes in terms of volatility of their values, both of these cases lack the capacity to 'predict' the future trend of their values for the future calculations.

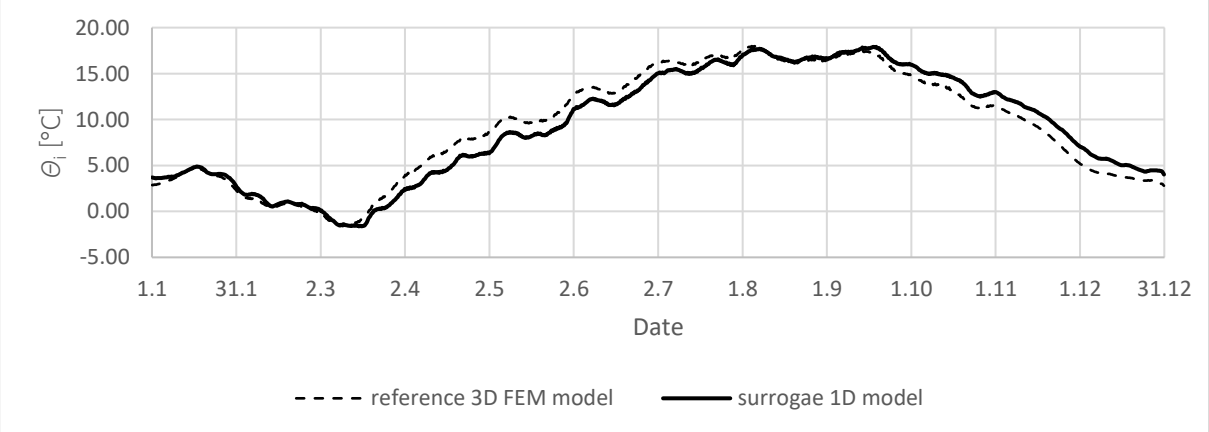

Fig. 4-13 Comparison of the free-float indoor air temperatures calculated on the 3D FEM model and the surrogate 1D model (indoor boundary condition for the core-zone element is the immediate indoor air temperature of the model)

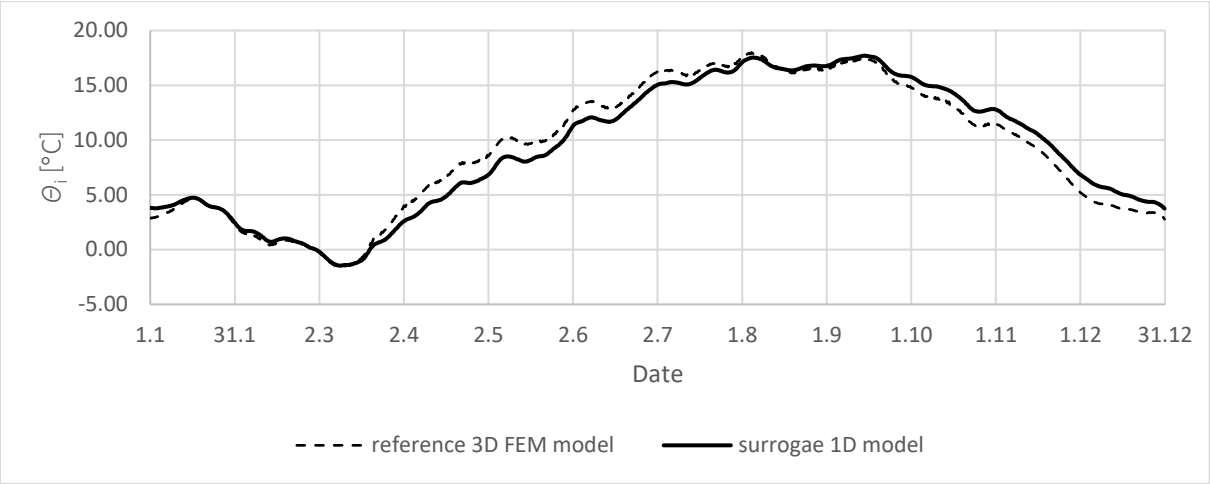

Fig. 4-14 Comparison of the free-float indoor air temperatures calculated on the 3D FEM model and the surrogate 1D model (indoor boundary condition for the core-zone element is the moving average of the indoor air temperature for the last 15 days)

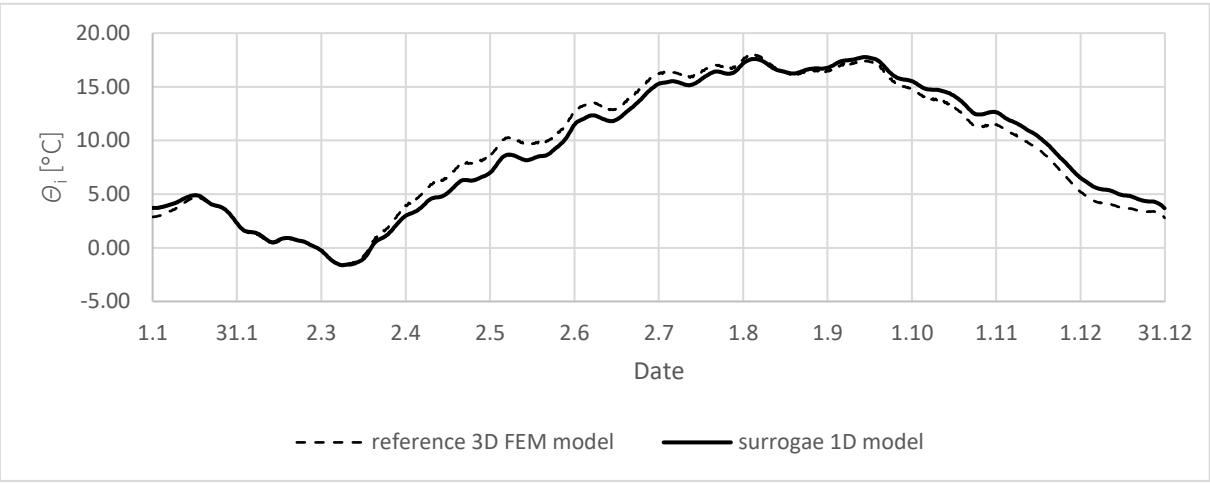

Fig. 4-15 Comparison of the free-float indoor air temperatures calculated on the 3D FEM model and the surrogate 1D model (indoor boundary condition for the core-zone element is the moving average of the indoor air temperature for the last 30 days)

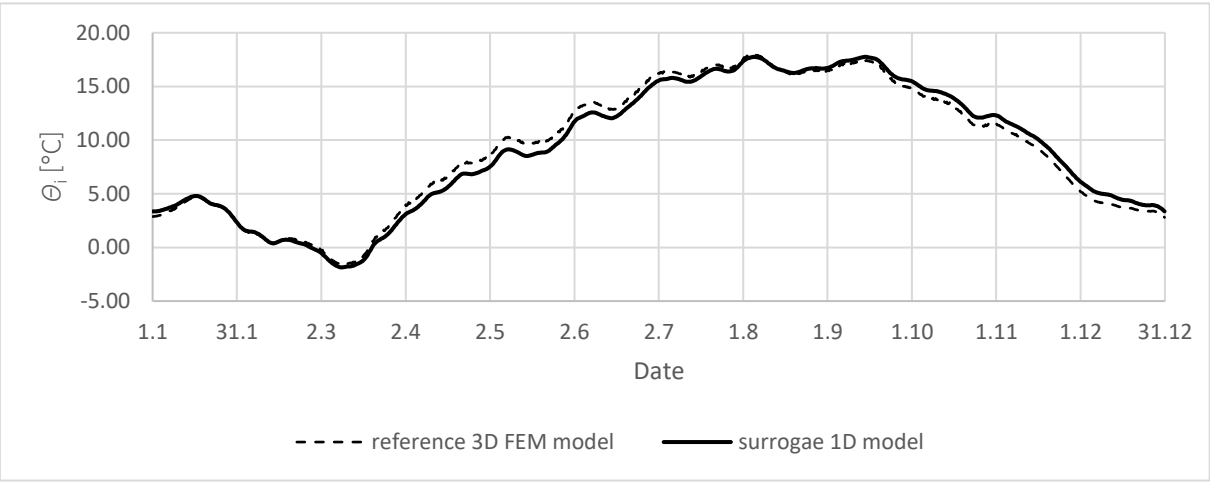

Fig. 4-16 Comparison of the free-float indoor air temperatures calculated on the 3D FEM model and the surrogate 1D model (indoor boundary condition for the core-zone element is the moving average of the indoor air temperature for the last 60 days)

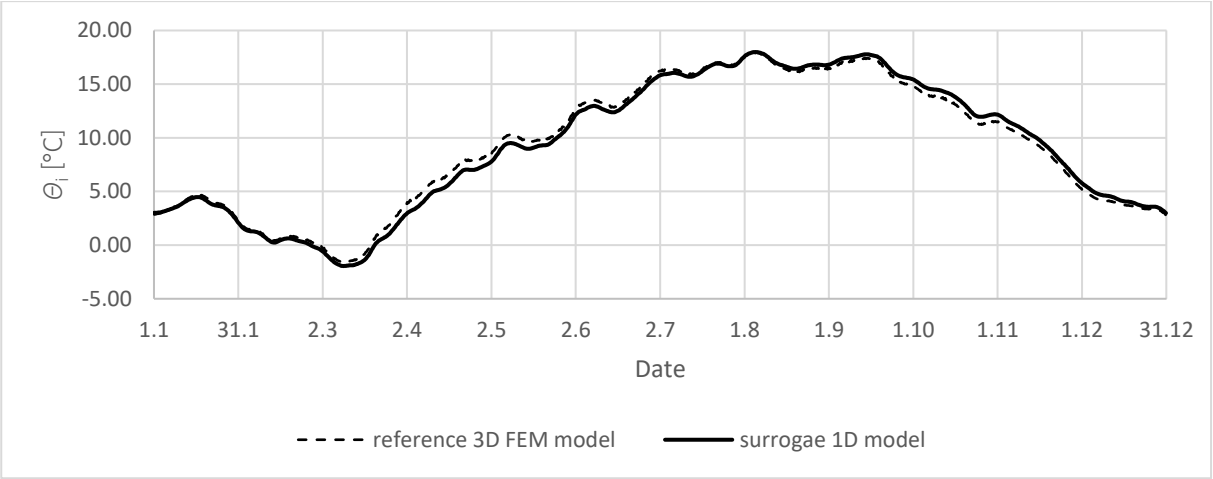

Fig. 4-17 Comparison of the free-float indoor air temperatures calculated on the 3D FEM model and the surrogate 1D model (indoor boundary condition for the core-zone element is the moving average of the indoor air temperature for the last 90 days)

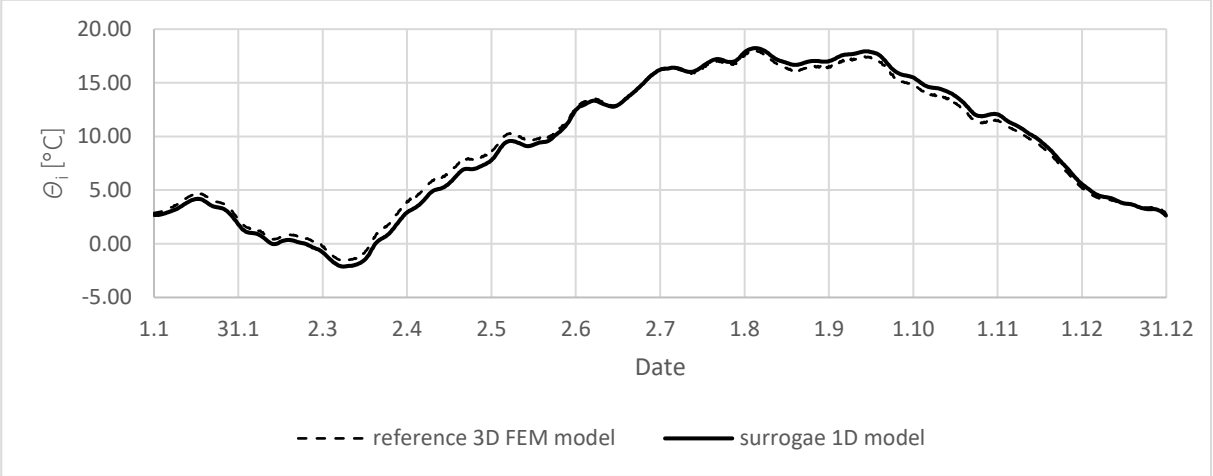

Fig. 4-18 Comparison of the free-float indoor air temperatures calculated on the 3D FEM model and the surrogate 1D model (indoor boundary condition for the core-zone element is the moving average of the indoor air temperature for the last 120 days)

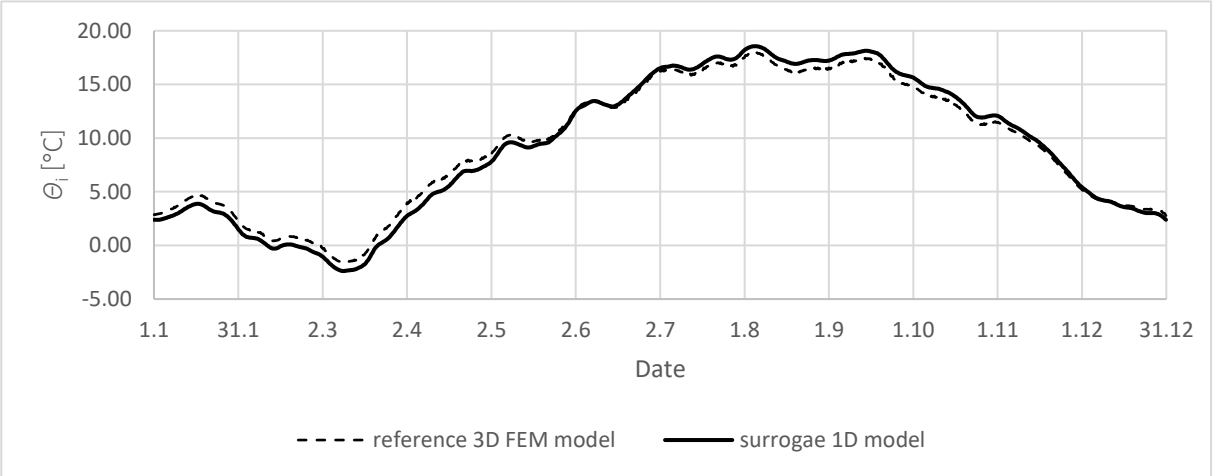

Fig. 4-19 Comparison of the free-float indoor air temperatures calculated on the 3D FEM model and the surrogate 1D model (indoor boundary condition for the core-zone element is the moving average of the indoor air temperature for the last 150 days)

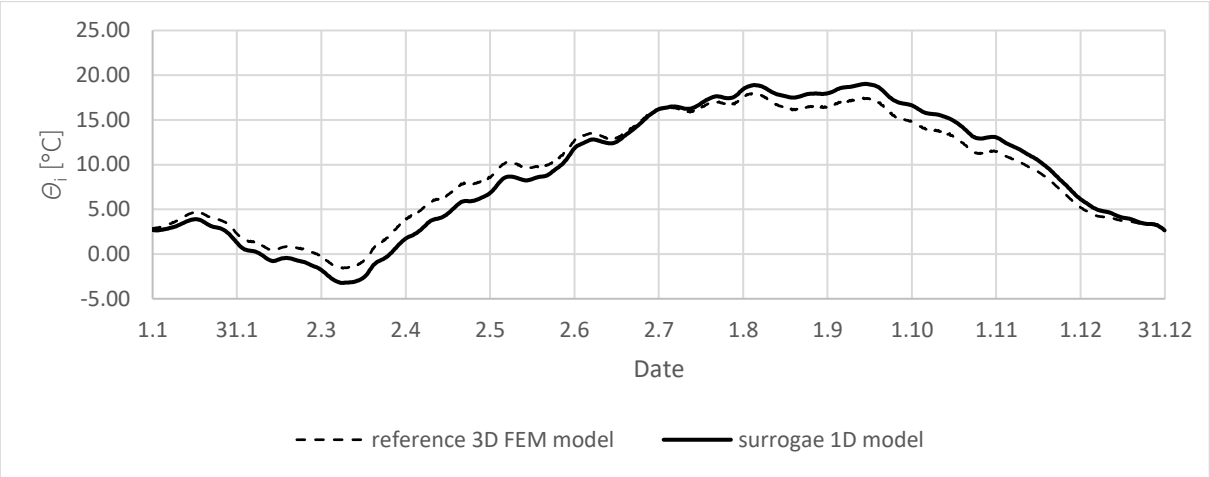

Fig. 4-20 Comparison of the free-float indoor air temperatures calculated on the 3D FEM model and the surrogate 1D model (indoor boundary condition for the core-zone element is the moving average of the indoor air temperature for the last 365 days)

Fig. 4-21 shows the maximal absolute difference of indoor air temperatures calculated on the reference 3D FEM model and on the surrogate 1D model in individual years. Fig. 4-22 shows the annual mean absolute difference of these temperatures in individual years. The figures confirm that the calculations on the surrogate 1D model using the immediate indoor air temperature and the moving average for the last 365 days as the indoor boundary condition for the core-zone element are performing the worst.

The best way to treat the indoor boundary condition for the core-zone element appears to be using the 90-days moving average. It is the same value as has been used for the outside boundary temperature. It is possible, that other cases would perform better, had the boundary temperatures used the moving average over the identical period. It is also possible, that the 90-days moving average gives the calculation a confident prediction of the future development as it is approximately the length of one climate season.

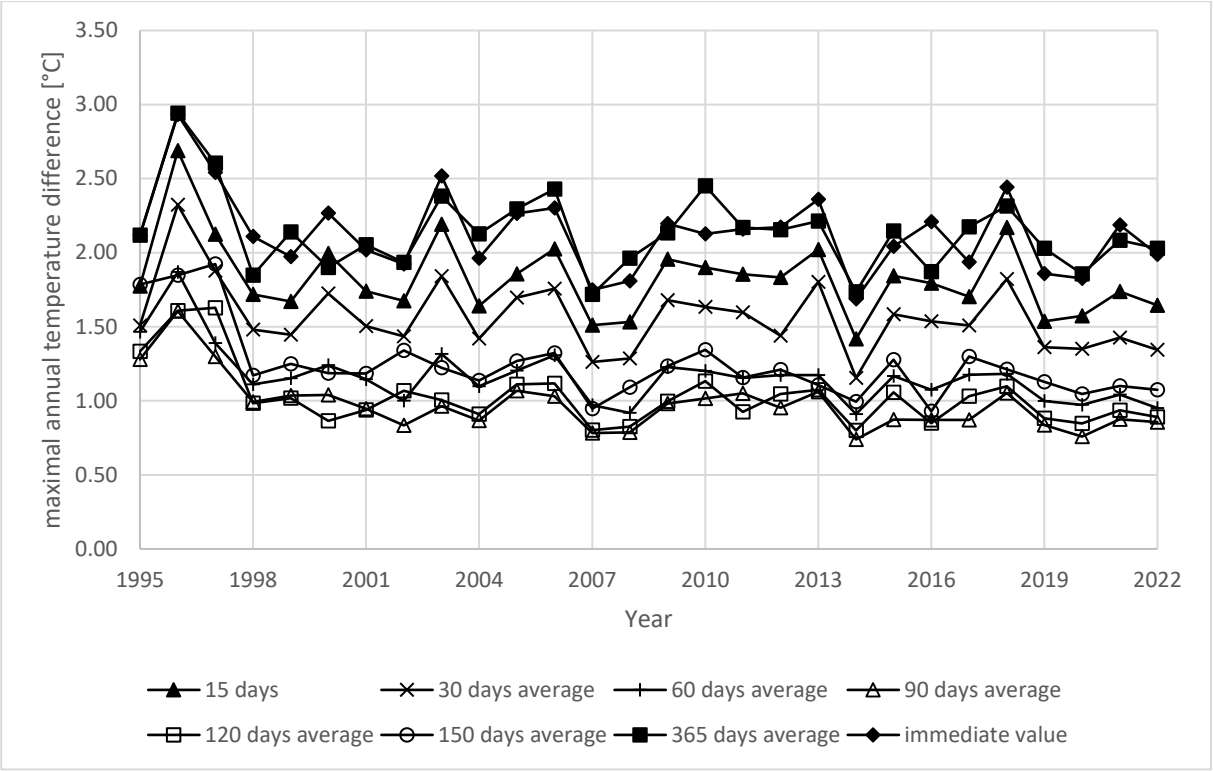

Fig. 4-21 Values of the maximal absolute difference of indoor air temperatures calculated on the 3D FEM model and the surrogate 1D model

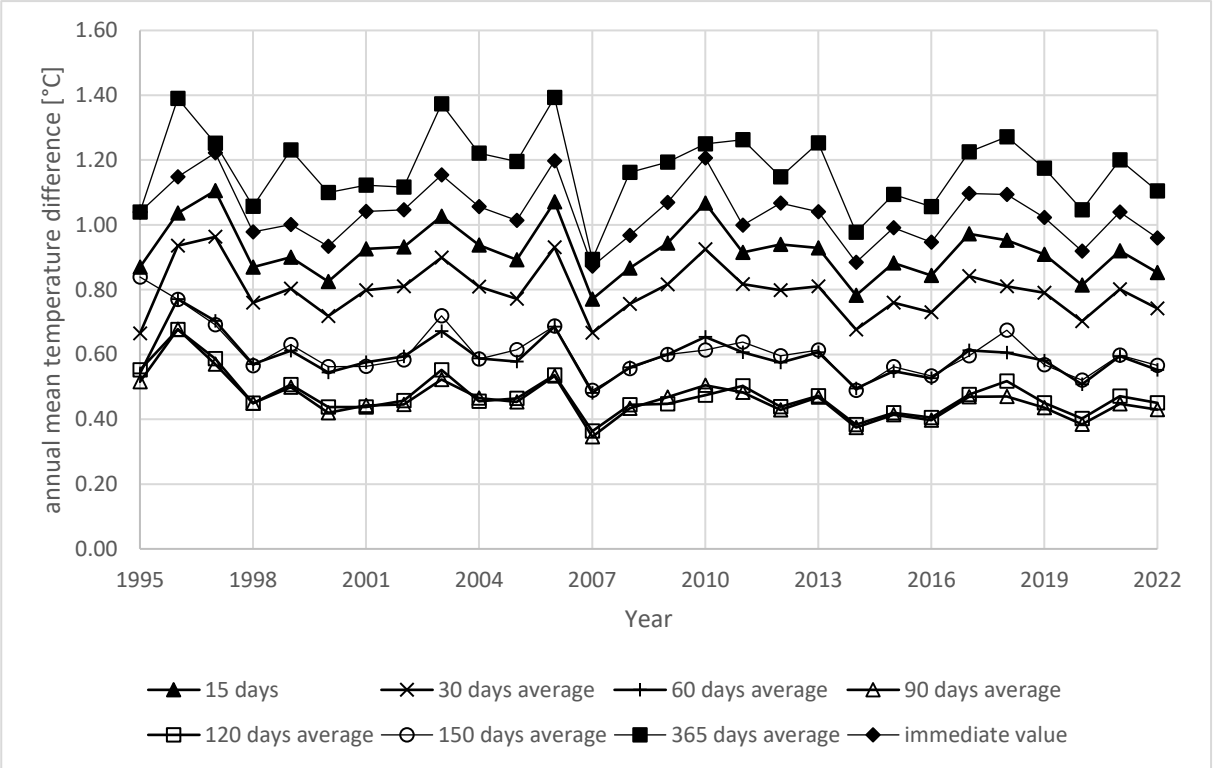

Fig. 4-22 Values of the annual mean absolute difference of indoor air temperatures calculated on the 3D FEM model and the surrogate 1D model

Partial conclusion

The behaviour of the developed surrogate 1D model has been analysed in a simplified whole-building simulation with free-floating indoor air temperature. The analysis was performed using hourly outdoor air temperature profile for 28 years. The purpose of the analysis was to determine the effect of the unknown internal air temperature making it impractical to determine its average value. The annual average value of the indoor air temperature has been considered in the model development as the indoor boundary condition for the core-zone element of the model to ensure the match of the reference heat fluxes through the slab-on-ground floors and the heat fluxes calculated using the developed model. The impossibility to determine the annual mean indoor temperature might have caused instability of the model causing an accumulation of errors over time.

The analysis has shown an approach to mitigate the error by replacing the annual mean indoor temperature by a moving average over different time periods before the calculation step. The commutation of errors was not confirmed. For all the considered time periods for the moving-average calculations, the mean and maximum differences of the indoor air temperatures calculated on the reference 3D model and the surrogate 1D model have oscillated around values specific for each case.

The best match was achieved by using the moving average of the indoor air temperature over the past 90 days. The maximal indoor air temperature difference between the models oscillated around ca 1 °C. The annual mean indoor air temperature difference between the models oscillated around ca 0.45 °C. These values present considerable good match of results. The computation time has been reduced from multiple hours (for a simulation of 1 year) for 3D FEM simulations to several minutes for the developed surrogate 1D model.

5. Upgrade with vertical perimeter thermal insulation

The model developed so far only focused on slab-on-ground floors without any perimeter thermal insulation. For these purposes it is applicable in simulations considering a wide range of thermal resistance of the slab R_{slab}. It is, however, reasonable to assume that the highly insulated slabs will also incorporate vertical thermal insulation around the perimeter. This part of the thesis therefore aims to analyse the possibility of introducing the effects of the vertical thermal insulation into the developed surrogate 1D model.

Method

The workflow is similar to the model development itself (see chapter 1). The individual model parameters are fine-tuned using reference 3D model results. These 3D models in this case also consider the vertical thermal insulation. Fine-tuning of individual parameters will presumably lead to different values than for the cases without the vertical thermal insulation. Therefore, the relationship between the original values for the cases without vertical thermal insulation, the new fine-tuned values, and the geometrical and thermal properties of the slab is sought through regression.

The additional insulation can have many qualitative forms. The vertical insulation's depth shall be denominated as h_i and its thickness as d_i (see Fig. 5-1). Within the scope of this work, two alternatives of its thickness have been considered: 5 cm and 15 cm. The considered thermal conductivity of the insulation material is λ = 0.04 [W/mK]. As these values may differ based on the material used in the construction, they are represented by the final thermal resistance of the vertical thermal insulation $R_{vertical}$.

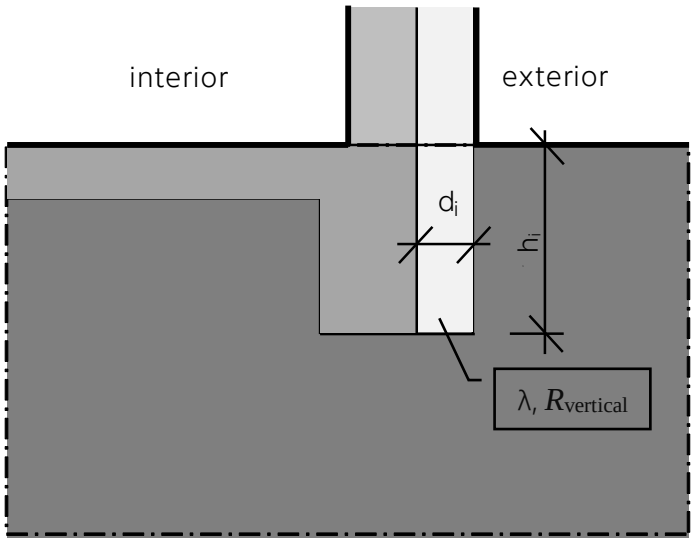

Fig. 5-1 Vertical thermal insulation

The analysis has been carried out considering the following slab-on-ground properties and their values:

- Geometrical properties of the building B' = {4; 5; 7; 10; 13; 15} [m]
- Slab-on-ground thermal resistance R_{slab} = {2; 3; ...; 8} [m²K/W]
- Depth of the vertical thermal insulation h_i = {0,7; 1,0; 1,5} [m]
- Thermal resistance of the vertical thermal insulation $R_{vertical}$ = {1.25; 3.75} [m²K/W]

Results

Perimeter zone element – length: The previous model development has identified the order of the model parameters fine-tuning (see chapter 3.2). The first parameter to be analysed is the length of the element representing the perimeter zone of the slab-on-ground floor $l_{transient}$. The additional length of this element needed to account for the effects of the vertical thermal insulation has been denominated $\Delta l_{transient}$ (Fig. 5-2).

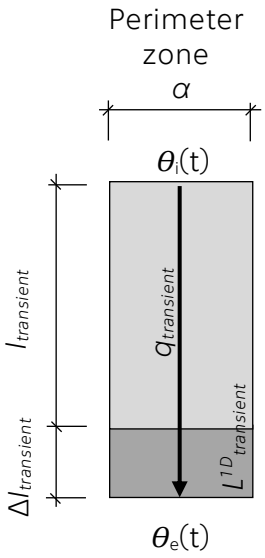

Fig. 5-2 Changes in the length of the perimeter zone element due to vertical thermal insulation

After the fine-tuning of the total length of the perimeter zone element for each of the considered test cases, the values of $\Delta l_{transient}$ have been identified. Fig. 5-3 shows the dependence of the calculated $\Delta l_{transient}$ on B' considering different values of $R_{slab.}$ This figure only shows this dependency for the case of vertical thermal insulation with characteristics h_i = 1.0 m and $R_{vertical}$ = 3.75 [m²K/W].

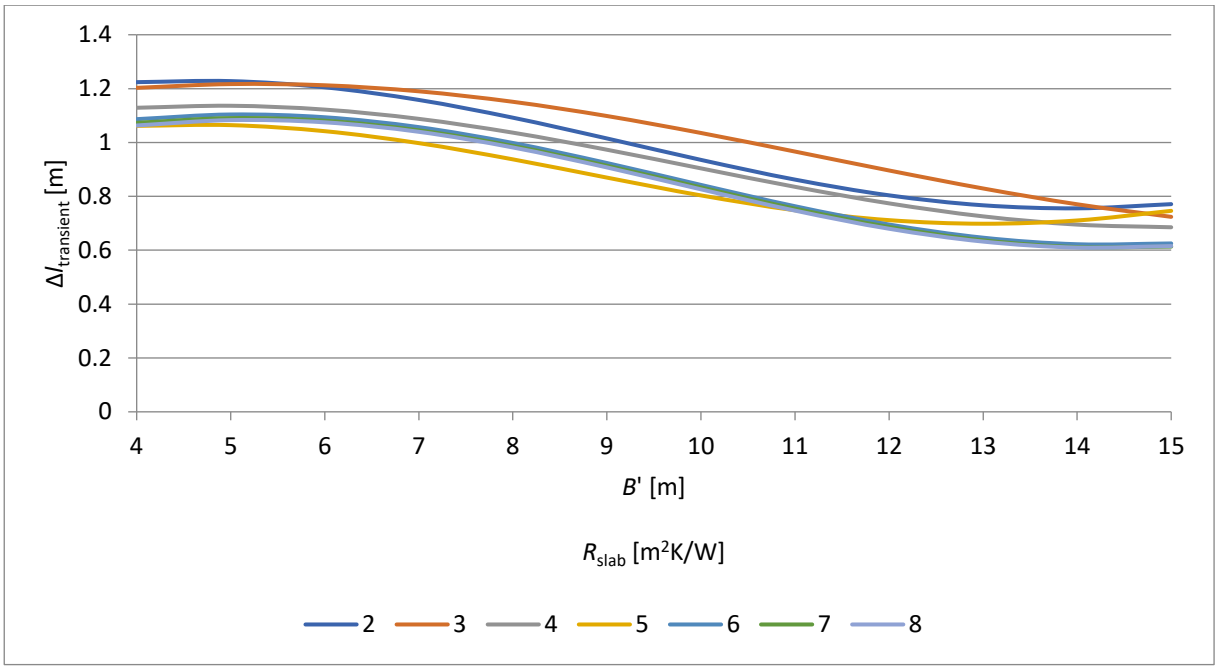

Fig. 5-3 Dependency of $\Delta l_{transient}$ on B' and R_{slab} for $R_{vertical}$ = 3.75 m²K/W and h_i=1.0 m

Similar analysis as shown in Fig. 5-3 has been carried out for all the combinations of the considered input values. When analysing the tuning process and results it has been observed, that for each combination of parameters R_{slab}, h_i and d_i is the $\Delta l_{transient}$ relation to the equivalent floor dimension a harmonic function:

$$\Delta l_{transient} = a \,.\, \sin(b \,.\, B' + c) + d \quad [\text{m}] \tag{5-1}$$

The values of parameters *a, b, c* and *d* differ, however, for each combination of R_{slab}, h_i and d_i. It can be therefore written, that $\Delta l_{transient} = f(B', R_{slab}, h_i, R_{perimeter})$. It has also been found, that the effect of R_{slab} can be neglected, resulting in:

$$a, b, c, d = f(h_i, R_{perimeter}), \tag{5-2}$$

The values of *a, b, c* and *d* are summarized in Tab. 5-1.

Tab. 5-1 Values of parameters *a, b, c* and *d* for $\Delta l_{transient}$ calculation

$R_{verticalr}$ [m².K.W⁻¹]	1.25			3.75		
h_i [m]	0.7	1	1.5	0.7	1	1.5
a	0.24	0.23	0.26	0.22	0.34	0.38
b	0.31	0.33	0.32	0.27	0.23	0.28
c	6.46	6.21	6.49	6.58	7.06	6.95
d	0.73	0.91	1.19	0.8	1.1	1.61

A linear interpolation is possible between these values.

Perimeter-zone element – width: The change of the width of the perimeter-zone element has been analysed in two alternatives:

- Seeking a multiplication coefficient of the existing values of α (Fig. 5-4, left),
- Seeking an additional part of the element (Fig. 5-4, right).

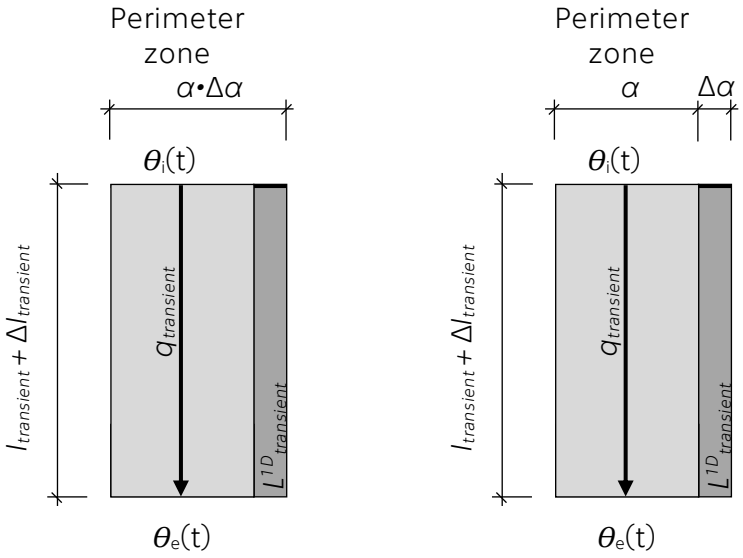

Fig. 5-4 Alternative approaches to interpret the change of the parameter α: by a multiplicator (left), by additional width (right)

First, the analysis for the variant of a multiplicator has been undertaken. Using the same approach of comparing the amplitudes (having accounted for the change in $l_{transient}$), the values of $\Delta\alpha$ have been found for each of the test cases. Fig. 5-5 shows the calculated values for the considered combinations of $R_{vertical}$ (first number in the combination's name in [W/m•K] and h_i (second number in the combination's name in [cm]) over R_{slab}. The data shown are valid for the cases with B' = 7 [m].

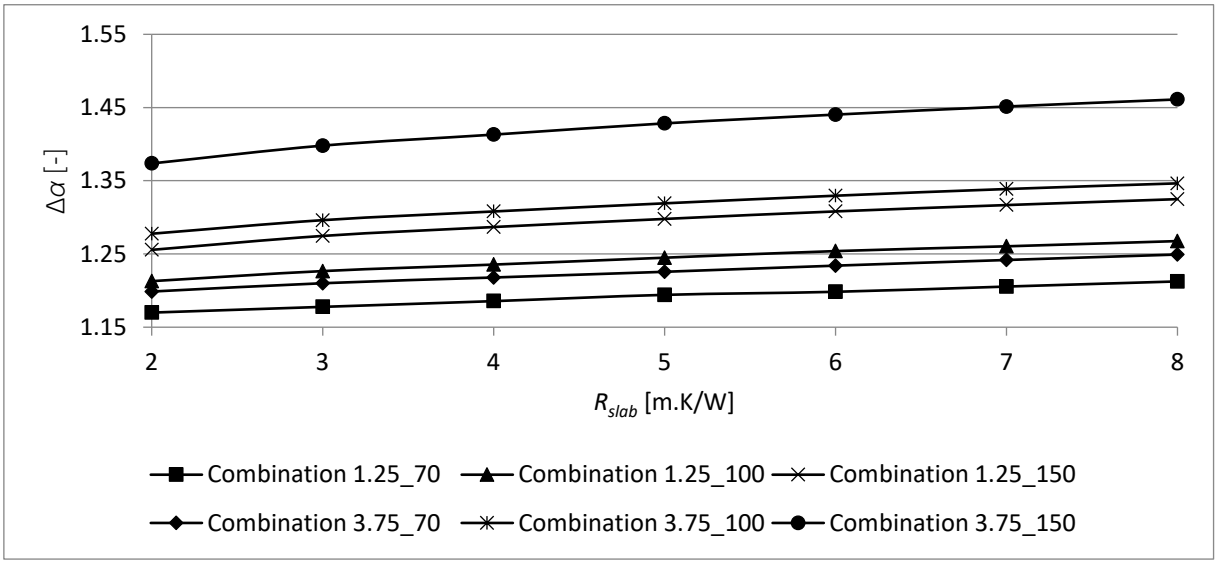

Fig. 5-5 Values of Δα for the possible combinations of $R_{vertical}$ and h_i over R_{slab} for B' = 7 m

The data analysis showed that the dependence on the R_{slab} can be described as a linear function:

$$\Delta\alpha \quad = a \cdot R_{slab} + b \quad [-] \tag{5-3}$$

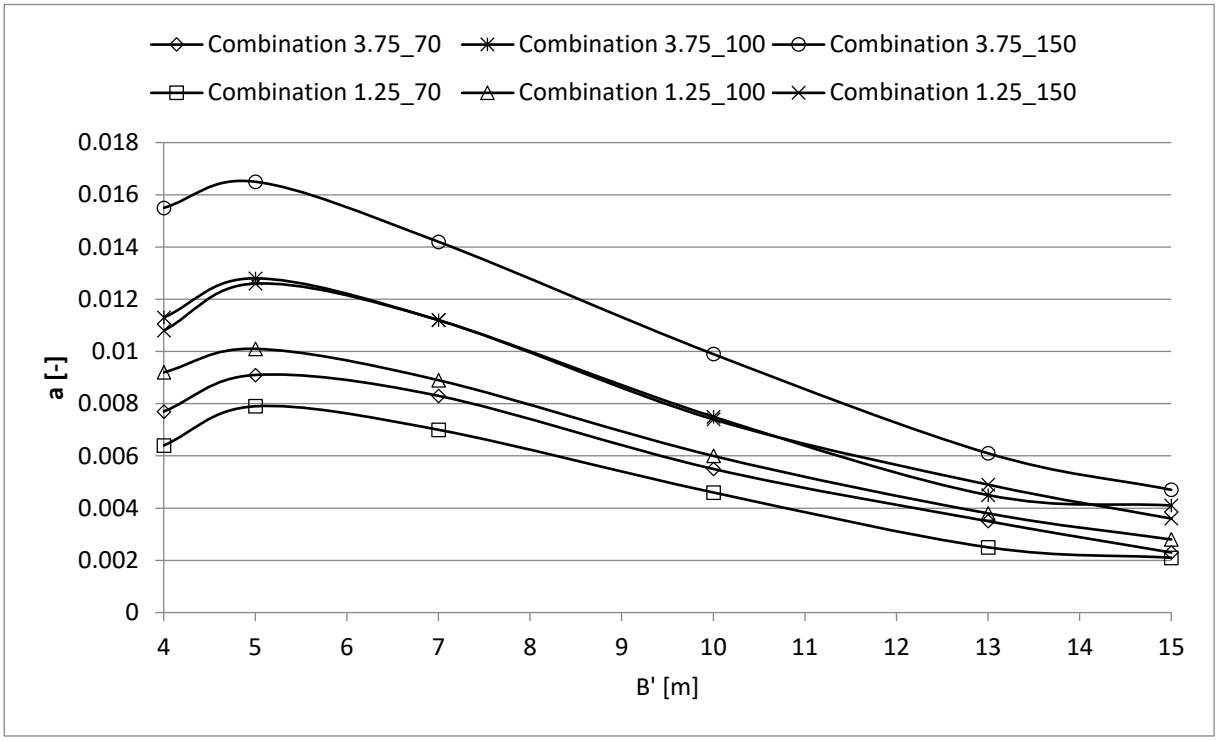

Fig. 5-6 Values of parameter a in equation (5-3) for the possible combinations of $R_{vertical}$ and h_i over B'

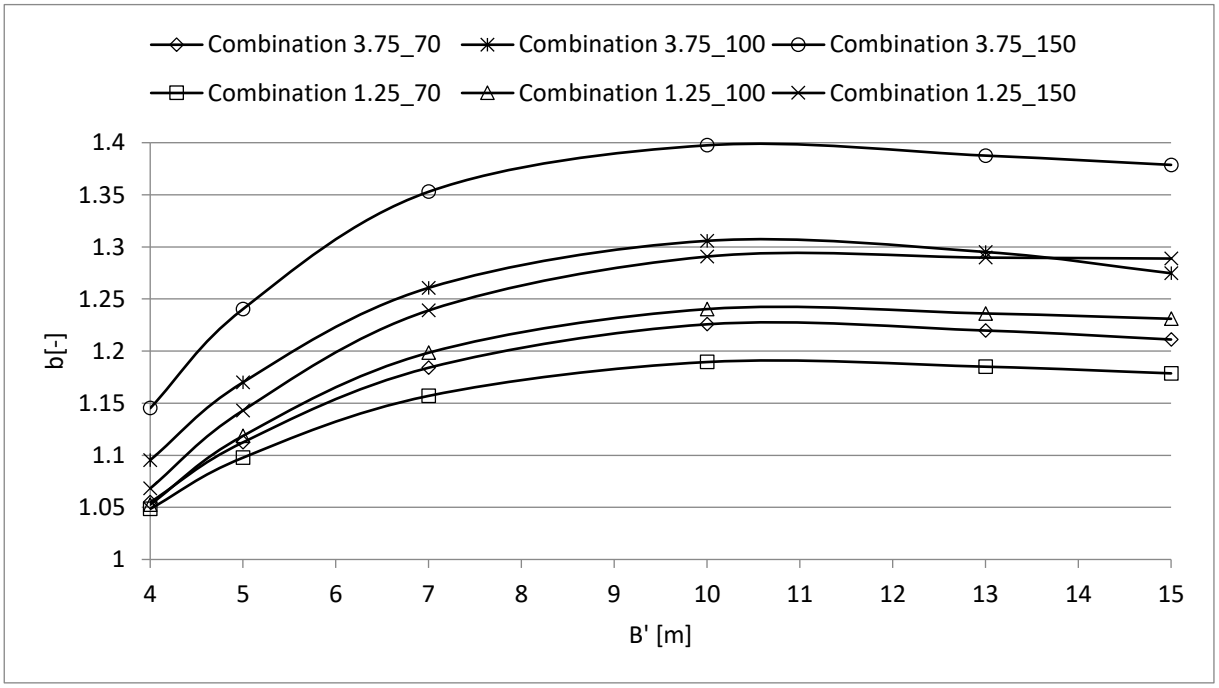

Fig. 5-7 Values of parameter b in equation (5-3) for the possible combinations of $R_{vertical}$ and h_i over B'

Through the mathematical regression, it has been found, that the parameter *b* in equation *(5-3)* would have to be described using the equation *(5-4)* and using the input matrix for $b_{m,n}$ shown in Tab. 5-2. This approach has been deemed inefficient. Therefore, the second alternative for treating the changes of *α* (as additional width, instead of a multiplier) has been further analysed.

$$b = \left(b_{1,1}\,.\,h_i^2 + b_{1,2}\,.\,h_i + b_{1,3}\right).B'^3 + \left(b_{2,1}\,.\,h_i^2 + b_{2,2}\,.\,h_i + b_{2,3}\right).B'^2 + \left(b_{3,1}\,.\,h_i^2 + b_{3,2}\,.\,h_i + b_{3,3}\right).B' + \left(b_{4,1}\,.\,h_i^2 + b_{4,2}\,.\,h_i + b_{4,3}\right) \quad (5\text{-}4)$$

Tab. 5-2 Input matrix for equation (5-4)

R_{slab} = 1.25 [m².K.W⁻¹]		n			R_{slab} = 3.75 [m².K.W⁻¹]		n		
		1	2	3			1	2	3
m	1	-0,00021	0,00072	-0,00020	m	1	0,00010	0,00005	0,00020
	2	0,00921	-0,02755	0,00570		2	-0,00160	-0,00931	-0,00309
	3	-0,10856	0,32884	-0,06395		3	-0,01140	0,16320	0,02450
	4	0,32620	-0,93490	1,21795		4	0,01790	-0,29910	0,87261

The values of Δ*α* as an additional part of the perimeter-zone element in [m] have been calculated for each combination of R_{slab}, $R_{vertical}$, and h_i. Their values over *B′* are shown in Fig. 5-8. The legend is not provided because of the large number of data series. It has been decided to neglect the influence of R_{slab} by calculating the average values for each combination of $R_{vertical}$, and h_i considering different *B′*. The resulting values of Δ*α* are shown over *B′* in Fig. 5-9.

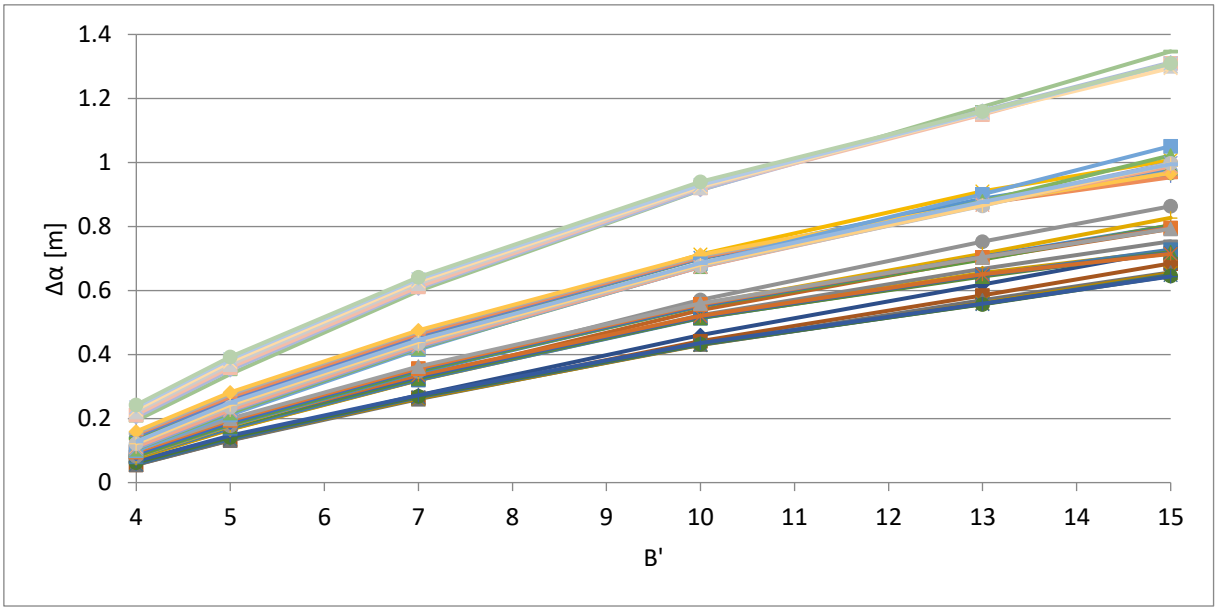

Fig. 5-8 Dependancy of Δα on B′ for the considered combinations of R_{slab}, $R_{vertical}$ and h_i (legend not provided due to the large number of data series)

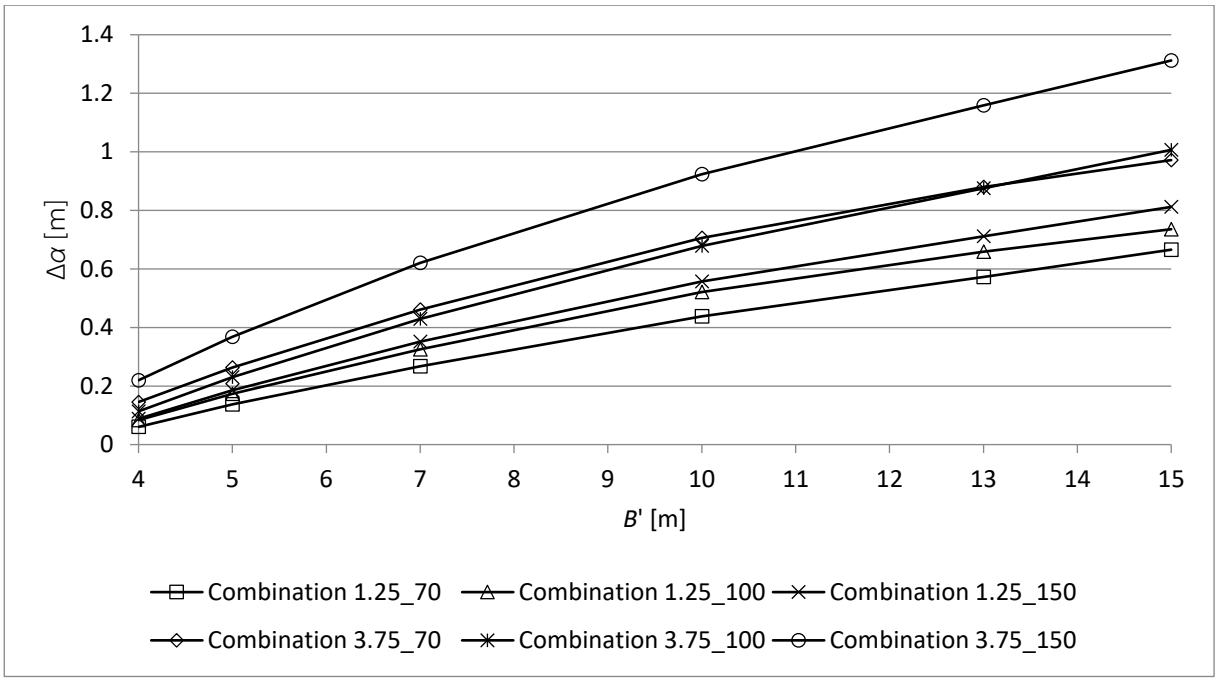

Fig. 5-9 Dependence of Δα on B′ for the considered combinations when neglecting R_{slab}

To simplify the equation governing Δα, an assumption of a second-grade polynomial has been made:

$$\Delta\alpha = a \,.\, B'^2 + b \,.\, B' + c \qquad [\text{m}] \tag{5-5}$$

The values of the parameters in this equation for different h_i and $R_{vertical}$ combinations are summarized in Tab. 5-3.

Tab. 5-3 Values of *a*, *b* and *c* for the Δα calculation

h_i [m]	0.7		1		1.5	
$R_{vertical}$ [m².K.W⁻¹]	1.25	3.75	1.25	3.75	1.25	3.75
a	-0.0016	-0.0027	-0.0024	-0.0037	-0.0024	-0.0036
b	0.084	0.111	0.111	0.145	0.126	0.167
c	-0.246	-0.316	-0.311	-0.375	-0.34	-0.39

After the application of this workflow it was possible to match the calculated values of Δα and their desired values calculated from the comparison of heat flux amplitudes shown in Fig. 5-8 with good confidence. Fig. 5-10 shows the relative error values for this comparison.

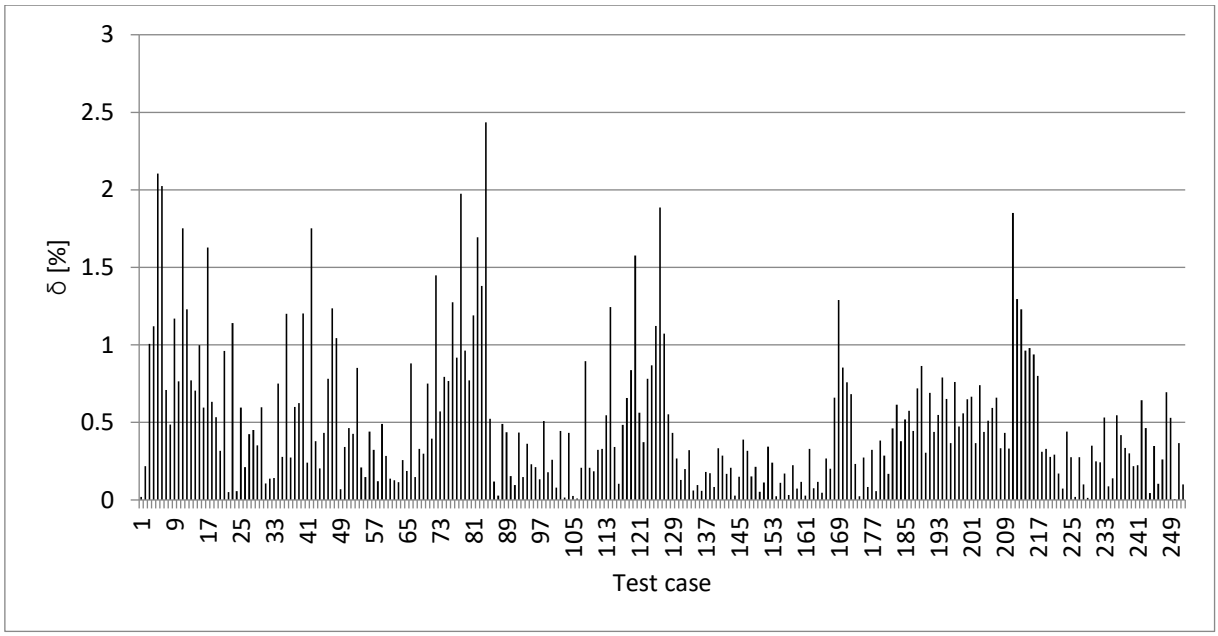

Fig. 5-10 Percentual Relative Error of the Δα values calculated using equation (5-5) *and Tab. 5-3 from the fine-tuned values shown in Fig. 5-8*

Length of the core-zone element: The changes in the previously analysed model parameters have focused on matching the time shift (by $\Delta l_{transient}$) and amplitude (by $\Delta\alpha$) of the heat flux profile calculated on the surrogate model to the reference 3D FEM calculations. As it has been described in Tab. 3-3, these changes have subsequently influenced the average value of the heat flux profile calculated on the surrogate models. This sole quality of the heat flux profile is influenced by the length of the core-zone element l_{steady}.

These changes have both influenced the desired value of the steady state heat flux through the core-zone element in their own ways. The fact that these changes are described by equations not perfectly matching the fine-tuned values means, that they would also introduce different levels of inaccuracies into further calculations. Furthermore, the parameter $\Delta\alpha$ effectively influences the width of the core-zone element, by which the heat specific heat flux is being multiplied in order to obtain the resulting total heat flux. All these complications have led to the decision, that it would be impractical to search for an additional block of soil which would account for the effects of the vertical thermal insulation as in the previous two parameters.

Instead, a whole new equation is suggested to determine the length of this component. Fig. 5-11 shows the new l_{steady} values relative to B′ for the considered properties of vertical insulation. A linear interpolation is assumed between the edge values using tripartite. For this purpose, an interpolation coefficient μ is suggested *(5-6)*. It combines the influence of R_{slab}, h_i and $R_{vertical}$. Its borderline values to be used in the tripartite are shown in

$$\mu = R_{slab} \cdot (h_i^2 \cdot R_{vertical}) \qquad (5\text{-}6)$$

Example of the calculation of the l_{steady} follows:

- Input parameters:
  - B' = 8.0 [m]; R_{slab} = 5 [m²K/W]; $R_{vertical}$ = 1.25 [m²K/W]; h_i = 1 [m]
  - μ= 7.81875
- Borderline values and corresponding μ:
  - Upper: l_{steady} = 2.8862 m (μ= 2.6125)
  - Lower: l_{steady} = 2.715 m (μ= 16.4375)
- Calculated value:
  - l_{steady} = 2.862 m

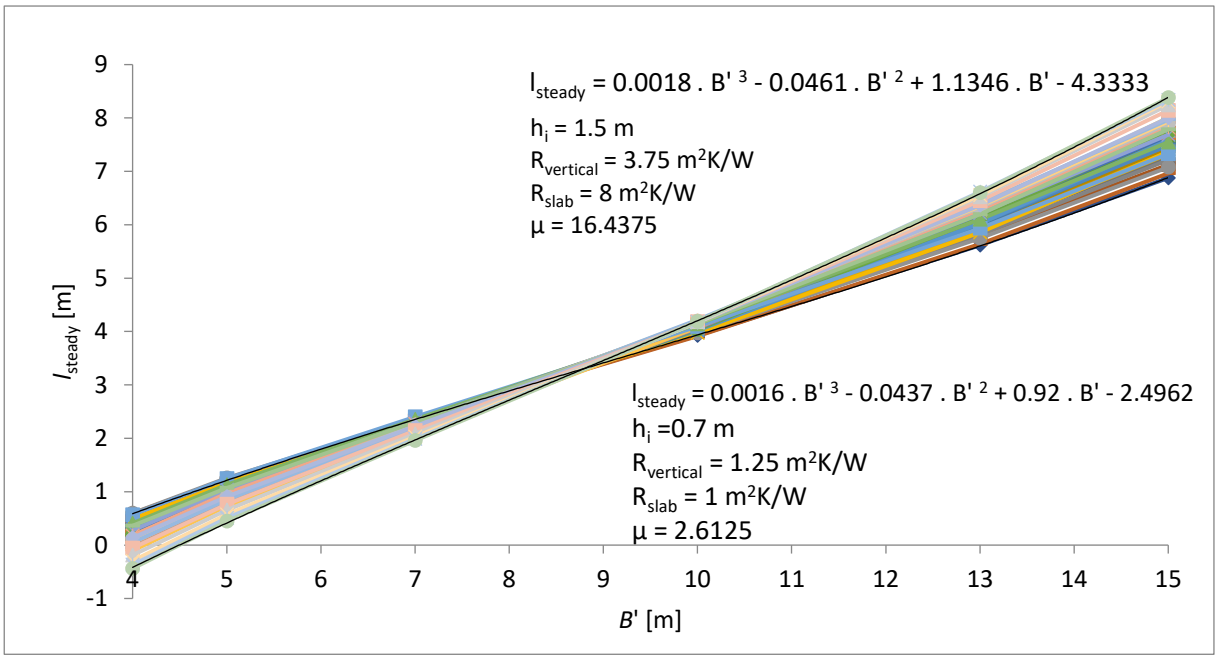

Fig. 5-11 Values of l_{steady} and the limit-case equations

Testing: The model considering above-described approach has been tested against 3D FEM models using the same *GoF* procedure as in the original development. For the considered harmonic boundary conditions lie all the 252 modelled cases in the interval $GoF \in$ <87,1; 99,8> [%]. From the mean relative error point of view do most of the cases report less then 4 % PMRE as shown in Fig. 5-12. There are however some cases which exceed this value. These are summarized in Tab. 5-4. Fig. 5-13 compares the heat fluxes obtained from the 3D FEM calculation and the surrogate 1D model for the worst performing scenario (case 1 in Tab. 5-4).

Tab. 5-4 Tested cases reporting PMRE exceeding 4 %.

	Case 1	Case 2	Case 3	Case 4
B' [m]	4	4	5	5
R_{slab} [m².K⁻¹.W⁻¹]	2	3	2	3
$R_{vertical}$ [m².K⁻¹.W⁻¹]	0.15	0.15	0.15	0.15
h_i [m]	1.5	1.5	1.5	1.5
GoF [%]	87.11	88.81	90.37	90.64
PMRE [%]	10.0	5.3	7.2	4.2

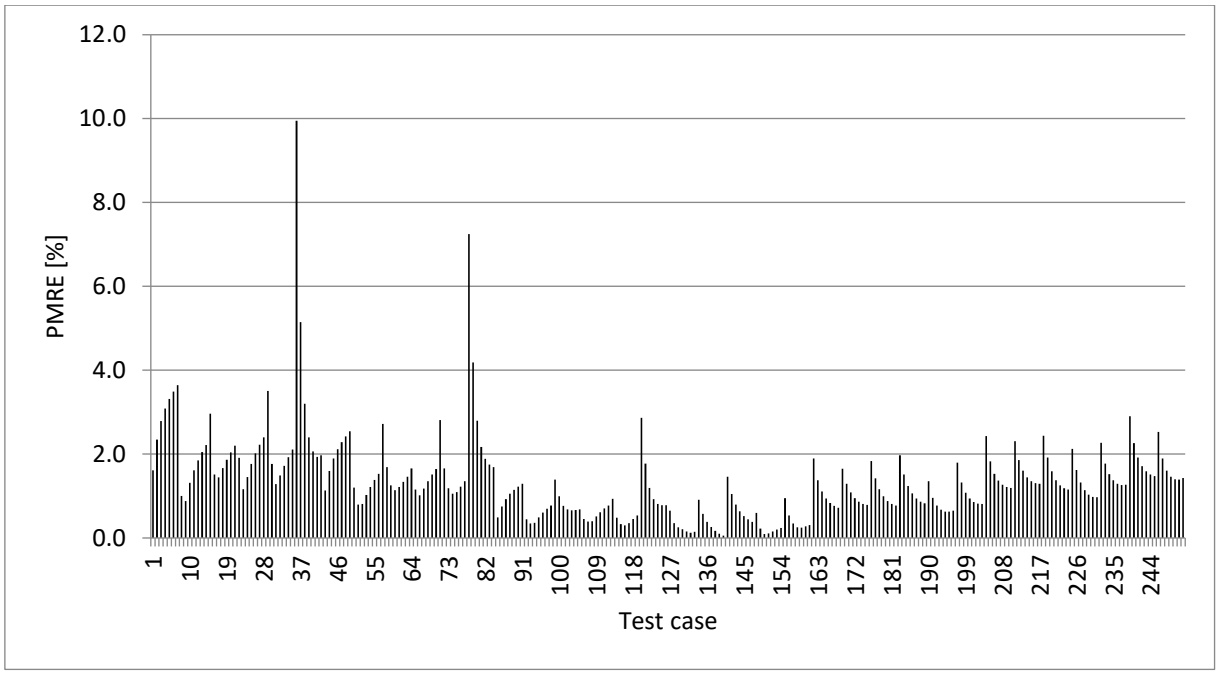

Fig. 5-12 PMRE values for considered scenarios

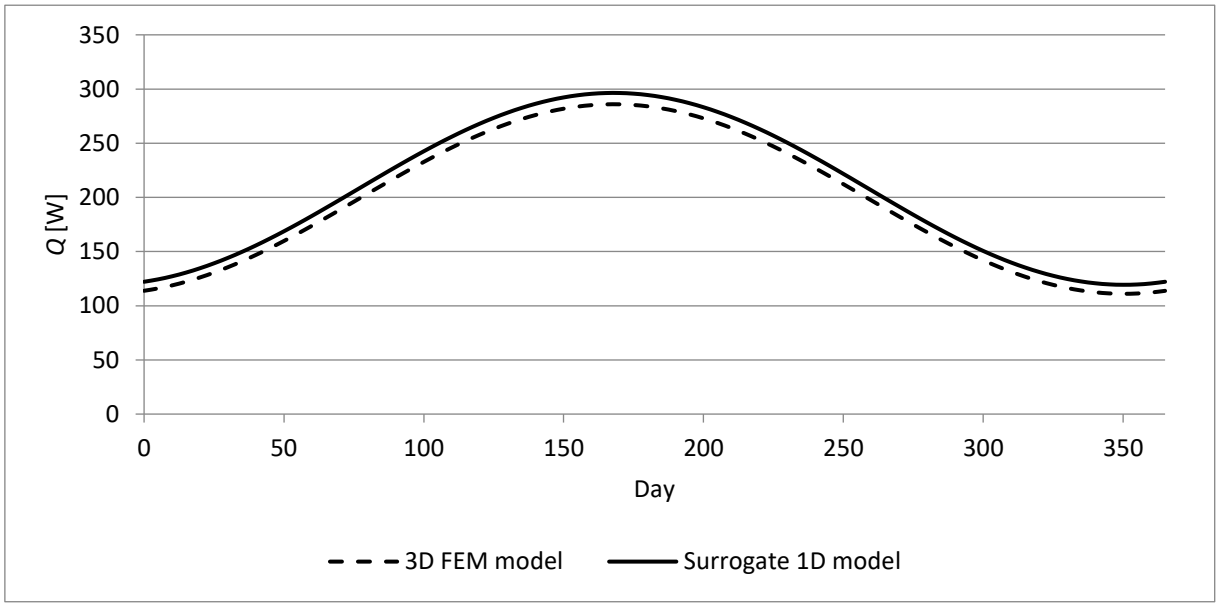

Fig. 5-13 Visualisation of the heat flux courses for the test case with the worst match of results

Partial conclusion

This part of the thesis has focused on the possible ways to incorporate the effects of a vertical thermal insulation on the developed surrogate 1D model geometry parameters. It used the same workflow as for the model development itself – fine-tuning and mathematical regression for individual model parameters in the order from the most influential parameter to the least influential parameter.

It has proposed a method to increase the dimensions of the perimeter-zone element of the developed surrogate 1D model and a method to calculate the length of the core-zone

element considering the relevant input parameters. The dimensions of the perimeter-zone element should be increased for values calculated using equations *(5-2)* and *(5-5)*, and tables Tab. 5-1 and Tab. 5-3. The value of I_{steady} should be calculated using the equations in Fig. 5-11 and the equation *(5-6)*.

The accuracy of the model considering the proposed workflow has been tested using 252 test cases by comparison of the resulting heat fluxes with 3D FEM calculations. The results have shown good confidence of results usable for early stages of the building design process.

6. Conclusion

This thesis has presented the problematics of the simplified dynamic thermal modelling of slab-on-ground floors. It has described the global context of energy efficiency in buildings and current trends in energy savings. These trends present a challenge for energy efficient building design and increased requirements on building performance modelling. As the energy demand in newly-built buildings is rapidly decreasing, the precision of thermal models plays a crucial role in the building design and also in building operation. An effective building design requires the evaluation of multiple variants with sufficient precision. Generally, increased precision leads to increased computation times and therefore makes it difficult to evaluate large numbers of design options.

Constructions in contact with the ground are one of the most difficult problems to evaluate in terms of heat loss calculations due to the large block of soil. The block of soil makes it impossible to model these constructions as 1D problems, similarly to other building envelope elements. There are different approaches to overcome this issue, be it by calculating virtual temperatures at the interface of the constructions and soil or by introducing simplified 2D and 1D computation models considering different input parameters. Different approaches are also used in individual whole-building simulation tools. These approaches always sacrifice some accuracy to shorten the computation time. Most of the available tools have their limitations and different tools are more suitable for different design cases.

This thesis has proposed a method to construct a surrogate 1D model of a slab-on-ground floor usable in RC modelling. The model consists of two separate 1D problems, each representing different zone of the slab-on-ground floor. Its geometrical interpretation is based on Anderson's [41] equivalent floor dimension. The geometrical parameters of the individual 1D problems within the developed surrogate 1D model have been described by equations considering the slab-on-ground floor geometry and the level of its thermal insulation. These equations have been found by fine-tuning the geometrical properties of the developed model in order to fit the resulting heat fluxes through the 1D system and the heat fluxes calculated on reference 3D FEM models. Annual harmonic temperature profiles have been used as the boundary conditions in the model development. The found values have then been analysed and used in mathematical regression to define the equations.

The developed model has then been tested using the same boundary conditions for test cases with different input parameters (geometry and level of thermal insulation) than the ones used for the model development. The accuracy of the results has then been compared with the standard 1D model of slab-on-ground floors according to the EN ISO 13370 [46]. In both cases have the results shown good confidence of results when

compared to the reference 3D FEM simulations while significantly decreasing the calculation time.

The developed model has then been tested for applicability in a simplified whole-building simulation in two scenarios: with conditioned indoor environment, and in a free-floating regime. In the case of the free-floating regime, different approaches to maximize the calculation accuracy have been considered. The model has performed with good confidence of results in both scenarios. The free-floating regime test has also found no accumulation of errors when simulating long time periods (28 years).

The possibility to account for vertical thermal insulation has also been researched. Through a similar process of fine-tuning and mathematical regression has been proposed a method to upgrade the developed model to be used for simulation of such cases. The testing using annual harmonic boundary temperatures showed good match of the results of the model when compared to the reference 3D FEM calculations.

The model has been developed considering an "unknown ground" according to the Czech version of EN ISO 13370 [46]. Its performance with other soil properties has not been investigated and can be a subject of further work. The equations found through mathematical regression describing model's geometrical properties can be considered complex. Their form has, however, been chosen to maximize the confidence of results obtained from the model. Future work can also focus on their further simplification, or finding other types within the mathematical regression process.

Especially complex can then be considered the process of incorporating the effects of vertical thermal insulation around the perimeter. This is caused by the chosen geometry interpretation. Future work can also focus on developing a separate set of equations for the cases with this type of insulation, instead on building it on top of the existing model. It might be easier for the user of this method to use two different sets of equations with the limitations for use – with and without vertical thermal insulation.

The thesis has proposed a method to deal with an unknown mean annual indoor temperature by using a moving average value of this variable. For conditioned spaces can the mean annual indoor temperature be estimated with sufficient accuracy for the calculations. For simulation of seasonally occupied buildings, this estimation might not be sufficient. The results of the free-float indoor air temperature show, that finding a suitable range for the moving average to substitute the annual mean value is necessary. Moving average of the values in the past 90 days has led to the best confidence of the results in the presented test case. The definition of a general method to determine this range for other cases can be researched further. Another option to overcome the unknown mean annual indoor temperature problem can be to run multiple simulations

and solve this problem iteratively. It would be, however, desirable to minimize the computation time as much as possible.

The confidence of results obtained from the developed model could be enhanced even more. One approach can be a refinement of the mathematical regression. It has, for, example, neglected the dependence of $I_{transient}$ on the level of thermal insulation of the slab-on-ground. This refinement would, however, have minor effect on the confidence of results and would only lead to more complex equations to determine the model parameter values. The second option is to narrow the range of the input parameters. This could mean excluding either smallest or largest buildings considered, or excluding low levels of floor thermal insulation. This could lead to easier curve-fitting and probably also to finding simpler equations. It would, however, also limit the model applicability.

Overall, the developed surrogate 1D model of slab-on-ground floors has shown a good confidence of results when compared to reference 3D FEM simulations under different conditions. Even with its current limitations it can be usable in early building design stages to evaluate multiple design possibilities in short time. The confidence of results even without specifying the mean annual indoor and outdoor temperatures after choosing the suitable moving average range can make it applicable in predictive building regulation systems to optimize the building performance.

List of figures

List of tables

References

[1] G. Pernigotto, A. Prada, M. Baratieri, P. Baggio, and A. Gasparella, 'Modelling Of The Thermal Behavior Of Walls And Floors In Contact With The Ground', presented at the International High Performance Buildings Conference, Purdue, Purdue, 2012.

[2] 'ČSN EN ISO 10211:2020 Thermal bridges in building construction - Heat flows and surface temperatures - Detailed calculations'. Úřad pro technickou normalizaci, metrologii a státní zkušebnictví, 2020.

[3] *Alliance for Buildings and Construction, International Energy Agency and the United Nations Environment Programme (2019): 2019 Global Status Report for Buildings and Construction: Towards a zero-emission, efficient and resilient buildings and construction sector*.

[4] '2020 Global Status Report for Buildings and Construction | Globalabc'. https://globalabc.org/resources/publications/2020-global-status-report-buildings-and-construction (accessed Nov. 03, 2022).

[5] '2021 Global Status Report for Buildings and Construction | Globalabc'. https://globalabc.org/resources/publications/2021-global-status-report-buildings-and-construction (accessed Nov. 03, 2022).

[6] 'Building Envelopes – Analysis', *IEA*. https://www.iea.org/reports/building-envelopes (accessed Dec. 21, 2021).

[7] 'ScienceDirect Search Results', *ScienceDirect*, Dec. 31, 2021. https://www.sciencedirect.com/search?qs=%22energy%20efficiency%20in%20buildings%22&lastSelectedFacet=articleTypes&articleTypes=FLA

[8] 'European Commission : CORDIS : Search : Results page'. https://cordis.europa.eu/search?q=contenttype%3D%27project%27%20AND%20(%27energy%20efficient%20buildings%27)&p=1&num=10&srt=Relevance:decreasing (accessed Dec. 31, 2021).

[9] J. Gupta and M. Chakraborty, '15 - Energy efficiency in buildings', in *Sustainable Fuel Technologies Handbook*, S. Dutta and C. Mustansar Hussain, Eds., Academic Press, 2021, pp. 457–480. doi: 10.1016/B978-0-12-822989-7.00016-0.

[10] H. Mahmudul, 'Investigation of Energy Efficient approaches for the energy performance improvement of commercial buildings', Queensland University of Technology, Brisbane, Australia, 2013. [Online]. Available: https://eprints.qut.edu.au/61050/1/M.__Hasan__Thesis.pdf

[11] P. Fairey and D. B. Goldstein, 'Metrics for Energy Efficient Buildings: How Do We Measure Efficiency?', presented at the 2016 ACEEE Summer Study on Energy Efficiency in Buildings, Washhington, D.C., Washhington, D.C.: American Council for an Energy-Efficient Economy, 2016. [Online]. Available: https://www.aceee.org/files/proceedings/2016/data/index.htm

[12] D. B. Goldstein and C. Eley, 'A classification of building energy performance indices', *Energy Effic.*, vol. 7, no. 2, pp. 353–375, Apr. 2014, doi: 10.1007/s12053-013-9248-0.

[13] D. Johnston, M. Siddall, O. Ottinger, S. Peper, and W. Feist, 'Are the energy savings of the passive house standard reliable? A review of the as-built thermal and space heating performance of passive house dwellings from 1990 to 2018', *Energy Effic.*, vol. 13, no. 8, pp. 1605–1631, Dec. 2020, doi: 10.1007/s12053-020-09855-7.

[14]P. J. C. Vogler-Finck, R. Wisniewski, and P. Popovski, 'Reducing the carbon footprint of house heating through model predictive control – A simulation study in Danish conditions', *Sustain. Cities Soc.*, vol. 42, pp. 558–573, Oct. 2018, doi: 10.1016/j.scs.2018.07.027.

[15]I. Sarbu and C. Sebarchievici, 'Aspects of indoor environmental quality assessment in buildings', *Energy Build.*, vol. 60, pp. 410–419, May 2013, doi: 10.1016/j.enbuild.2013.02.005.

[16]L. Rohde, T. Larsen, R. Jensen, E. Loukou, and K. Jønsson, 'Historical Development of IEQ in Danish Dwellings -Has Energy Efficiency Requirements Inhibited Positive IEQ Developments?', presented at the E3S Web of Conferences, Apr. 2020. doi: 10.1051/e3sconf/201911102055.

[17]N. Simões and C. Serra, 'Ground contact heat losses: Simplified calculation method for residential buildings', *Energy*, vol. 48, no. 1, pp. 66–73, Dec. 2012, doi: 10.1016/j.energy.2012.04.013.

[18]M. H. Adjali, M. Davies, C. Ni Riain, and J. G. Littler, 'In situ measurements and numerical simulation of heat transfer beneath a heated ground floor slab', *Energy Build.*, vol. 33, no. 1, pp. 75–83, Nov. 2000, doi: 10.1016/S0378-7788(00)00067-0.

[19]J. Neymark and R. Judkoff, 'International Energy Agency Building Energy Simulation Test and Diagnostic Method (IEA BESTEST) In-Depth Diagnostic Cases for Ground Coupled Heat Transfer Related to Slab-On-Grade Construction', National Renewable Energy Laboratory, Colorado, USA, Technical Report NREL/TP-550-43388, Sep. 2008. [Online]. Available: https://www.nrel.gov/docs/fy08osti/43388.pdf

[20]H. Zhou, B. Lin, J. Qi, L. Zheng, and Z. Zhang, 'Analysis of correlation between actual heating energy consumption and building physics, heating system, and room position using data mining approach', *Energy Build.*, vol. 166, pp. 73–82, May 2018, doi: 10.1016/j.enbuild.2018.01.042.

[21]J. Šála, L. Keim, Z. Svoboda, and J. Tywoniak, 'Komentář k ČSN 73 0540 Tepelná Ochrana Budov', Česká energetická agentura, Praha, Oct. 2007. [Online]. Available: https://www.mpo-efekt.cz/upload/7799f3fd595eeee1fa66875530f33e8a/Publikace_Komentar_k_CSN_730540_Tepelna_ochrana_budov_2220047206.pdf

[22]D. Pompl, 'Vývoj tepelně-technických vlastností budov a zateplovacích systémů', bachelor thesis, Czech Technical University in Prague, Faculty of Mechanical Engineering, Prague, 2017. [Online]. Available: https://dspace.cvut.cz/bitstream/handle/10467/70871/F2-BP-2017-Pompl-Dominik-Bakalarska_prace.pdf?sequence=1&isAllowed=y

[23]V. Shemelin and Z. Malík, '"D2.1 Framework on Energy Efficient Buildings" of the HORIZON 2020 project POWERSKIN+. EC Grant Agreement No. 869898', CVUT, Praha, Czech Republic, 2021. [Online]. Available: https://www.powerskinplus.eu/filedelivery.php?docId=322

[24]M. P. Deru and A. T. Kirkpatrick, 'Ground-Coupled Heat and Moisture Transfer from Buildings Part 1–Analysis and Modeling*', *J. Sol. Energy Eng.*, vol. 124, no. 1, pp. 10–16, May 2001, doi: 10.1115/1.1435652.

[25]J. Claesson and C.-E. Hagentoft, 'Heat loss to the ground from a building—I. General theory', *Build. Environ.*, vol. 26, no. 2, pp. 195–208, Jan. 1991, doi: 10.1016/0360-1323(91)90027-9.

[26]C.-E. Hagentoft, 'Heat loss to the ground from a building : slab on the ground and cellar', doctoral thesis, Lund University, Lund, 1988. [Online]. Available: https://portal.research.lu.se/en/publications/heat-loss-to-the-ground-from-a-building-slab-on-the-ground-and-ce

[27]'Welcome to ESP-r'. http://www.esru.strath.ac.uk/Courseware/ESP-r/tour/ (accessed Jan. 03, 2022).

[28]J. W. Hand, 'Strategies for Deploying Virtual Representations of the Built Environment (aka The ESP-r Cookbook)'. Energy Systems Research Unit Department of Mechanical and Aerospace Engineering University of Strathclyde, Glasgow, UK., May 01, 2018. [Online]. Available: http://www.esru.strath.ac.uk/Courseware/ESP-r/tour/Downloads/strategies_may_2018.pdf

[29]I. Beausoleil-Morrison and G. Mitalas, 'BASESIMP: a Residential-Foundation Heat-Loss Algorithm for Incorporating into Whole-Building Energy-Analysis Programs', in *Proc. of Building Simulation'97*, 1997, pp. 1–8. [Online]. Available: http://www.ibpsa.org/proceedings/bs1997/bs97_p051.pdf

[30]I. Beausoleil-Morrison, G. Mitalas, and H. Chin, 'Estimating Three-Dimensional Below-Grade Heat Losses from Houses Using Two-Dimensional Calculations', in *Thermal Performance of the Exterior Envelopes of Buildings VI*, Clearwater Beach USA: ASHRAE, pp. 95–99. [Online]. Available: https://web.ornl.gov/sci/buildings/conf-archive/1995%20B6%20papers/012_Beausoleil.pdf

[31]G. P. Mitalas, 'Basement heat loss studies at DBR/NRC', National Research Council of Canada. Division of Building Research, Sep. 1982. doi: 10.4224/20378029.

[32]G. P. Mitalas, 'Calculation of Below-Grade Residential Heat Loss: Low-Rise Residential Building'.

[33]'Ground Heat Transfer in EnergyPlus: Auxiliary Programs — EnergyPlus 8.3'. https://bigladdersoftware.com/epx/docs/8-3/auxiliary-programs/ground-heat-transfer-in-energyplus.html (accessed Jan. 03, 2022).

[34]W. Bahnfleth and J. Amber, 'Algorithms for Slab-on-Grade Heat Transfer Calculations', US Army Corps of Engineers Research Laboratory, Champaign, Illinois, Technical report E90/15, Sep. 1990. [Online]. Available: https://www.researchgate.net/publication/235156117_Algorithms_for_Slab-on-Grade_Heat_Transfer_Calculations

[35]W. Bahnfleth, 'Three-Dimensional Modelling of Heat Transfer from Slab Floors', US Army Corps of Engineers Research Laboratory, Champaign, Illinois, technical manuscript E89/11, Jul. 1989. [Online]. Available: https://www.researchgate.net/publication/235109133_Three-Dimensional_Modelling_of_Heat_Transfer_from_Slab_Floors

[36]W. Bahnfleth and C. O. Pederson, 'Three-dimensional numerical study of slab-on-grade heat transfer', presented at the ASHRAE Transactions, Jan. 1990. [Online]. Available: https://www.researchgate.net/publication/235156117_Algorithms_for_Slab-on-Grade_Heat_Transfer_Calculations

[37]'EnergyPlus™ Version 9.6.0 Documentation: Input Output Reference'. U.S. Department of Energy. [Online]. Available: https://energyplus.net/assets/nrel_custom/pdfs/pdfs_v9.6.0/InputOutputReference.pdf

[38]'Ground Heat Transfer Calculations using Foundation:Kiva: Engineering Reference — EnergyPlus 9.6'. https://bigladdersoftware.com/epx/docs/9-6/engineering-reference/ground-heat-transfer-calculations-using-kiva.html#ground-heat-transfer-calculations-using-foundationkiva (accessed Jan. 03, 2022).

[39]'Kiva | Big Ladder Software'. https://bigladdersoftware.com/projects/kiva/ (accessed Jan. 04, 2022).

[40]N. J. F. Kruis, 'Development and Application of a Numerical Framework for Improving Building Foundation Heat Transfer Calculations', doctoral thesis, University of Colorado, 2015.

[41]B. R. Anderson, 'Calculation of the steady-state heat transfer through a slab-on-ground floor', *Build. Environ.*, vol. 26, no. 4, pp. 405–415, Jan. 1991, doi: 10.1016/0360-1323(91)90067-L.

[42]'Welcome | TRNSYS : Transient System Simulation Tool'. http://www.trnsys.com/ (accessed Jan. 03, 2022).

[43]T. Kusuda, 'Earth temperature and thermal diffusivity at selected stations in the United States', U.S. Department of Commerce, National Buerau of Standards, 8972, 1965. [Online]. Available: https://nvlpubs.nist.gov/nistpubs/Legacy/RPT/nbsreport8972.pdf

[44]'BSim — BSim - Building Simulation'. https://build.dk/bsim/Pages/BSim_Building_Simulation.aspx (accessed Feb. 11, 2023).

[45]H. Janssen and J. E. Christensen, 'Hygrothermal optimisation of museum storage spaces', *Energy Build.*, vol. 56, pp. 169–178, Jan. 2013, doi: 10.1016/j.enbuild.2012.08.043.

[46]'ČSN EN ISO 13370:2019 Thermal performance of buildings - Heat transfer via the ground - Calculation methods'. Úřad pro technickou normalizaci, metrologii a státní zkušebnictví, 2019.

[47]Z. Malík and P. Kopecký, 'Tepelná strata podlahou na zemine: redukcia 3D referenčného modelu na ekvivalentný 2D model', *Tepelná Ochr. Budov*, vol. 18, no. 5, pp. 18–22, 2015.

[48]HTflux, 'Characteristic floor dimension (B')'. https://www.htflux.com/en/documentation/psi-g-ground-contact-calculations/characteristic-floor-dimension-b/ (accessed Feb. 20, 2023).

[49]'Comsol Multiphysics'. COMSOL, Inc., Burlington, MA. [Online]. Available: comsol.com

[50]'ČSN 730540-2:2011 Thermal protection of buildings - Part 2: Requirements'. Úřad pro technickou normalizaci, metrologii a státní zkušebnictví, 2011.

[51]'WUFI® Plus | WUFI (en)'. https://wufi.de/en/software/wufi-plus/ (accessed Jan. 06, 2022).

[52]'Matlab'. MathWorks, Inc. [Online]. Available: https://www.mathworks.com/products/matlab.html

[53]'Microsof Excel'. Microsoft corporation.

[54]K. Staněk, 'TEPELNÝ TOK ZEMINOU - PODLAHA NA TERÉNU (dle ČSN EN ISO 13370 - podrobně dle příloh A a F)'. Czech Technical University in Prague, 2014.

[55] van Schijndel A. W. M., 'Round robin experiment CE1 design of the test box experiment methodologies and preliminary results', *Expert Meet. Int. Energy Agency Annex 58 2-4 April 2012 Bilbao Spain*, pp. 1–57, 2012.

[56]'Simulink'. [Online]. Available: https://www.mathworks.com/products/simulink.html

[57]'Oikolab Weather Downloader', Oikolab, Ltd., Sheung Wan, Hong Kong, Hong Kong SAR. [Online]. Available: https://weatherdownloader.oikolab.com/downloader

List of candidate's publications and R&D outcomes

TYWONIAK, J., et al. Exteriérový zastiňovací systém s fotovoltaickými lamelami pro střešní okna. [Functional Sample] 2021.

TYWONIAK, J., et al. Exteriérový zastiňovací systém s integrovanými funkcemi pro střešní okna- základní řešení. [Functional Sample] 2021.

LUPÍŠEK, A., et al. Resilientní bytové domy - Metodika pro hodnocení bytových domů z pohledu resilience, mitigace klimatických změn a adaptace na klimatické změny. [Certified Methodology (for RIV)] 2020.

MALÍK, Z., P. ŠENFELDR, and M. VOLF. Integrovaný prefabrikovaný dílec obálky budovy. [Prototype] 2020.

VOLF, M., et al. Resilient and Environmentally Efficient Residential Buildings - Assessment Method and Interim Outcomes. In: IOP Conference Series: Earth and Environmental Science. BEYOND 2020 – World Sustainable Built Environment Online conference, Gothenburg, 2020-11-02/2020-11-04. Bristol: IOP Publishing Ltd, 2020. vol. 588. ISSN 1755-1307. DOI 10.1088/1755-1315/588/3/032035.

VOLF, M. and Z. MALÍK. Horizontálně osazovaný modulární obvodový plášť. [Verified Technology] 2020.

SOUST-VERDAGUER, B., et al. Implications of Using Systematic Decomposition Structures to Organizebuilding LCA Information: A Comparative Analysis of National Standardsand Guidelines- IEA EBC ANNEX 72. In: IOP Conference Series: Earth and Environmental Science. BEYOND 2020 – World Sustainable Built Environment Online conference, Gothenburg, 2020-11-02/2020-11-04. Bristol: IOP Publishing Ltd, 2020. vol. 588. ISSN 1755-1307.

České vysoké učení technické v Praze, Praha 6, Dejvice, CZ. Prefabrikovaný kompozitní dílec pro rychlou a snadnou montáž výplňových konstrukcí. Inventors: M. VOLF, Z. MALÍK, and A. LUPÍŠEK. Czech Republic. Utility Model CZ 33659. 2020-01-28. Available from: https://isdv.upv.cz/doc/FullFiles/UtilityModels/FullDocuments/FDUM0033/uv033659.pdf

VOLF, M., et al. Prefabrikovaný dílec obálky budovy s integrovanou zelení. [Functional Sample] 2019.

TYWONIAK, J., et al. Remarks on application of building physics in changing climatic conditions. In: Sustainable Built Environment Conference 2019 PROCEEDINGS book. Sustainable Built Environment Conference 2019, Scilla, 2019-05-16/2019-05-17. IiSBE Italia R&D srl, 2019. p. 192-196. ISBN 9791220057387. Available from:

https://www.sbe19scilla.org/media/attachments/2020/01/15/scilla_proceedings_v4_l.pdf

MALÍK, Z. Ekvivalentná tepelná vodivosť vzduchu vo vzduchových dutinách priečniku fasádneho systému a jej vplyv na tepelnú priepustnosť detailu v porovnaní s CFD modelom. Vytápění, větrání, instalace. 2019, 28(5), 266-271. ISSN 1210-1389.

České vysoké učení technické v Praze, Praha 6, Dejvice, CZ. Systém pro zkvalitňování vnitřního prostředí budov pomocí pěstování rostlin. Inventors: D. ADAMOVSKÝ, et al. Czech Republic. Utility Model CZ 33355. 2019-11-05. Available from: https://isdv.upv.cz/doc/FullFiles/UtilityModels/FullDocuments/FDUM0033/uv033355.pdf

MALÍK, Z., et al. Tepelnětechnické posouzení kotevního prvku pro předsazené konstrukce. TZB info. 2019, 21(35), ISSN 1801-4399. Available from: https://stavba.tzb-info.cz/prostup-tepla-stavebni-konstrukci/19487-tepelnetechnicke-posouzeni-kotevniho-prvku-pro-predsazene-konstrukce

SCHULER, M., K. DVOŘÁKOVÁ, and Z. MALÍK. A Zero Energy House for and by Frank Gehry. In: SOJKOVÁ, K., et al., eds. Central Europe towards Sustainable Building (CESB19). Central Europe towards Sustainable Building 2019, Praha, 2019-07-02/2019-07-04. Bristol: IOP Publishing Ltd, 2019. IOP Conference Series:Earth and Environmental Science. vol. 290. ISSN 1755-1307. DOI 10.1088/1755-1315/290/1/012108.

ADAMOVSKÝ, D., et al. KlimaOkno pro obvodový plášť budovy. [Functional Sample] 2018.

CALTA, V., et al. Vyhodnocení provozu administrativní budovy Otevřená zahrada v Brně (2. část). Vytápění, větrání, instalace. 2018, 27.(5), 272-276. ISSN 1210-1389.

MALÍK, Z. and P. KOPECKÝ. Dynamická tepelná simulácia celej budovy s použitím odvodeného zjednodušeného modelu podlahy na zemine. In: 41. vědecká mezinárodní konference ústavů a kateder pozemních staveb České a Slovenské republiky. Dlouhá Lhota, 2018-09-19/2018-10-21. Praha: ČVUT, Fakulta stavební, Katedra konstrukcí pozemních staveb, 2018. p. 37-42. ISBN 978-80-01-06494-8.

CALTA, V., et al. Vyhodnocení provozu administrativní budovy Otevřená zahrada v Brně (1. část). Vytápění, větrání, instalace. 2018, 27.(3), 130-135. ISSN 1210-1389.

MALÍK, Z. and P. KOPECKÝ. Aplikácia zjednodušeného dynamického modelu prenosu tepla cez podlahu na zemine v simulácii celej budovy. Vytápění, větrání, instalace. 2017, 26(4), 200-204. ISSN 1210-1389.

MALÍK, Z. and P. KOPECKÝ. Aplikácia zjednodušeného dynamického modelu prenosu tepla cez podlahu na zemine v simulácii celej budovy. In: JAROŠ, M. and M. BARTÁK, eds. Simulace budov a techniky prostředí 2016 - sborník 9. konference IBPSA-CZ. Simulace

budov a techniky prostředí 2016: 9. konference IBPSA-CZ, Brno, 2016-11-10/2016-11-11. Praha: IBPSA-CZ, 2016. p. 33-38. ISBN 978-80-270-0772-1.

MALÍK, Z. and P. KOPECKÝ. Simplified Dynamic Thermal Models of Slab on Ground Floors. In: HÁJEK, P., et al., eds. Central Europe towards Sustainable Building 2016 - Innovations for Sustainable Future. Central Europe towards Sustainable Building 2016 Innovations for Sustainable Future, Prague, 2016-06-22/2016-06-24. Praha: GRADA PUBLISHING, 2016. p. 837-844. 1st edition, Prague, June 2016, Complete edition - printed version + Flash disk with full paper version. ISBN 978-80-271-0248-8.

BUREŠOVÁ, V., et al. Rešerše české, německé a rakouské legislativy související s energetickou náročností budov. [Research Report] Buštěhrad: ČVUT v Praze, UCEEB, 2015.

RŮŽIČKA, J., et al. Optimalizace návrhu konstrukčních detailů, stanovení lineárních součinitelů prostupu tepla vybranných stavebních detailů v rámci projektu rodinných domů Praha 13 - Stodůlky. [Research Report] Buštěhrad: ČVUT v Praze, UCEEB, 2015.

MALÍK, Z. and P. KOPECKÝ. Tepelná strata podlahou na zemine: redukcia 3D referenčného modelu na ekvivalentný 2D model. Tepelná ochrana budov. 2015, 18(5), 18-22. ISSN 1213-0907.

ANNEXES

Annex 1: The development of the required U-values for selected envelope components in other countries

This annex provides further overview of the development of the required U-values for selected building envelope components in other European countries (chapter 2.1)

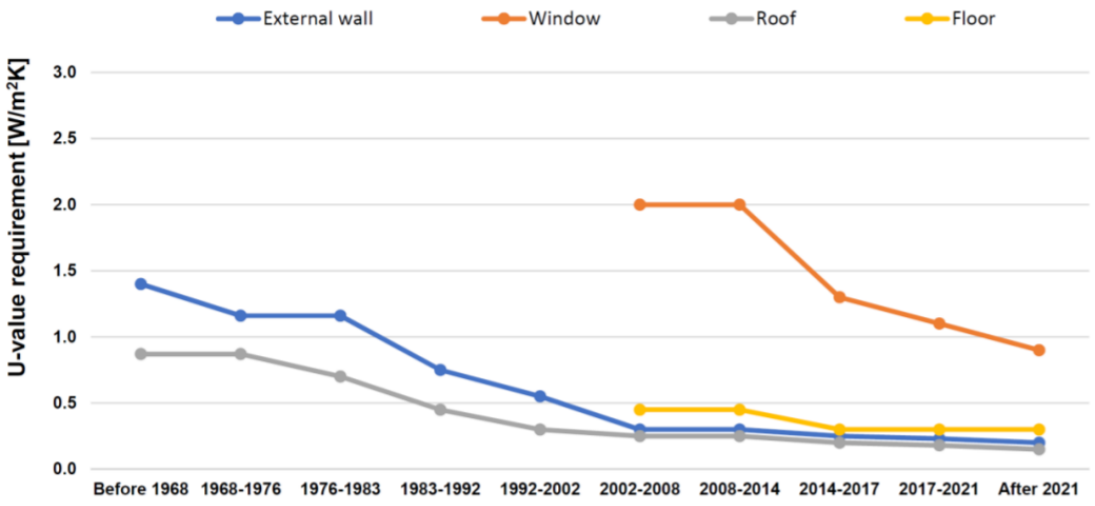

Fig. 0-1 Development of the required U-values for different building construction periods in Poland [23]

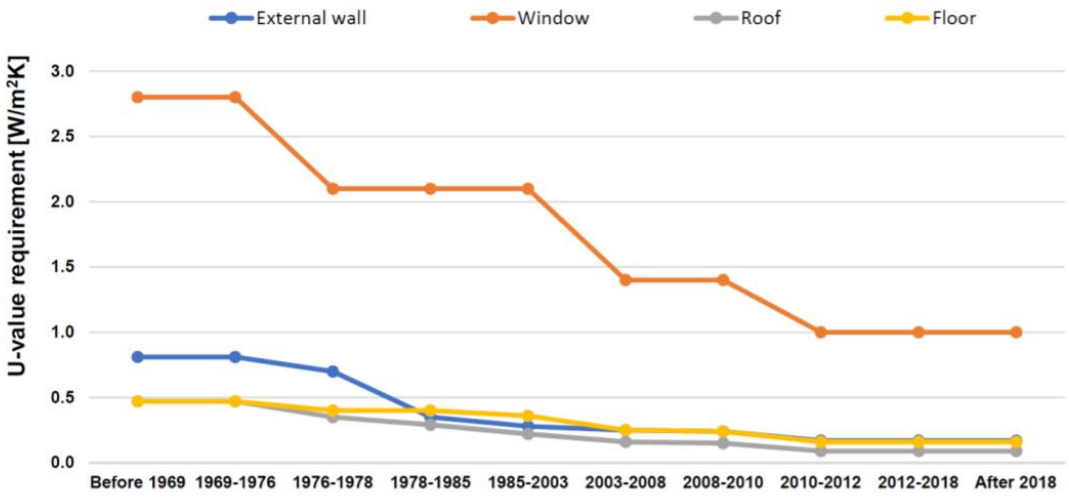

Fig. 0-2 Development of the required U-values for different building construction periods in Finland [23]

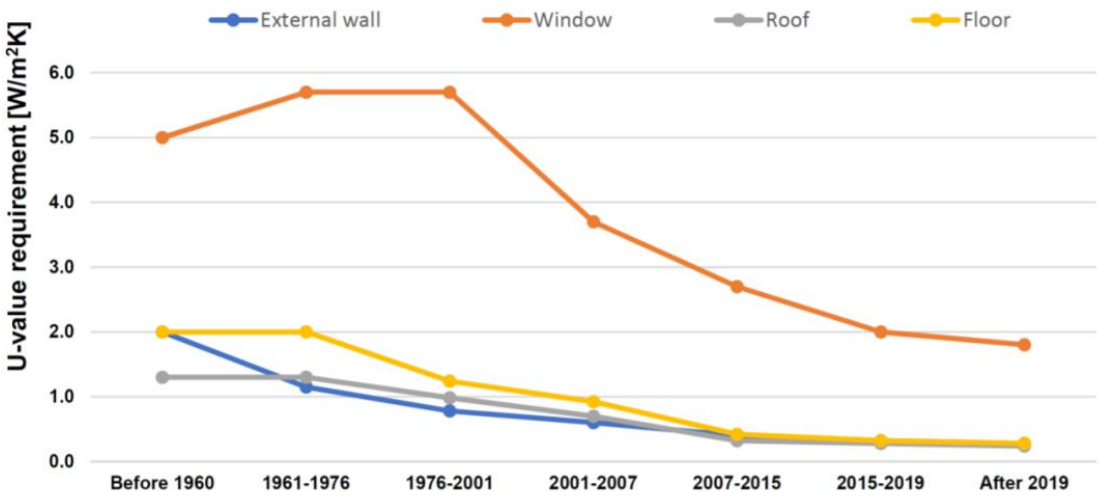

Fig. 0-3 Development of the required U-values for different building construction periods in Italy (Rome) [23]

Annex 2: Overview of other TRNSYS types for ground-coulped heat transfer

Type 1244:

- Is intended for slab-on-grade, basement, crawlspace, and buried zone heat transfer from Type 56 buildings
- Data file is typically created by hand using a spreadsheet. The top surface (X-Y plane) noding can be performed by the TESS Plug-in to Google SketchUp which maps the nodes to the surfaces and then pulled into the spreadsheet. For each soil node in the z-direction (depth), the user must specify the full X-Y map.
- The slab edge heat transfer is not accounted for in slab-on-grade or slab-in-grade constructions. Subsurface walls and floors have edge effects.
- The insulation can be added to the Type 56 walls. No additional insulation is allowed.
- The footer material is not accounted for.
- Only one soil layer is modelled
- Soil surfaces are uniform and horizontal
- The far-field heat transfer can be modelled as conductive or adiabatic and can be set for the X and Y directions independently, while for the far-field temperatures two options are introduced: (a) Surface temperature set by the Kusuda correlation with far-field soil temperatures driven by 1-dimensional conduction from the surface, or (b) Surface temperature of the far-field is set by an energy balance considering convection, conduction to the soil, incident solar radiation and long-wave radiation exchange with the sky. Far-field soil temperatures are then set by 1-dimensional conduction from the calculated surface temperature.
- Deep earth heat transfer can be conductive or adiabatic, while the deep earth temperatures are set by Kusuda correlation as a function of soil properties, time of year and depth.
- For the near-field surface temperatures, two options are introduced: (a) Surface temperatures set by the Kusuda correlation. In this case, the presence of the building does not influence the surface temperatures, just the sub-surface temperatures, or (b) Surface temperatures are calculated with a surface energy balance considering convection, conduction to the soil, incident solar radiation

and long-wave radiation exchange with the sky (building presence impacts soil temperatures).

- Heat flows from Type 56 slabs/walls are passed in as inputs. Average slab/soil boundary temperatures passed back to the Type 56 model.
- Sub-surface heat transfer is calculated using a 3-dimensional conduction using a finite difference approach.

Type 1255:

- Intended to model slab-on-grade and slab-in-grade construction for non-Type 56 buildings.
- The data file is generally created using a TESS Plug-In for Google Sketchup.
- Floor slab is assumed to be uniform across all thermal zones (thickness, materials, etc.)
- Slab edge heat transfer calculated to both the ambient air and the soil.
- The user can specify top surface or bottom surface insulation on each slab. The user can also specify skirt (slab edge) insulation. This skirt insulation, assumed to start at the top edge of the slab, can stop partway down the slab edge, stop at the bottom edge of the slab, or continue down beneath the slab. All insulation is assumed to be infinitesimally thin. Skirt insulation is not located between thermal zones – only between the zone and the soil/ambient.
- The footer material is not accounted for.
- Only one soil layer is modelled
- Soil surfaces are uniform and horizontal
- The far-field heat transfer can be modelled as conductive or adiabatic and can be set for the X and Y directions independently, while for the far-field temperatures, the same two options as in Type 1244 are introduced.
- Deep earth heat transfer can be conductive or adiabatic, while the deep earth temperatures are set by Kusuda correlation as a function of soil properties, time of year and depth.
- For the near-field surface temperatures, the same two options as in Type 1244.
- Slab surface temperatures are calculated from a surface energy balance.
- Sub-surface heat transfer is calculated using a 3-dimensional conduction using a finite difference approach.

Type 1267:

- Intended to model most on-grade, and sub-surface heat transfer for Type 56 buildings, non-Type buildings, storage tanks etc.
- Data file is typically created by hand using a spreadsheet. The top surface (X-Y plane) noding can be performed by the TESS Plug-in to Google SketchUp which maps the nodes to the surfaces and then pulled into the spreadsheet. For each soil node in the z-direction (depth), the user must specify the full X-Y map.
- Slab edge heat transfer is accounted for in the model (both to air and soil or other materials).
- The user can specify insulation R-values on the faces of any of the materials defined in the model, can specify the insulation as its own material (density, conductivity, specific heat) in the model, or have the insulation be a part of Type 56 building surface.
- The footer material can be accounted for in the model.
- Multiple soil layers are allowed
- The soil surface is completely user-defined.
- The far-field heat transfer is adiabatic. Users should specify a far-field distance sufficiently far away from the heat transfer.
- Deep earth heat transfer is conductive, but the user can specify bottom-surface insulation on the lowest soil material. The deep earth temperatures are provided by the user as a parameter.
- For the near-field surface temperatures, the same two options as in Type 1244 and Type 1255.
- For the zone/soil heat transfer calculation, two options are introduced: (a) Heat flows from Type 56 slabs/walls are passed in as inputs. Average slab/soil boundary temperatures passed back to the Type 56 model, or (b) Material/air boundary temperatures are calculated from a surface energy balance.
- Sub-surface heat transfer is calculated using a 3-dimensional conduction using a finite difference approach.

Annex 3: Comparison of 3D vs. 2D calculation results and 3D vs. 1D calculation results

This annex shows two figures. One figure represents the comparison of the results obtained from a reference 3D FEM calculation and the 2D FEM calculations for the worst performing test case (chapter 3.1). The second shows the comparison of the results obtained from a reference 3D FEM calculation and the 1D calculations on the developed model (chapter 4.1). It can be seen, that both the inaccuracy of both simplified models is comparable.

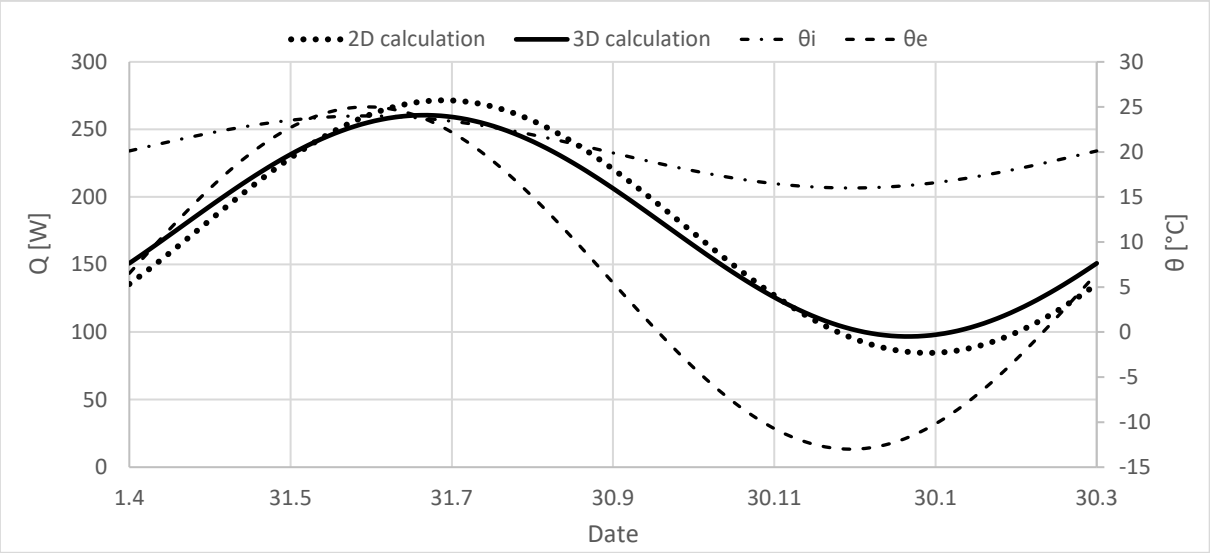

Fig. 0-4 Annual heat flux to the interior under harmonic boundary temperatures for the floor plan 6,0 [m] x 8,4 [m]; B'/2 = 1,75 [m]; GoF = 80,2 [%] (3D vs. 2D calculation)

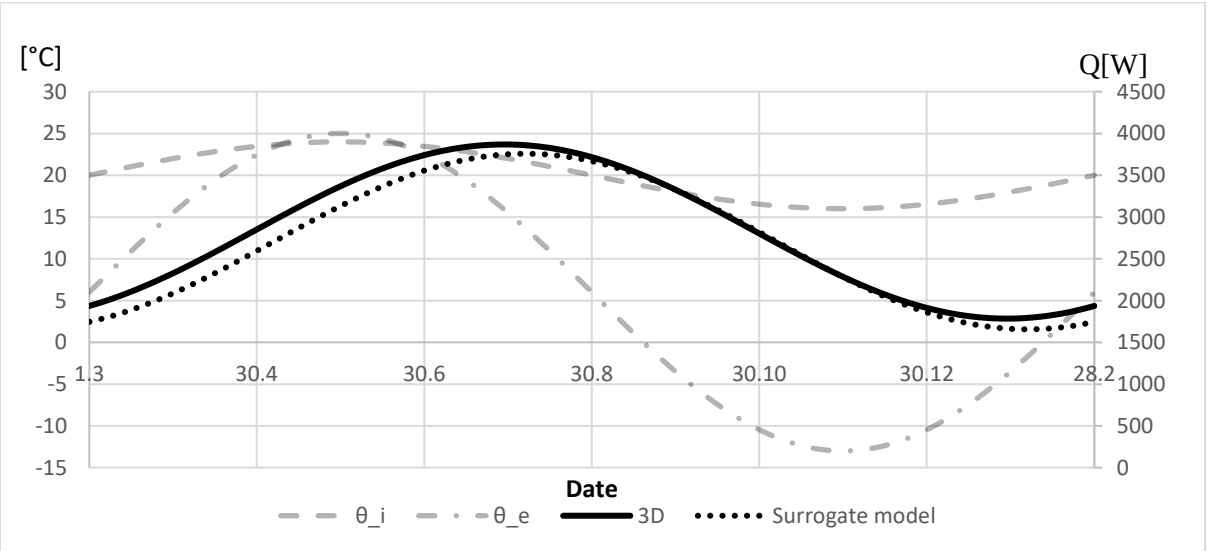

Fig. 0-5 Comparison of referential 3D results with surrogate model results for the worst case (floor 60x12 m, 3D vs. 1D calculation)

Annex 4: Results of comparison: developed model, 3D FEM model and EN ISO 13370 1D model

This annex presents the rest of the comparisons of results from the developed model, 3D FEM model and EN ISO 13370 1D calculation carried out in chapter 4.2.

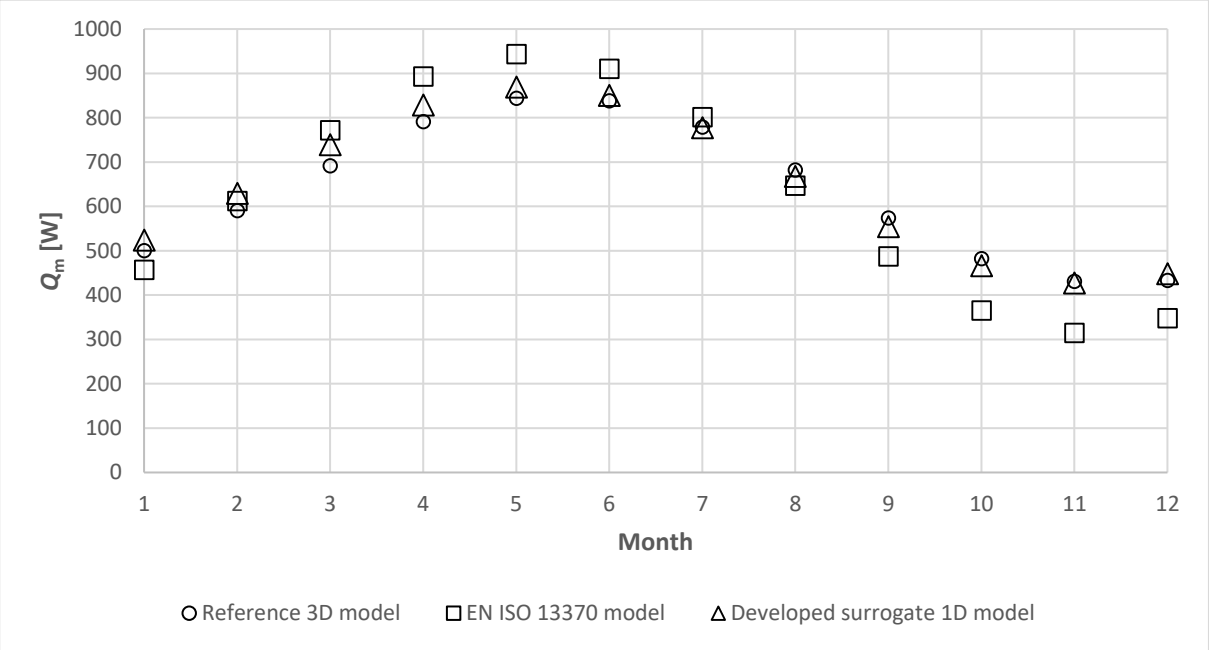

Fig. 0-6 Comparison of the mean heat fluxes through the slab-on-ground floors (floor plan 18x12 m)

Tab. 0-1 Comparison of the mean heat fluxes through the slab-on-ground floors (floor plan 18x12 m)

	Q [W]		
month	Reference 3D model	ISO13370 model	Developed surrogate 1D model
January	500	456	524
February	590	611	629
March	691	771	739
April	791	893	828
May	843	943	869
Jun	838	910	850
July	779	801	777
August	682	646	667
September	574	487	554
October	482	365	466
November	430	314	427
December	433	348	448
PMRE [%]		12.6	3.4
GoF [%]		45.7	82.9

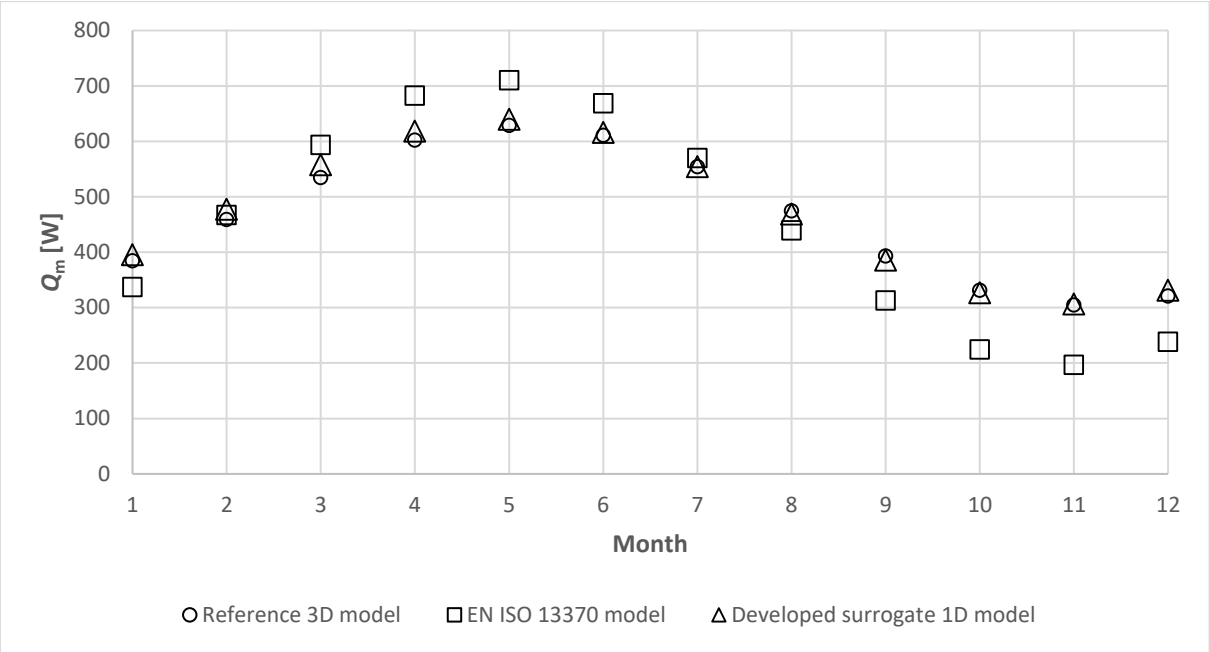

Fig. 0-7 Comparison of the mean heat fluxes through the slab-on-ground floors (floor plan 10x15 m)

Tab. 0-2 Comparison of the mean heat fluxes through the slab-on-ground floors (floor plan 10x15 m)

	Q [W]		
month	Reference 3D model	ISO13370 model	Developed surrogate 1D model
January	384	337	396
February	459	467	477
March	535	594	558
April	602	682	618
May	629	710	640
Jun	611	669	616
July	554	570	554
August	475	440	469
September	393	313	386
October	331	224	326
November	304	197	306
December	321	238	331
PMRE [%]		15.4	2.1
GoF [%]		38.1	89.8

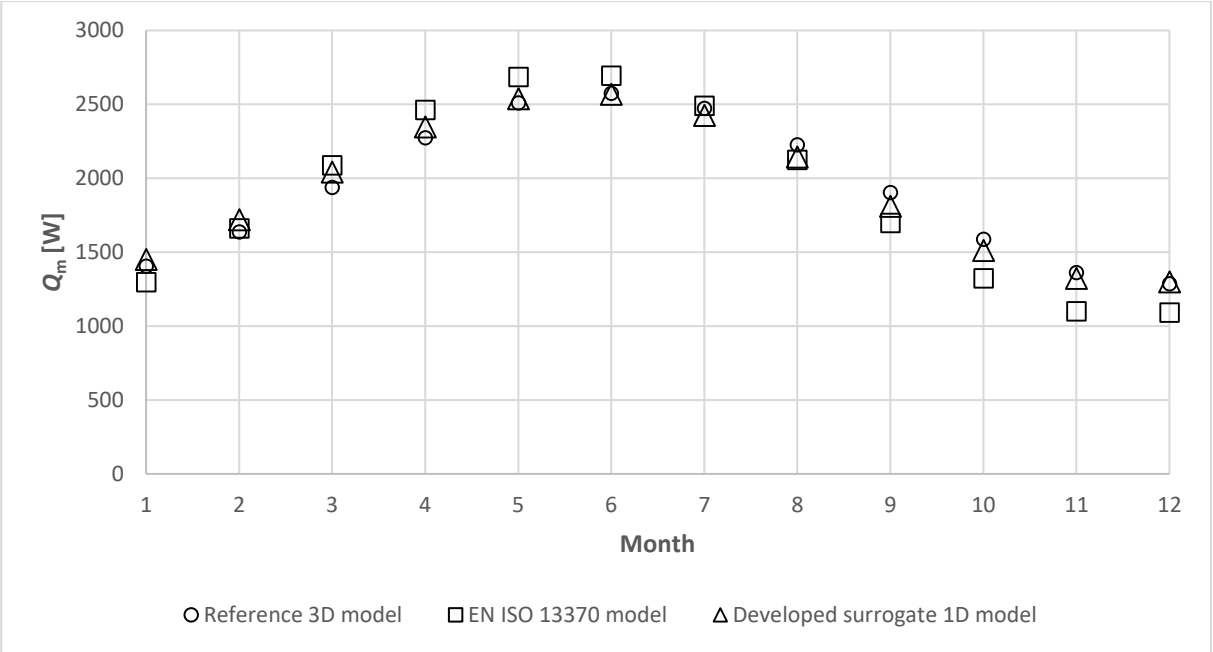

Fig. 0-8 Comparison of the mean heat fluxes through the slab-on-ground floors (floor plan 60x12 m)

Tab. 0-3 Comparison of the mean heat fluxes through the slab-on-ground floors (floor plan 60x12 m)

	Q [W]		
month	Reference 3D model	ISO13370 model	Developed surrogate 1D model
January	1 405	1 296	1 450
February	1 636	1 661	1 719
March	1 937	2 088	2 042
April	2 274	2 463	2 346
May	2 509	2 685	2 538
Jun	2 575	2 695	2 567
July	2 472	2 489	2 424
August	2 226	2 124	2 144
September	1 903	1 697	1 811
October	1 587	1 322	1 510
November	1 361	1 100	1 322
December	1 286	1 090	1 300
PMRE [%]		8.7	3.1
GoF [%]		62.6	85.6